



Terhi Hirvikorpi

Thin Al_2O_3 barrier coatings grown on bio-based packaging materials by atomic layer deposition

VTT PUBLICATIONS 770

Thin Al₂O₃ barrier coatings grown on bio-based packaging materials by atomic layer deposition

Terhi Hirvikorpi

Doctoral dissertation for the degree of Doctor of Science in Technology to be presented with due permission of the Aalto University School of Chemical Technology for public examination and debate in Room 26 at Dipoli Congress Centre (Espoo, Finland) on the 18th of November, 2011, at 12 noon.



ISBN 978-951-38-7750-7 (soft back ed.)

ISSN 1235-0621 (soft back ed.)

ISBN 978-951-38-7751-4 (URL: <http://www.vtt.fi/publications/index.jsp>)

ISSN 1455-0849 (URL: <http://www.vtt.fi/publications/index.jsp>)

Copyright © VTT 2011

JULKAISIJA – UTGIVARE – PUBLISHER

VTT, Vuorimiehentie 5, PL 1000, 02044 VTT

puh. vaihde 020 722 111, faksi 020 722 4374

VTT, Bergsmansvägen 5, PB 1000, 02044 VTT

tel. växel 020 722 111, fax 020 722 4374

VTT Technical Research Centre of Finland, Vuorimiehentie 5, P.O. Box 1000, FI-02044 VTT, Finland
phone internat. +358 20 722 111, fax + 358 20 722 4374

Terhi Hirvikorpi. Thin Al₂O₃ barrier coatings grown on bio-based packaging materials by atomic layer deposition [Ohuet biopohjaisille pakkausmateriaaleille atomikerroskasvatetut Al₂O₃-barrier-pinnoitteet]. Espoo 2011. VTT Publications 770. 74 p. + app. 42 p.

Keywords: atomic layer deposition, aluminium oxide, thin film, barrier, biopolymer, packaging material

Abstract

Growing environmental concerns related to the use of synthetic non-biodegradable polymers in the packaging industry have led to the need for new, especially bio-based, materials. Currently, petroleum-based synthetic polymers are widely used due to their relatively low cost and high performance. Biodegradable plastics and fibre-based materials have been proposed as a solution to the waste problems related to these synthetic polymers. Fibre-based packaging materials have many advantages over their non-biodegradable competitors, such as stiffness vs. weight ratio and recyclability. However, poor barrier properties and sensitivity to moisture are the main challenges restricting their use. Application of a thin coating layer is one way to overcome these problems and to improve the barrier properties of such materials.

Atomic layer deposition (ALD) is a well suited technique for depositing thin inorganic coatings onto temperature-sensitive materials such as polymer-coated boards and papers and polymer films. In the present work, thin and highly uniform Al₂O₃ coatings were deposited at relatively low temperatures of 80, 100 and 130 °C onto various bio-based polymeric materials employing the ALD technique. The study demonstrates that a 25-nm-thick ALD-grown Al₂O₃ coating significantly enhances the oxygen and water vapour barrier performance of these materials. Promising barrier properties were obtained with polylactide-coated board, hemicellulose-coated board as well as various biopolymer (polylactide, pectin and nanofibrillated cellulose) films after coating with a 25-nm-thick Al₂O₃ layer.

Thin Al₂O₃ coatings can improve the properties of biopolymers, enabling the use of these renewable polymers in the production of high-performance materials for demanding food and pharmaceutical packaging applications. The future roll-to-roll ALD technology for coating polymers with inorganic thin films will increase the industrial potential of these materials and could lead to further opportunities for their commercialization.

Terhi Hirvikorpi. Thin Al₂O₃ barrier coatings grown on bio-based packaging materials by atomic layer deposition [Ohuet biopohjaisille pakkausmateriaaleille atomikerroskasvatetut Al₂O₃-barrier-pinnoitteet]. Espoo 2011. VTT Publications 770. 74 p. + app. 42 p.

Avainsanat: atomic layer deposition, aluminium oxide, thin film, barrier, biopolymer, packaging material

Tiivistelmä

Pakkausteollisuuden tietoisuus synteettisten biohajoamattomien muovien ympäristöhaitoista on lisännyt tarvetta ekologisemmille biopohjaisille pakkausratkaisuille. Nykyisin öljypohjaisia synteettisiä polymeerejä käytetään useissa pakkauksissa, koska ne ovat halpoja ja ominaisuuksiltaan hyviä. Biohajoavia muovi- ja kuitupohjaisia materiaaleja pidetään ratkaisuna öljypohjaisten synteettisten muovien aiheuttamalle jäteongelmalle. Kuitupohjaisilla pakkausmateriaaleilla on monia hyviä ominaisuuksia verrattuna niiden biohajoamattomiin kilpailijoihin, kuten painoon suhteutettu kestävyys ja kierrätettävyys. Niiden heikkoutena on kuitenkin huono kosteuden sietokyky sekä korkea vesihöyrynläpäisy, jotka estävät tuotteiden laajamittaisen käytön. Materiaalien läpäisynestoa voidaan parantaa sopivilla pinnoituksilla.

Atomikerroskasvatus ohutpinnoitteiden valmistustekniikkana soveltuu hyvin epäorgaanisten pinnoitteiden kasvatukseen lämpöherkille materiaaleille, jollaisia esimerkiksi polymeeripinnoitetut kartongit ja paperit sekä polymeerikalvot ovat. Tässä työssä kasvatettiin ohuita Al₂O₃-kalvoja suhteellisen alhaisissa lämpötiloissa (80, 100 ja 130 °C:ssa) ALD-tekniikalla monenlaisille biopohjaisille polymeerisubstraateille. Ohuet (25 nm) ALD-tekniikalla valmistetut Al₂O₃-pinnoitteet mahdollistavat huomattavan parannuksen biopohjaisten pakkausmateriaalien hapen- ja vesihöyrynläpäisyn estokykyyn. Polylaktidilla ja hemiselluloosalla päällystetyt kartongit sekä polylaktidista, pektiinistä ja nanoselluloosasta valmistetut kalvot olivat lupaavia hapen ja vesihöyrynläpäisyä estäviä materiaaleja, kun ne oli päällystetty 25 nm:n paksuisella Al₂O₃-kerroksella.

Nämä ohuet pinnoitteet aikaansaavat niin merkittävän parannuksen esto-ominaisuuksissa, että biopolymeerien käyttö vaativissakin pakkaussovelluksissa, kuten elintarvike- ja lääkepakkauksissa, mahdollistuu. ALD-teknologian kehitys kohti rullalta rullalle -prosessia mahdollistaa epäorgaanisten pinnoitteiden valmistamisen teollisessa mittakaavassa, mikä on elintärkeää tässä työssä esiteltujen uusien pakkausmateriaalien kaupallistumiselle.

Academic dissertation

Custos

Academy Professor Maarit Karppinen
Department of Chemistry, School of Chemical Technology,
Aalto University, Finland

Supervisor

Academy Professor Maarit Karppinen
Department of Chemistry, School of Chemical Technology,
Aalto University, Finland

Instructors

Doctor Mika Vähä-Nissi
VTT Technical Research Centre of Finland, Espoo, Finland
Professor Ali Harlin
VTT Technical Research Centre of Finland, Espoo, Finland

Preliminary examiners

Professor David Cameron
Lappeenranta University of Technology, Finland
Professor Mikael Hedenqvist
Royal Institute of Technology (KTH), Sweden

Opponent

Docent Eeva-Liisa Lakomaa
Vaisala Oyj, Helsinki, Finland

*Kuka vain, minä vain, sinä vain
Kaiken avain, voit muuttaa suuntaa*

Teräsbetoni,
Maailma tarvitsee sankareita

Preface

The experimental work for this thesis was carried out at Oy Keskuslaboratorio – Centrallaboratorium Ab (KCL) and at VTT Technical Research Centre of Finland between November 2007 and December 2010.

I would like to express my sincere gratitude to my supervisor Academy Prof. Maarit Karppinen of the Laboratory of Inorganic Chemistry at the Aalto University School of Chemical Technology for investing such enormous time and effort in guiding this work. I also extend my appreciation to my instructors at VTT, Dr. Mika Vähä-Nissi and Prof. Ali Harlin, for their valuable guidance and for the opportunity to work on this subject, which is close to my heart. My sincere thanks go also to the pre-examiners of this thesis for their work and helpful advice. I am deeply thankful to my co-workers and friends at VTT and especially to Ms. Jenni Sievänen, Ms. Hanna Heinonen, Dr. Riku Talja and Dr. John Kettle for bringing laughter and joy to work and always being there for me.

I would like to thank all of the co-writers who have made a contribution to the included papers. I would especially like to thank everyone at Picosun for their help and guidance. Mr. Jari Malm of Aalto University is also much appreciated for his help and friendship.

Finally, I would like to thank my parents Ritva and Taisto Kujanpää as well as my sister Kirsi Kemppainen, her husband Janne, their two adorable sons Aaro and Elias, and my close friend Heikki Kiili for their love and support which I will never forget. Most of all, this work could not have been possible without my husband Mika. You are everything I could ever ask for. Our newborn daughter, Emma, and you are the best reasons to strive, step-by-step, to save nature and to change the world for the better.

Espoo, September 2011

Terhi Hirvikorpi

List of publications

The thesis consists of an introductory summary and the six publications listed below. The publications are referred to in the text by the roman numerals I–VI.

- I T. Hirvikorpi, M. Vähä-Nissi, A. Harlin and M. Karppinen, Comparison of some coating techniques to fabricate barrier layers on packaging materials, *Thin Solid Films* **518** (2010) 5463–5466.
- II T. Hirvikorpi, M. Vähä-Nissi, T. Mustonen, E. Iiskola and M. Karppinen, Atomic layer deposited aluminum oxide barrier coatings for packaging materials, *Thin Solid Films* **518** (2010) 2654–2658.
- III T. Hirvikorpi, M. Vähä-Nissi, J. Nikkola, A. Harlin and M. Karppinen, Thin Al₂O₃ barrier coatings onto temperature-sensitive packaging materials by atomic layer deposition, *Surface and Coatings Technology*, **205** (2011) 5088–5092.
- IV T. Hirvikorpi, M. Vähä-Nissi, A. Harlin, J. Marles, V. Miikkulainen and M. Karppinen, Effect of corona pre-treatment on the performance of gas barrier layers applied by the atomic layer deposition onto polymer-coated paperboard, *Applied Surface Science* **257** (2010) 736–740.
- V T. Hirvikorpi, M. Vähä-Nissi, J. Vartiainen, P. Penttilä, J. Nikkola, A. Harlin, R. Serimaa and M. Karppinen, Effect of heat-treatment on the performance of gas barrier layers applied by atomic layer deposition onto polymer-coated paperboard, *Journal of Applied Polymer Science* **122** (2011) 2221–2227.
- VI T. Hirvikorpi, M. Vähä-Nissi, A. Harlin, M. Salomäki, S. Areva, J.T. Korhonen and M. Karppinen, Enhanced water vapor barrier properties for biopolymer film by polyelectrolyte multilayer and atomic layer deposited Al₂O₃ double-coating, *Applied Surface Science* **257** (2011) 9451–9454.

Contributions of the author

- I** Designed the experiments, carried out the thickness measurements, supervised the characterizations (ICP-AES, AFM, OTR and WVTR), evaluated all of the results and had a major role in writing the manuscript.
- II** Designed the experiments, carried out the TG analyses, supervised the characterizations (SEM, AFM, OTR and WVTR), evaluated all of the results and had a major role in writing the manuscript.
- III** Designed the experiments, carried out the ALD coatings and some of the CA, SE and OTR measurements, supervised the CA, SE, OTR and WVTR measurements, evaluated all of the results and had a major role in writing the manuscript.
- IV** Designed the experiments, carried out the corona treatments and CA and SE analyses, supervised the OTR and WVTR measurements, evaluated all of the results and had a major role in writing the manuscript.
- V** Designed the experiments, carried out the ALD coatings, some of the thermal treatments and the CA and SE analyses, supervised the characterizations (AFM, OTR and WVTR) evaluated all of the results and had a major role in writing the manuscript.
- VI** Designed the experiments, carried out the fabrication of the PE solutions, PEM coatings on silicon wafer and characterizations (thickness, M_v , cytotoxicity and CA), supervised the fabrication of PEM coatings on PLA and characterizations (SEM and WVTR), evaluated all of the results and had a major role in writing the manuscript.

Contents

Abstract	3
Tiivistelmä.....	4
Academic dissertation	5
Preface	9
List of publications.....	10
Contributions of the author	11
List of abbreviations	14
List of symbols	17
1. Introduction	18
2. Polymeric packaging materials	20
2.1 The use of biopolymers as packaging materials	20
2.2 The selection of suitable packaging materials	21
3. Permeation through polymeric materials.....	23
3.1 Mass transfer interactions	23
3.2 Oxygen and water vapour barrier measurement	26
3.3 Reliability of OTR and WVTR measurements	29
4. Deposition of high-quality thin-film barriers	31
4.1 Conventional barrier coatings.....	31
4.2 Atomic layer deposition (ALD).....	32
4.3 The ALD process for Al ₂ O ₃ coatings	33
4.4 ALD fabricated barrier coatings.....	35
5. Experimental	38
5.1 Objectives	38
5.2 Substrate materials	38
5.3 Thin-film depositions.....	40
5.4 Pre-treatments for polymeric materials	41
5.5 Pre-coatings prior to ALD-Al ₂ O ₃ coating	42
5.6 Sample characterizations	42
6. Results and discussion.....	45
6.1 Characterization of thin Al ₂ O ₃ coatings grown on polymers.....	45
6.1.1 Properties of polymeric substrates.....	45
6.1.2 Comparison of barrier properties obtained by different thin-film deposition techniques	47
6.2 ALD growth process for Al ₂ O ₃ coatings on polymeric materials	48

6.3	Barrier properties of ALD-Al ₂ O ₃ coatings on biopolymeric materials	51
6.4	Influence of pre-treatments and pre-coating layers on barrier properties.....	56
6.4.1	Enhanced surface polarity by corona treatment.....	56
6.4.2	Enhanced polymer crystallinity by thermal treatment.....	57
6.4.3	Epoxy-SG layer as a pre-barrier for Al ₂ O ₃ -coated biopolymeric substrates	59
6.4.4	Polyelectrolyte multilayer film as a pre-coating for Al ₂ O ₃ -coated biopolymeric substrates	61
7.	Conclusions	64
	References	66
Appendices		
	Publications I–VI	

List of abbreviations

AFM	Atomic force microscopy
ALD	Atomic layer deposition
ALG	Sodium alginate
B	Board
BfR	Bundesinstitut für risikobewertung (German federal institute for risk assessment)
CA	Contact angle (°)
CHI	Chitosan
CVD	Chemical vapour deposition
DIM	Diiodomethane
EBE	Electron beam evaporation
EDS	Energy dispersive spectroscopy
EVOH	Ethylene vinyl alcohol
FDA	Food and drug administration
GGM	Galactoglucomannan
GPC	Growth per cycle
ICP-AES	Inductively-coupled plasma atomic emission spectroscopy
LbL	Layer-by-layer
LDPE	Low-density polyethylene
MLD	Molecular layer deposition

MS	Magnetron sputtering
NFC	Nanofibrillated cellulose
OTR	Oxygen transmission rate ($\text{cm}^3/\text{m}^2/10^5 \text{ Pa/day}$)
OWRK	Extended Fowkes theory
PC	Polycarbonate
PE	Polyethylene
PECVD	Plasma-enhanced chemical vapour deposition
PEM	Polyelectrolyte multilayer film
PEN	Polyethylene naphthalene
PET	Polyethylene terephthalate
PHB	Polyhydroxybutyrate
PLA	Polylactide
PMMA	Polymethyl methacrylate
PP	Polypropylene
PS	Polystyrene
PVC	Polyvinyl chloride
PVD	Physical vapour deposition
R_a	Average roughness (m)
RH	Relative humidity (%)
RT	Room temperature
SCCM	Standard cubic centimetres per minute
SEM	Scanning electron microscopy
SG	Sol-gel
TG	Thermogravimetry
TMA	Trimethylaluminium

UNC	Uncoated
WAXS	Wide-angle X-ray scattering
WVTR	Water vapour transmission rate (g/m ² /day)
XPS	X-ray photoelectron spectroscopy

List of symbols

A	Effective area of permeation (m^2)
a	Mark–Houwink parameter (-)
c	Concentration of the permeant molecule (mol/l)
D	Diffusion coefficient (m^2/s)
E_d	Activation energy of diffusion (kJ/mol)
F	Diffusing rate per unit of area ($\text{g/m}^2\text{s}$)
k	Boltzmann constant ($1.380650 \cdot 10^{-23} \text{ JK}^{-1}$)
K	Mark–Houwink parameter (ml/g)
l	Thickness of the packaging material (m)
M_v	Molecular weight (g/mol)
P	Permeability coefficient (g/msPa)
q	Quantity of permeant molecule (volume or mass) passing through the packaging material (m^3 or kg)
S	Solubility coefficient ($\text{g}/(\text{m}^3\text{Pa})$)
t	Evaluation time (s)
T	Temperature (K)
x	Direction of diffusion (-)
$[\eta]_{in}$	Intrinsic viscosity (ml/g)
Δp	Pressure difference between both sides of the packaging material (Pa)
γ_s	Total surface energy (mN/m)
γ^d	Dispersive component of surface energy (mN/m)
γ^p	Polarity component of surface energy (mN/m)

1. Introduction

Synthetic non-biodegradable polymers derived from petroleum-based resources, such as polyethylene, polypropylene, polyethylene terephthalate, etc., are widely used materials in food and pharmaceutical packaging applications due to their relatively low cost and high performance. However, growing environmental concerns related to the use of these polymers has led to the need for new solutions, and biopolymers (modified natural polymers, and biodegradable synthetic polymers of bio-based monomers) have been considered to be the environmentally-friendly solution for packaging materials in the future [1]. In many cases, however, poor barrier properties, especially of natural polymers, and sensitivity to moisture are preventing the wider use of these materials. In order to commercialize novel materials from renewable sources, the properties of these materials must be improved to a level that matches or exceeds the properties of the materials currently in use without sacrificing recyclability. One way to improve the barrier properties of biopolymers is to coat them with a thin inorganic layer.

Atomic layer deposition (ALD) is an advanced thin-film deposition technique that enables the production of high-quality coatings on a range of materials [2,3]. The technique's layer-by-layer growth assures precise control of film thickness even at relatively low process temperatures. Similar process control, mild deposition conditions and high film quality combined with low thickness is difficult to obtain with other thin-film deposition techniques. The goal of the present work was to deposit ultra-thin high-quality barrier coatings onto polymeric materials. The emphasis was on biopolymeric materials, such as polylactide (PLA). The ALD-grown Al_2O_3 coatings were shown to produce significantly enhanced oxygen and water vapour barrier materials when coated onto temperature-sensitive biopolymeric materials.

Nowadays biopolymers are used in relatively few packaging products. Thin (25 nm or less) Al_2O_3 coatings can extend the use of these polymers towards more demanding packaging applications such as dry food and pharmaceutical packages. The fabrication of recyclable and biodegradable barrier materials represents a new approach to utilizing the ALD technique. The results led to optimization of the ALD process parameters (most suitable oxygen source, deposition temperature, and film thickness) for biopolymeric materials. In addition, the effects on barrier properties of various pre-treatments and pre-coatings carried out prior to the ALD process were studied.

Numerous non-biodegradable and bio-based polymers have been developed as commercial barrier materials by companies and research institutes. The polymers currently in use are presented in Chapter 2. ALD coatings offer the potential to raise the properties of these materials to new, improved levels. However, due to the highly complex nature of the barrier phenomena involved, this goal is not easy to achieve. The gas barrier phenomena in question are briefly presented in Chapter 3. In addition to a description of the ALD process, the currently used thin-film deposition techniques related to the packaging industry are discussed in Chapter 4.

The experimental section, including a description of the substrate materials and the characterization techniques employed during the work, is presented in Chapter 5. The main characterization methods utilized were the barrier testing methods, i.e. oxygen and water vapour transmission rates (OTR, WVTR). The oxygen and water vapour barrier properties of temperature-sensitive bio-based materials combined with ALD-grown Al_2O_3 coatings have not been as extensively studied before. Chapter 5 also describes the methods applied to improve the barrier properties of the polymeric materials prior to the ALD process. Chapters 6 and 7 summarize the results. Chapter 7 also describes the current development status of these materials and provides recommendations for future research.

The future of the materials studied here looks bright. The future use of roll-to-roll ALD technology to produce inorganic coatings on polymers will increase the industrial potential of these materials as the process becomes more cost-effective [4]. This development is being supported by new competence and research tools and evidenced by new inventions and patent applications [5–7]. Process development is also essential for the commercialization of these novel packaging materials, which is predicted to be a reality within the next few years.

2. Polymeric packaging materials

2.1 The use of biopolymers as packaging materials

The use of polymers from renewable sources, i.e. biopolymers, as a replacement for synthetic non-biodegradable polymers as packaging materials is believed to offer a future means of significantly reducing non-compostable packaging waste and mitigating the greenhouse effect [8]. The use of biopolymers as packaging materials is increasing due to their advantageous properties. For instance, in many cases they are completely biodegradable within the composting cycle. Due to similar properties with petroleum-based polymers, biopolymers, such as polylactide (PLA) can be used to replace conventional polymers, such as polystyrene (PS) or polypropylene (PP). In addition, biopolymers can be fabricated from renewable biomass which will not eventually run out as will the feedstock of petrochemicals making biopolymers a sustainable alternative for the packaging industry. However, when compared to synthetic thermoplastic polymers such as polypropylene or polyethylene, the use of biopolymers is limited due to their naturally poor moisture barrier properties. The recyclable packaging materials currently on the market are mainly based on starch or PLA. In the packaging industry, biopolymers are used in applications such as biodegradable waste bags, fast food service-ware, and food containers.

Biopolymers are classified according to their source of extraction or the production method used [9]. Biopolymers are referred to as natural polymers if they have been extracted or removed from biomass [10,11]. Natural polymers are formed during the natural growth processes of organisms. Biopolymers can be produced by classical chemical synthesis starting from renewable bio-based monomers, or they can be produced by micro-organisms. Thermoplastic, biodegradable PLA is a biopolymer produced by polymerization of lactic acid monomers or cyclic lactide dimers [12]. Biodegradable polymers of fossil origin

also exist, such as polycaprolactone, although these cannot be defined as biopolymers.

The diversity of packed food and pharmaceutical goods will increase in the future, as will the requirement for more sustainable packaging materials [12]. Fibre-based materials refer to materials made from cellulosic fibre networks, such as paper and board. Paper and board products must compete with plastics for market share. Paper and board base materials are often coated with polymers or treated in some other way to enhance their mechanical and barrier properties. Fibre-based materials have advantages and disadvantages similar to biopolymers [13]. These materials are often compostable within the composting cycle but their moisture resistance is poor. In addition, their stiffness vs. weight ratio is also excellent and hard to beat. Due to problems in the recycling process posed by synthetic non-biodegradable polymers, novel, easily recyclable, fibre-based materials have been developed for these applications [1,14].

Polymer waste can be managed in three ways: mechanical recycling, energy recovery, or biological recycling [14]. Additionally, monomer recycling has also been proposed for several polymers such as polyvinyl chloride, although the concept has not proven feasible to date. Mechanical recycling is the most beneficial approach in cases where the recycled polymer only partially replaces the polymer in the primary product. The main obstacle in the recycling process is thermal decomposition of the polymer. In addition, polymers often contain impurities after recycling. Energy recovery from polymers is potentially a beneficial option, as petroleum-based polymers contain large amounts of energy and could be used as a partial replacement for fossil fuels. However, the formation of toxic gases during the incineration of polymers remains a key problem in this respect. Biological recycling refers to the composting of organic matter, i.e. the returning of polymers to biomass. Biological recycling is the most beneficial method where mechanical recycling and energy recovery are inefficient, for example in the case of food packages containing food waste.

2.2 The selection of suitable packaging materials

The choice of packaging material for a given application depends on a range of factors. The type of packed good, its chemical composition, size, storage conditions, expected shelf life, moisture content, aromas and appearance are just a few characteristics to be considered in the material selection. The chosen material must protect both the packed item and the environment. In the case of

2. Polymeric packaging materials

food and pharmaceutical packages, health and hygiene must also be accounted for. The approved packaging materials for food and pharmaceutical products are restricted by law. In the USA, the Food and Drug Administration (FDA) regulates factors affecting migration and changes in odour and flavour. In Europe, one major regulator is the German Federal Institute for Risk Assessment (Bundesinstitut für Risikobewertung, BfR) [15–17]. In addition, the European Union and its legislation on packaging and packaging waste regulate the suitability of packaging materials in Europe.

In order to provide sufficient protection the packaging material must be multifunctional, as it must serve as a barrier against gases, moisture, light, grease and aromas. In addition, it must be durable and sealable. This must also be achieved at low production cost and with low energy consumption [18]. Polyethylene (PE) as a commercial synthetic petroleum-based polymer is a poor oxygen barrier, but has good water and water vapour barrier properties. Besides low- and high-density PE, the common non-biodegradable moisture barrier polymers include PP and polyethylene terephthalate (PET) [19,20]. Other similar polymers with moisture barrier properties include cyclo-olefin copolymers, liquid-crystal polymers and nano-composites [21,22]. In addition, vinyl alcohol polymers, such as ethylene vinyl alcohol (EVOH) are examples of petroleum-based polymers that have good oxygen, but poor water vapour barrier properties due to their polar groups, which cause them to be hydrophilic [1]. Hygroscopic materials, such as many biopolymers (especially polymers from natural sources), typically lose their barrier properties at high relative humidity [23]. This is mainly due to the adsorption of moisture from the environment by the biopolymer which causes the polymer structure to swell, resulting in a more porous structure. Although PLA lacks high oxygen and moisture barrier properties as such, it has potential due to the fact that it is recyclable and fulfils the requirements for direct contact with aqueous, acidic and fatty foods [24].

Often single polymer lacks sufficient barrier properties for demanding applications. Multilayer structures are employed as a means of improving barrier performance by combining the desirable barrier properties of individual materials [25]. Traditionally, multilayer structures incorporating aluminium foil and polymer films or metallized aluminium films have been used as barriers for gases, moisture and light [19,20]. However, the key drawback of aluminium foil is its lack of recyclability. The development of replacements for aluminium foil has therefore gained considerable attention, and improved water vapour and oxygen barrier properties for polymers have been achieved using thin SiO_x coatings [21,26].

3. Permeation through polymeric materials

3.1 Mass transfer interactions

In a polymeric packaging system, numerous interactions take place between the packed items and the packaging material. The internal and external environments of a package have different concentrations of specific compounds [27]. The fundamental driving force behind the interactions is chemical potential, which causes molecules to diffuse into and through the packaging material. These molecules tend naturally to move from the side of higher concentration to that of lower concentration. The interactions can be classified into three groups: mass transfer, biological exchange, and energy exchange interactions. This chapter focuses exclusively on mass transfer interactions, as these have the biggest influence on gas and water vapour barrier properties during the shelf-life of a packaged product [27]. Shelf-life refers to the time from fabrication to opening of the package. The mass transfer phenomena are illustrated in Figure 1.

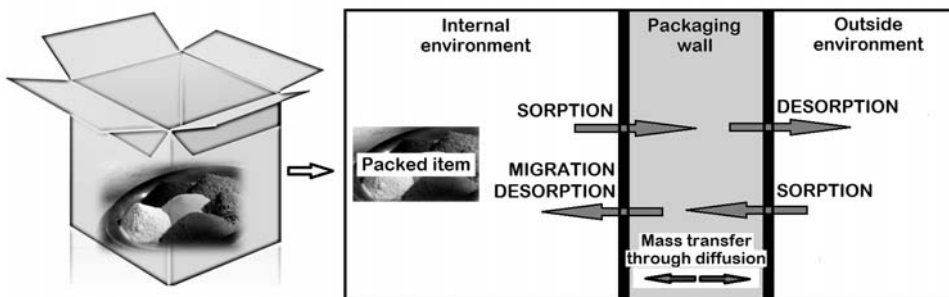


Figure 1. Mass transfer processes through and from a polymeric packaging wall (modified from Hernandez et al. [27]).

3. Permeation through polymeric materials

Mass transfer processes involve the process of permeation. Permeation refers to the movement of molecules between the packed item and the outside environment. Permeation is a complex process which involves sorption of the permeant into the polymer from the high concentration side, diffusion through the material, and desorption from the polymer on the low concentration side. Transfer of permeants between the packaging material and the immediate environment or product includes sorption, desorption and migration. The molecules move to the packaging wall by sorption and out of the packaging wall to the outside environment by desorption. Sorption also describes the dissolution of the permeant molecules at the packaging wall surface prior to diffusing through the wall. Migration refers to the release of migrating species directly from the packaging material into the packed item. In such a case, the packed item must be in direct contact with the packaging wall. In cases where the packaging wall is in contact with the protecting gas, i.e. the protecting atmosphere in the package, the molecules move by desorption from the packaging wall into the gas. Migrating species typically consist of small residues of monomer from the polymerization process, plasticizers or other additives [15], but may also include chemicals from the packaging board, printing inks or the package's sealing adhesives [28,29]. Migration is controlled by diffusion and driven by concentration gradients. If the packed item comes into contact with the packaging material, species may migrate causing possible health risks.

Permeants consist of low molecular weight molecules such as aromatic compounds, oxygen (O₂), carbon dioxide (CO₂) and water (H₂O). The degree of permeation of these molecules through a specific packaging material can be described by the permeability coefficient (*P*) of the material. Diffusion, solubility and permeability are among the parameters used to describe the mass transfer for a specific combination of polymer and permeant [13]. Permeability is an important parameter for measuring the overall transfer rate through a polymer layer. The permeability coefficient can be expressed using a solubility coefficient (*S*) and a diffusion coefficient (*D*) as follows [27]:

$$P=SD=\frac{ql}{At\Delta p} \quad (1)$$

In Equation (1), *S* is a thermodynamic term describing the amount of permeant that can dissolve in the polymer. *D* is a kinetic term indicating the velocity of the permeant in a specific polymer host. In addition, it affects the time required to

reach steady state after diffusion. D is typically described by Arrhenius type equation as follows [27]:

$$D = D_0 \exp(-E_d / kT) \quad (2)$$

The size of the permeant influences the diffusion coefficient. Geometrical and thermal properties also affect the value of D . The size of the permeant and the porosity of the polymeric material will affect D_0 whereas the temperature will affect the exp term. The temperature change can also affect D_0 if temperature changes the porosity of the polymeric material. If D is low, either the permeants are relatively large, the polymer is tightly packed, or the temperature is low [13]. Parameter q is the quantity of permeant transferred by a unit of area (A) in a specific time (t). Parameter l is the thickness of the material, and Δp is the partial pressure difference. Permeability properties are additionally influenced by chemical structure, wettability, degree of free volume in the polymer, crystallinity, orientation, tacticity and crosslinking [30].

Fick's laws of diffusion quantitatively describe the permeation processes [27]. These laws describe the processes by which matter is transported from one part of a polymer film to another as a result of random molecular motions. Fick's first law, i.e. Equation (3) expresses the approximation of the transfer rate (F) of the diffusing substance per unit area in the steady state by D , the concentrations of the permeant molecules at opposite sides at the packaging wall (c_1 and c_2), and the direction of diffusion (x) as follows:

$$F = -D \frac{\partial c}{\partial x} \Rightarrow F = -D \frac{c_1 - c_2}{x} \quad (3)$$

Permeants in polymers often induce interactions. Swelling, plasticizing and even morphological changes can take place. When a large amount of permeant molecules enters the polymer matrix, it swells [31,32]. The swelling of the polymer by the permeant increases the diffusivity. With interacting penetrants the diffusion coefficient can vary as a function of the concentration and time due to swelling and plasticization of polymer [33,34]. This has usually a stronger effect on diffusion than on solubility.

3.2 Oxygen and water vapour barrier measurement

Term ‘barrier property’ refers to a material’s ability to resist the diffusion of specific species (molecules, atoms or ions) into and through itself. The barrier properties of polymeric materials are influenced by a wide range of variables, making conclusions regarding these properties sometimes difficult to draw [33,35]. With polymer films, permeability is affected by the chemical and physical structure of the polymer, the chemical structure and concentration of the permeant, temperature and humidity. In addition, the mechanical strength and barrier properties of amorphous or semicrystalline materials, such as polymers, are affected by their glass transition temperature (T_g) [12]. When the polymer is cooled below its T_g , it becomes hard and brittle. Above T_g the polymer is soft and flexible due to higher mobility of amorphous polymer chains. Many properties of both the polymer and the permeant affect gas and vapour permeation, and these must be taken into consideration when interpreting barrier results. The main factors are presented in Table 1 [36].

Table 1. The main properties of polymers and permeants affecting permeation.

Factor	Effect
Permeant size and shape	Small permeants permeate rapidly
Polarity	Impairs water vapour barrier properties
Polymer crystallinity	Less permeable due to fewer intermolecular spaces
Polymer orientation	The more ‘regular’ the polymer, the less permeable

There are many methods that can be employed for measuring gas and vapour permeability through polymers and polymer-coated boards [27]. Here, the objective was to determine oxygen and water vapour permeation properties measured as transmission rates through the samples.

The prevention of oxygen gas permeation is important because oxygen often permanently damages the quality of the packed item. Oxygen can be strongly and irreversibly absorbed into the polymers present in a food product [37]. The definition of oxygen transmission rate (OTR) is the quantity of O_2 gas passing through an area in a certain time under specified conditions of temperature, humidity and pressure [38]. In this work, the OTR values were measured mainly using Mocon Oxtran 2/20 equipment (Figure 2).



Figure 2. Equipment employed in measuring oxygen transmission rates.

In addition, a Systech M8001 unit was used for comparison of the obtained results. Polymer films and polymer-coated papers and boards were clamped into the diffusion cell, which was purged from residual O_2 using an oxygen-free carrier gas (N_2 added with 2% H_2). The carrier gas was routed to the sensor until a stable zero level was established. Pure O_2 was then introduced into the outside chamber of the diffusion cell. The flux of O_2 diffusing through the sample to the inside chamber was conveyed to the sensor by the carrier gas. The OTR was measured from two to eight parallel samples. The measurements were done using humid gases at room temperature (23 °C, 50% relative humidity) and the results were expressed as $cm^3/m^2/10^5 Pa/day$.

The water vapour transmission rate (WVTR) refers to the amount of water vapour transmitted through an area in a certain time under specified conditions of temperature and humidity. There are many standard procedures for measuring WVTR using gravimetric methods [39–43]. Here, the WVTR was measured using the gravimetric cup method, where the substrate is sealed in an absorbent ($CaCl_2$) containing cell and exposed to humid air in a controlled environment (Figure 3). This is the method most commonly used for determining the WVTR of polymeric materials [44].

3. Permeation through polymeric materials

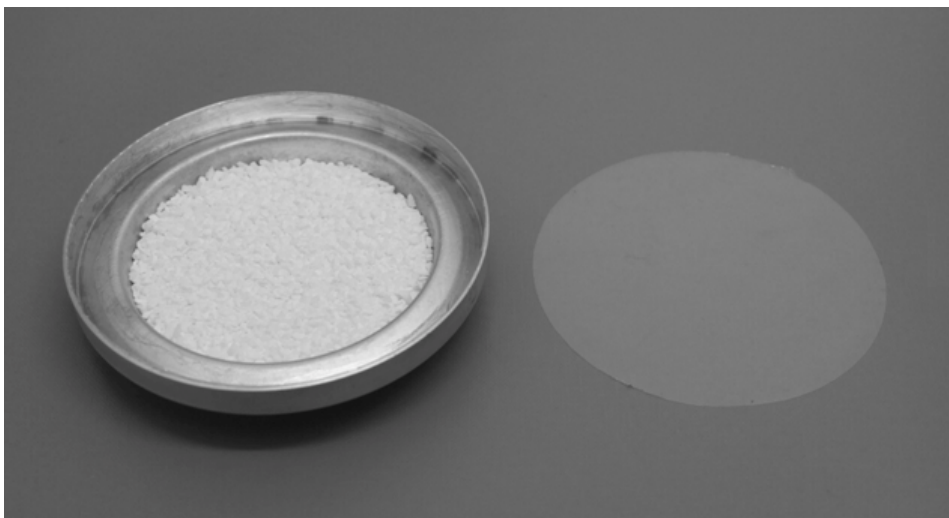


Figure 3. Aluminium dish employed in the determination of WVTR values.

The permeated compounds were collected on the low-concentration side of the cell, and the weight gain was monitored as a function of time. The WVTR values were measured from three to five parallel samples according to the modified gravimetric methods ISO 2528:1995 and SCAN P 22:68 and were expressed as $\text{g}/\text{m}^2/\text{day}$. The $\text{g}/\text{m}^2/\text{day}$ unit is not a standard SI-unit, but its use is justified on the basis that it is widely used in the industry to express WVTR values. The test conditions were $23\text{ }^\circ\text{C}$ and 75% relative humidity. The WVTR of polymeric materials decreases exponentially with increased coating layer or film thickness if cracking of the barrier layer does not occur. Permeation takes place mainly through coating defects such as cracks, voids and pinholes or through the amorphous regions of polymer films [45]. In addition to layer thickness, the WVTR is affected by temperature and humidity, with the WVTR increasing with increased temperature and humidity [13]. The permeation process is also affected by the surface chemistry. Less polar surfaces are considered to improve water vapour barrier properties, as adsorption of polar water molecules is more difficult.

3.3 Reliability of OTR and WVTR measurements

The reliability of the obtained OTR and WVTR values may be hindered by a number of general sources of error, as described below. To minimize the impact of these errors, two to eight parallel samples were always fabricated and characterized. The number of parallel samples characterized depended on the variation of the obtained OTR and WVTR values between parallel samples. For this reason, the standard deviation value was also determined together with the average OTR and WVTR values obtained for an individual sample. When a low standard deviation value was obtained, the properties of the parallel samples were considered to be homogenous and the number of parallel measurements was smaller.

The main sources of error in OTR and WVTR measurements are due to the properties of the substrates. Permeability properties are greatly affected by the thickness and the coat weight of the sample [33,35]. In addition, the properties of the polymer itself and the coating method used influence the repeatability of the results. The coat weight and thickness of different polymeric substrates can vary greatly even within the same polymer sheet. The impact is usually greater when the substrates have been fabricated, for example, by a lab sheet coater or by solution casting. Commercial polymeric products are considered to be more homogenous, diminishing the variation of barrier properties between parallel samples. Sample heterogeneity increases mechanical stress in the polymeric material, possibly leading to increased numbers of defects. This may cause internal cracking of the sample material during measurement. In addition, to gain good repeatability of results, i.e. low standard deviation, carefulness in handling the samples is crucial due to the sensitivity of both the polymeric material and the thin Al₂O₃ coating. It was noted, that board-based samples were easier to handle due to the stiff base material.

The measurement conditions also affect the repeatability of the results, making stable conditions a necessity. However, some variation in temperature (23 °C ± 0.1 °C) and humidity (relative humidity % ± 2–5%) may nevertheless occur, causing the polymer to shrink or swell. In WVTR measurement by the cup method the sample is sealed against the aluminium dish with hot wax. This can induce thermal stresses in some polymers. In addition, air escaping from the dish may cause bubbles in the wax layer, and impurities or hot wax may lead to poor adhesion between the wax seal and the aluminium dish. Such samples are to be rejected. In addition, as the WVTR measurement is based on change in

3. Permeation through polymeric materials

weight, there is a risk of error during weighing. Depending on the precision of the weighing appliance, a very low WVTR may require prolonging the weighing intervals. On the other hand, an extremely high WVTR can cause saturation of the salt within the dish, thus limiting the measurable values. In OTR measurement, however, side leakage, often referred to as the 'by-pass stream' or 'zero', can be determined. When measuring the properties of relatively good barrier materials, the detection limits of the measurements ($0.01 \text{ cm}^3/\text{m}^2/10^5 \text{ Pa/day}$ for OTR, $\sim 1 \text{ g/m}^2/\text{day}$ for WVTR [36]) set some limitations. In addition, it is beneficial to measure, for example, polymer-coated board or paper with the polymer layer facing the carrier gas stream. Due to the porous structure of the fibrous material the reverse set-up could cause lateral leakage of oxygen from the surrounding atmosphere along the material to the inside chamber. In addition, the carrier gas flow can pick up permeant molecules from the porous structure. In order to avoid leakage, the sample is sealed against the test cell with vacuum grease. However, this grease can spread onto the sample and affect the polymer properties. Based on the fact that the sources of errors described here were taken into account during this work, the OTR and WVTR values obtained are considered reliable.

Instead of using the cup method, the WVTR values could be measured with similar equipment as the OTR values. With this kind of equipment, the detection limit for water vapour can be as low as $5 \cdot 10^{-4} \text{ g/m}^2/\text{day}$ thus enabling the study of high barrier materials. As the minimum detectable WVTR with the cup method is $\sim 1 \text{ g/m}^2/\text{day}$, even with a perfect barrier the result would not be better. This was the main limitation concerning the use of the cup method.

The main difference between the cup method and several automated systems is the means of detection. While cup method is a gravimetric method, the others are usually based on chemical detection of water molecules. In addition, the automated systems utilize gas flows on both sample surfaces. The advantage of continuous gas flow is a constant concentration gradient over the sample. In cup method the salt absorbs the moisture and becomes eventually saturated. On the other hand, a continuous carrier gas flow can affect the results in the case of porous materials. Measuring low WVTR values is easier with an automated system, while the cup method allows a wide test range and several parallel measurements with lower investment costs. This is the case especially when dealing with moderate test conditions. High test temperature and humidity can cause softening of the wax sealant and fast saturation of the salt.

4. Deposition of high-quality thin-film barriers

4.1 Conventional barrier coatings

The oxides SiO_x and AlO_x are commonly used barrier coating materials for polymers in packages. SiO_x , in particular, has been used to replace aluminium foil in applications such as fibre-based packages for dry food mixes, drinks, sauces and seasonings, polymer composite cans, and packages for snacks, coffee and pet foods. Coatings of AlO_x have been used in applications, such as laminated heat-sealable packages for snack foods.

Industrial thin SiO_x coatings for packages are mainly fabricated using vacuum deposition techniques, such as sputtering, evaporation or plasma enhanced chemical vapour deposition (PECVD) [19,46]. In addition, plasma deposition has been used to apply films roll-to-roll from liquid precursors at atmospheric pressure with reasonable high speed. One configuration is that the plasma nozzles are moving in x-direction as the sample moves in y-direction. The distance from the sample to the nozzle head can be kept constant. Liquid precursor is atomized into droplets and sprayed directly into the plasma and then onto the substrate. The atmospheric plasma deposition technique for fabrication of barrier coatings has not yet been employed for industrial use. In PECVD the chemical reactions of vapour precursors take usually place on a batch-type vacuum reactor. However, the PECVD can also be employed also as roll-to-roll process at atmospheric pressure [47].

The sputtering, evaporation and PECVD techniques have been used to fabricate coatings with thicknesses of 10–100 nm on polymers. Of these techniques, the PECVD deposition technique gives the best barrier properties [19]. The fabricated SiO_x coatings are transparent, water-resistant and, in terms of barrier properties, comparable to metallic aluminium coatings. The problem

4. Deposition of high-quality thin-film barriers

with SiO_x coating is its poor mechanical resistance, which can be solved by varnishing or laminating [21]. The barrier properties of thin-film-coated materials depend strongly on the properties of the polymer. Gas permeation through thin-film-coated polymer is also affected by defects in the inorganic layer [48–53].

Besides the techniques mentioned above, a number of other deposition techniques can be utilized to fabricate thin SiO_x , AlO_x or metallic aluminium coatings onto polymers for various applications [21,54–75]. Relevant techniques for the present work (magnetron sputtering (MS), electron beam evaporation (EBE), sol-gel (SG) deposition, and atomic layer deposition (ALD)) are well described in literature [69–75], and in the case of Al_2O_3 coatings, in Publication I. The sol-gel coating (SG) technique as a wet chemical method differs from other, vacuum-based techniques discussed here. The technology is simple and can be applied as several different variants. However, industrially, these layers are typically thick, morphologically different and cannot be considered as thin film technology.

4.2 Atomic layer deposition (ALD)

The ALD technique is considered to be an advanced version of the CVD technique. There are many drawbacks with conventional CVD when fabricating thin films on polymeric substrates. The operating temperature range for a typical CVD process is around 300–500 °C, which is too high for sensitive polymers as it exceeds their melting point. In addition, with CVD the use of precursor gases cannot be effectively controlled and thus the thickness of the film cannot be tightly controlled. Some drawbacks, such as high deposition temperature, can be somewhat overcome with plasma-enhanced CVD. However, the film quality is typically poorer when the CVD or PECVD process is applied compared to ALD. CVD and PECVD leave defects and pinholes in the inorganic film [48,49,53,76]. The advantages of the ALD technique are the possibility to employ relatively low deposition temperatures and yet still grow thin films in a highly controlled manner. With ALD, the thin film grows layer-by-layer based on self-limiting gas-solid reactions. This technique is well suited to producing high-performance gas diffusion barrier coatings on porous materials as it allows the preparation of dense and pinhole-free inorganic films that are uniform in thickness even deep inside pores, trenches and cavities of various dimensions [63,68,77,78]. The layer-by-layer film growth and the surface saturation through chemisorption

enables precise control of the film growth and thickness [79,80]. This is the main difference between ALD and CVD; in CVD chemisorption is also applied but without surface saturation, making the growth primarily controlled by the dosage of the precursor.

The chemical reactions take place in a vacuum chamber. The precursors are fed alternately into the chamber in vaporized form. The precursor pulses are separated by an inert gas purge. During the purge, unreacted excess precursor molecules are removed together with the gaseous by-products. After the purge, the surface is saturated with the first precursor and can react with the second one. Finally, the surface is purged again with inert gas and the ALD cycle is completed. The ALD technique was developed in the 1970s in Finland by Suntola and Antson [81]. The first applications for ALD were large-area flat panel electroluminescence displays. Nowadays a wide range of ALD-grown materials and applications have been developed, from catalysts to electroluminescent displays to microelectronics and beyond [82].

4.3 The ALD process for Al₂O₃ coatings

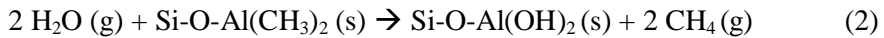
The focus of the present work was to grow Al₂O₃ films from trimethylaluminium (TMA; Al(CH₃)₃) and water (H₂O) or ozone (O₃). The TMA-H₂O process is considered to be a near-ideal ALD process and the reaction mechanisms are well understood. The chemical reactions involved in the formation of an Al₂O₃ layer on a silicon wafer substrate using H₂O and O₃ as an oxygen source are briefly discussed in the following [81,83–99]. Al₂O₃ is non-toxic and non-flammable and has a melting point of 2050 °C [90]. In controlled conditions Al₂O₃ forms highly even and uniform surface films, and is for this reason considered to be an excellent diffusion barrier. The growth of Al₂O₃ films is relatively straightforward by means of ALD. In this chapter, the fundamental reactions taking place during the TMA-H₂O process on smooth surfaces such as silicon wafer are briefly described.

Water vapour in the air is adsorbed onto most surfaces, forming hydroxyl (OH) groups. On silicon wafer, water vapour forms Si-O-H (s) groups. When the silicon wafer is placed in an ALD reactor chamber and TMA is pulsed into the chamber, the TMA (g) reacts with the Si-O-H (s) groups on the surface of the silicon as shown in reaction (1). Methane (CH₄ (g)) is simultaneously produced as a by-product.

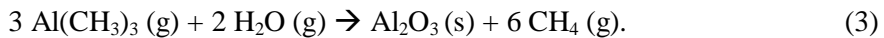
4. Deposition of high-quality thin-film barriers



The reaction continues until the surface is passivated with $\text{Si-O-Al}(\text{CH}_3)_2 (\text{s})$. TMA does not react with itself, which terminates the reaction to one layer. The deposition continues by pulsing H_2O into the reaction chamber. H_2O reacts with the methyl groups (CH_3) forming O-Al bridges and OH^- groups as shown in reaction (2). Again, CH_4 is produced as the by-product, and pumped away.

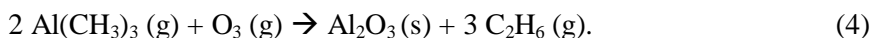


The excess H_2O again does not react with the OH^- groups, thus terminating the reaction to one atomic layer. After these two half reactions, one ALD cycle is completed. The whole ALD cycle can be described as reaction (3):



The number of surface OH^- -groups influences the number of chemisorbed species. Although considered near-ideal, there are some drawbacks to the TMA- H_2O process. Steric hindrance of precursors can influence on the film growth. In addition, the applied layer does not always form a fully smooth surface and the layer can have islets [80].

The use of O_3 instead of H_2O as the oxygen source is in some cases desired due to the higher activity of O_3 in ligand elimination [91]. Another reason for favouring O_3 is that it does not absorb as easily as H_2O into the reactor walls, thus facilitating purging. Due to these properties, better quality films could be obtained. On the other hand, a morphological characterization study [91] has shown that O_3 can also yield lower-quality films than H_2O . The films can be less dense and rougher, especially at low growth temperatures. When O_3 is used as the oxygen source for the preparation of Al_2O_3 films, the following reaction (4) is suggested to take place [92]:



The complex reaction mechanism and the use of O_3 in the fabrication of Al_2O_3 layers have been previously studied mainly for the needs of microelectronic applications [89,93–99]. It is assumed that during the O_3 pulse, O_3 decomposes into O_2 and monoatomic O which is the active species [91]. The efficiency of

this decomposition reaction is believed to be temperature-dependent [93]. The study of O₃ decomposition [91] showed that the use of O₃ could yield lower growth per cycle (GPC) rates compared to the corresponding H₂O process. The different growth mechanism and high reactivity of O₃ may result in a different film structure.

In a work by Goldstein *et al.* [98], the TMA-O₃ process at 90–377 °C was studied by in-situ measurements. It was revealed that CH₄ (g) and CO₂ (g) were the reaction by-products. In addition, it was recently noticed that besides CH₄ (g) and CO₂ (g), H₂O is also produced as a by-product in this process [99], and the researchers proposed a reaction mechanism where TMA chemisorbs on the surface, releasing CH₄ (g), and the following O₃ pulse partly combusts the remaining CH₃ (g) ligands to form CO₂ (g) and H₂O (g).

4.4 ALD fabricated barrier coatings

Applications for ALD-grown barrier coatings have previously been mostly related to electronics. In addition, the ALD-coated polymeric substrates have mainly been non-biodegradable. The most common ALD-grown gas and water vapour barrier material has been Al₂O₃ [63–65,68,77,100–102]. In these studies the Al₂O₃ films have mainly been fabricated using the TMA-H₂O process, but studies also show that O₃ can also be used as the oxygen source when depositing on polymers [103].

The advantages of ALD-grown Al₂O₃ coating are superior moisture protection and relatively low deposition temperature. For the purposes of protecting electronic parts, water vapour transmission rates of the order of $1 \cdot 10^{-3}$ g/m²/day and oxygen transmission rates below $5 \cdot 10^{-3}$ cm³/m²/10⁵ Pa/day were reported for less than 25 nm thick Al₂O₃ coatings on synthetic, non-biodegradable polymers [64]. In addition, Park *et al.* [77] reported a water vapour transmission rate of 0.03 g/m²/day at 38 °C and 100% relative humidity for an ALD-grown Al₂O₃ barrier that was 30 nm thick and deposited on both sides of a poly(ethersulfone) substrate, whereas Carcia *et al.* [68] showed that 25 nm thick Al₂O₃ barrier films on poly(ethylene naphthalene) substrates can have a water vapour transmission rate of less than $1 \cdot 10^{-5}$ g/m²/day. These results are, however, only partly comparable with the results presented in the present study, in which the substrates are mainly biopolymeric materials.

The focus of this work is on the novel benefits of ALD-grown films as oxygen and water vapour barrier materials. Prior to this thesis, there have been no

4. Deposition of high-quality thin-film barriers

studies covering a wide range of different bio-based substrates combined with less than 100 nm thick ALD-grown Al_2O_3 layers. The barrier level required for food and pharmaceutical packaging applications is not as low as that needed for the protection of electronics. Barrier requirements for sensitive food products presented in Figure 4 have been reported to vary between 0.01 to 100 $\text{cm}^3/\text{m}^2/10^5$ Pa/day for OTR and 0.01 to 100 $\text{g}/\text{m}^2/\text{day}$ for WVTR [104].

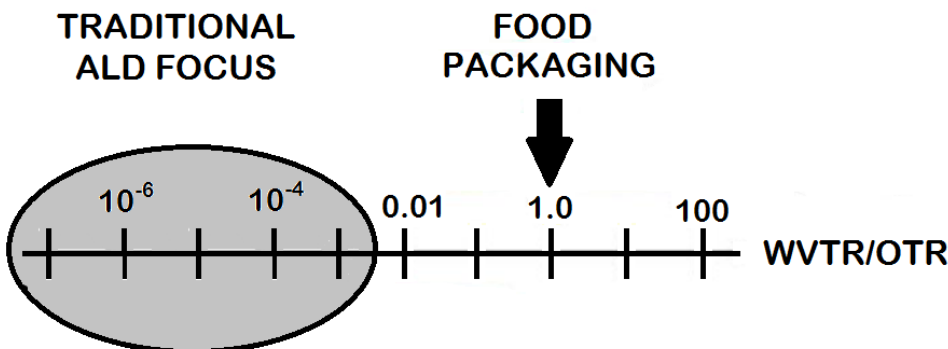


Figure 4. The oxygen and water vapour barrier level required for commercial applications (modified from Beneq Ltd marketing material).

The polymeric substrate materials employed in the present work are temperature-sensitive, which in practice makes thin layer formation more demanding, thus essentially limiting the number of possible ALD processes and ALD-grown coatings which can be applied on these materials as barrier layers. In addition, due to dust and other particles on the substrates, the ALD coatings on polymeric materials cannot be fabricated in a cleanroom environment. This also limits the use of impurity-sensitive ALD processes.

In this thesis the ALD-grown coating material was Al_2O_3 , although other ALD-grown oxides, such as silicon dioxide (SiO_2) [105] and titanium dioxide (TiO_2) [103], could also be employed as barrier layers. In addition, SiO_2 has been grown as a part of a nanolaminate structure. Nanolaminates are structures made up of alternating layers of different materials, and the properties of the nanolaminate usually differ from the properties of the individual materials used to build the nanolaminate structure. Nanolaminates using SiO_2 and Al_2O_3 have been found to improve barrier properties [65]. In addition, tungsten and Al_2O_3 nanolaminates have been grown for thermal barrier purposes [106].

Pure tungsten has also been deposited at 80 °C as gas diffusion barrier layers on polymer films and polymer particles [107]. Other metals, such as iridium, have been employed as copper diffusion barriers to prevent diffusion into silicon in copper interconnected structures [108]. ALD-grown nitrides, such as tungsten nitride (WN) [109], niobium nitride (NbN_x) [110], tantalum nitride (TaN_x) [111] and zirconium nitride (ZrN) [112] have been shown also to effectively prevent copper diffusion.

The most recent development in polymer related ALD research concerns molecular layer deposition (MLD). With MLD, organic-inorganic hybrid films can be grown by a sequential, self-limiting surface chemistry process by using an inorganic precursor, such as TMA, and an organic precursor, such as ethylene glycol [113]. These could have potential as barrier materials, especially in applications that demand flexibility.

5. Experimental

5.1 Objectives

The first task of this thesis was to study whether high-quality barrier coatings with similar or better barrier properties could be fabricated on polymeric materials by utilizing thin-film deposition methods other than ALD. The hypothesis was that of all thin-film deposition techniques, ALD provides the most defect-free films. Thereafter, the task was to perform the ALD coatings at 80, 100 or 130 °C on biopolymeric materials. This temperature range was selected based on the fact that most biopolymers are known to be temperature-sensitive. ALD-grown Al₂O₃ coatings were deposited onto several polymeric substrates at target thicknesses ranging from 10 to 900 nm. The ALD process parameters (most suitable oxygen source, deposition temperature, and film thickness) were optimized for these biopolymers. This enabled the investigation of the oxygen and water vapour barrier properties of the Al₂O₃ coatings on polymer films and polymer-coated papers and boards. An additional objective of the study was to improve the barrier properties of ALD-coated materials by employing treatments and coatings on the substrates prior to the ALD process.

5.2 Substrate materials

The objective was to study the influence of thin Al₂O₃ coatings on the barrier properties of polymeric materials, concentrating mainly on bio-based substrate materials. To focus on the impact of the coating, commercial polymeric materials were chosen as the main substrates. Commercial products have more homogenous surface chemistry, thus minimising the variation in properties between parallel samples. Commercial paperboards (provided by Stora Enso Oyj) with bio-based polylactide (B(PLA)) coatings on one side were used as the

main substrate materials. A wide range of other commercial polymer films were also used as substrate materials. In addition, non-commercial biopolymer materials were also used as substrate materials in order to widen the scope of investigation of potential ALD-coated materials. The materials employed are presented in Table 2. It should be noted that the barrier properties of the pristine substrate materials could not be compared as such due to differences in polymer layer thickness, coat weight, coating and film fabrication processes, possible additives such as plasticizers in the substrate materials, the base material type, e.g. paper and board, and surface roughness values.

Table 2. Packaging materials employed in the present work as substrates.

Code	Description	Commercial	Publication
B1(PLA)	Poly lactide-coated board; PLA 35 g/m ² on board 310 g/m ²	x	I, III, IV
B2(PLA)	Poly lactide-coated board; PLA 35 g/m ² on board 210 g/m ²	x	II, III
B3(PLA)	Poly lactide-coated board; PLA 27 g/m ² on board 210 g/m ²	x	III, V
B(GGM)	Galactoglucomannan-coated board; GGM approx. 9 g/m ² on pigment-coated board 200 g/m ²		III
B(PE)	Low-density polyethylene-coated board; LDPE 15 g/m ² on board 210 g/m ²	x	I–V
P(UNC)	Uncoated paper; 80 g/m ²	x	II
P(PIG)	Pigment-coated and calendered paper; 60 g/m ²	x	II
P(LDPE)	Low-density polyethylene-coated paper	x	II
PLA1	Poly lactide film; 20 µm	x	III, VI
PLA2	Poly lactide film; 75 µm	x	III
PLA3	Poly lactide film; 25 µm	x	II
NFC	Nanofibrillated cellulose film; approx. 60 g/m ²		III
PHB	Polyhydroxybutyrate film; 180 µm	x	III
Pectin	Pectin film; 160 µm (solution-casted)		III
PEN	Polyethylene naphthalene film; 50 µm	x	II
PP	Polypropylene film; 30 µm	x	II
PET	Polyethylene terephthalate film; 50 µm	x	II

5.3 Thin-film depositions

Besides ALD, other thin-film deposition techniques were employed in the present work, including magnetron sputtering (MS), electron beam evaporation (EBE) and sol-gel (SG) coating. These techniques were chosen for the comparison of the ALD technique as they are widely studied and also used in commercial barrier applications. In addition, the chosen deposition methods are thought to be more cost-efficient and faster than conventional batch-type ALD. The techniques also enabled the fabrication of thin Al_2O_3 coatings at relatively low temperature. The depositions were made at $100\text{ }^\circ\text{C}$ on B1(PLA). The deposition processes are described in detail in Publication I.

The ALD coatings were mainly done with a SUNALE R-200 reactor from Picosun presented in Figure 5. The target thicknesses of the fabricated Al_2O_3 coatings (25–100 nm) were as similar as possible for all of the thin-film deposition techniques used.



Figure 5. During this thesis VTT invested in a new SUNALE R-200 ALD-reactor which is not limited by clean room conditions.

Due to differences in the controllability of the processes, some variation between sample thicknesses did nevertheless occur. The best control of Al_2O_3 coating thickness was achieved with the vacuum-based methods (MS, EBE and ALD). In contrast, precise thicknesses were difficult to achieve using SG coating due to the nature of the coating application method (spraying). For example, with 100 nm Al_2O_3 coatings, the thickness varied 10–15% from the target thickness. Of the studied methods, ALD enabled the most precise control of film thickness. The levels of control and film quality enabled by ALD are unobtainable with the other studied thin-film deposition techniques. Furthermore, it should be noted that purely inorganic Al_2O_3 coatings are not possible to fabricate using the SG technique due to the presence of organic molecules from the precursor solution in the deposited film. In addition to Al_2O_3 coatings, pure aluminium films were also grown using the MS technique. This was included in the study because metallic Al, as a thicker film, is considered to be a high performance barrier.

5.4 Pre-treatments for polymeric materials

Pre-treatments (corona and thermal) were employed to improve the surface properties of the polymeric materials prior to the ALD process. Corona treatment is an electrical process utilizing ionized air to increase the polarity of the surfaces by oxidation. The surface is bombarded with O_3 , O_2 and free O radicals in order to increase the surface energy and lead, potentially, to higher quality coatings. In this work, the hypothesis was that the increased polarity could increase adhesion between the polymer surface and the first ALD-grown Al_2O_3 layer, possibly enabling the growth of a more uniform Al_2O_3 coating. The corona treatment was performed on B(PE) and B1(PLA) substrates using a widely used method [114]. After the corona treatment, the substrate materials were coated with Al_2O_3 at 100 °C.

The barrier properties of polymeric films or coatings are affected by their chemical structure and morphology [115]. The impact of thermal treatments on barrier properties has been previously studied [116,117]. With extruded PLA-coatings, polymer crystallinity has been found to be inversely related to the difference between the melt temperature and the quenching temperature [118] leading sometimes to formation of a totally amorphous structure. Diffusion of gas permeants occurs through the amorphous regions, while crystalline regions are more or less impermeable. The WVTR of PLA decreases with increasing crystallinity [119]. Drawing on these findings, the idea of the current work was

5. Experimental

to utilize the ability of thermal pre-treatment to increase crystallinity and thus to improve the barrier properties of the substrate prior the Al_2O_3 coating and possibly to even out the surface chemistry and topography due to more ordered polymer structure. The B3(PLA) substrate was thermally treated in a convection oven at 130 °C for 4, 9 or 16 minutes followed by quenching at room temperature. After thermal treatment, the substrate materials were coated with a 25-nm-thick Al_2O_3 layer grown by ALD at 80 °C.

5.5 Pre-coatings prior to ALD- Al_2O_3 coating

Besides pre-treatments, the barrier properties of polymeric materials can be improved by pre-blocking the largest pinholes in the substrate using a coarser method than ALD. In addition, pre-coatings can be utilized to alter the surface topography prior to ALD. In this study, the pre-barrier layers were generated using two separate methods; layer-by-layer (LbL) deposition of polyelectrolytes [120,121], and sol-gel deposition of an epoxy-coating (epoxy-SG). The epoxy-SG coatings with a target coat weight of 2 g/m² were prepared using 3-(trimethoxysilyl)propyl glycidyl as the epoxy source, ethanol as a solvent, and water as an initiator for the hydrolysis and condensation reactions. The coatings were applied on corona pre-treated B2(PLA) surfaces using a spraying method, dried at 120 °C and further coated with an ALD-grown Al_2O_3 layer at 80 °C. A corona treatment unit (ET1 from Vetaphone) with a treatment time of 60 seconds was used for better wetting and adhesion properties between the coating and the substrate.

The polyelectrolyte multilayer (PEM) films from sodium alginate (ALG) and chitosan (CHI) were fabricated according to the LbL method on PLA1. The samples were coated with an ALD-grown Al_2O_3 layer at 100 °C.

5.6 Sample characterizations

Thermogravimetric (TG) analyses were employed to reveal the possible thermal limitations of different polymer coatings for use as substrates for thin-film depositions. Scanning electron microscopy (SEM) and atomic force microscopy (AFM) were used to image surfaces and their roughness. In addition, AFM acquires information on surface topography, friction, and adhesion [122]. For Publication II, the SEM employed was a Hitachi S-3400 N VP-SEM with an operating voltage of 15 keV, and for publications III and VI a JEOL JSM-

7500FA was used. In Publication II, a multimode scanning probe AFM (Nanoscope III from Digital Instruments Inc.) was employed, and in publications I, III and V an AFM XE-100 (Park Systems with 905-ACTA cantilever) was used. Non-contact ‘tapping’ mode was used for the AFM imaging [123,124].

The thin-film film growth rates and actual film thicknesses on the polymeric substrates could not be directly measured. Instead, the film thicknesses and the ALD layer growth rates were estimated with a Nanospec AFT4150 reflectometer, ellipsometer or UV-Vis spectrophotometer from films grown on a silicon Si(100) wafer. The surface coverage of ALD-grown Al₂O₃ layers were determined by X-ray photoelectron spectroscopy (XPS) analyses. The amount of Al in the Al₂O₃ layers was determined by inductively coupled plasma atomic emission spectroscopy (ICP-AES) analysis.

The effects related to pre-treatments and pre-coatings were characterized by contact angle (CA) and surface energy measurements. The CA measurement is the oldest and still the most popular method of evaluating wettability [125]. Wide-angle x-ray scattering (WAXS) was utilized to study the level of crystallinity of the substrates due to its allowance of the characterization of distinctions between different polymers [126]. The molecular weights of the components in the PEM film were determined by viscosity and density measurements. The Mark–Houwink equation (4) gives a relation between intrinsic viscosity $[\eta]_{in}$ and molecular weight M_v by utilizing the Mark–Houwink parameters K and a [127–131].

$$[\eta]_{in} = KM_v^a \quad (4)$$

Although many characterization methods were employed during the research, the emphasis was on oxygen (OTR) and water vapour transmission (WVTR) rates. Table 3 presents the main characterization methods employed and the information obtained.

5. Experimental

Table 3. Characterization methods applied and the information obtained.

Method	Information obtained	Publication
Thermogravimetric analysis (TG)	Polymer degradation temperature	II
Scanning electron microscopy (SEM)	Structure and thickness of the Al ₂ O ₃ coating	II, III, VI
Atomic force microscopy (AFM)	Structure, morphology and roughness of the polymeric material prior to and after Al ₂ O ₃ coating	I–III, V
Scanning ellipsometry	Al ₂ O ₃ coating thickness (20–100 nm)	I, II, VI
UV/Vis spectrophotometer	Al ₂ O ₃ coating thickness (50–100 nm)	I, III, V
Reflectometer	Al ₂ O ₃ coating thickness (25–100 nm)	I, III–VI
X-ray photoelectron spectroscopy (XPS)	Polymer surface coverage by the Al ₂ O ₃ coating	II
Inductively coupled plasma atomic emission spectroscopy (ICP-AES)	Amount of Al in the Al ₂ O ₃ coating	I
Contact angle (CA)	Surface wetting	III–VI
Surface energy (γ_s)	Surface polarity	III–V
Wide-angle x-ray scattering (WAXS)	Surface morphology	V
Microviscometer and density meter	Molecular weight of the polyelectrolyte	VI
Oxygen transmission rate (OTR)	Oxygen barrier property of the sample	I–V
Water vapour transmission rate (WVTR)	Water vapour barrier property of the sample	I–VI

6. Results and discussion

6.1 Characterization of thin Al₂O₃ coatings grown on polymers

6.1.1 Properties of polymeric substrates

The main scope of the present work was to investigate whether ALD-grown Al₂O₃ coatings could extend the use of polymeric materials as oxygen and water vapour barriers. The substrate materials were mainly bio-based, although some synthetic, non-biodegradable polymeric materials were also investigated. It should be noted, that the pristine substrates could not be compared as such. The surfaces of different polymeric materials vary greatly, due mainly to different coating methods and coat weights and the effect of these on material thickness and surface smoothness. Figure 6 shows AFM images of the surfaces of the two most studied substrate materials in publications related to this thesis, B(PE) and B1(PLA).

6. Results and discussion

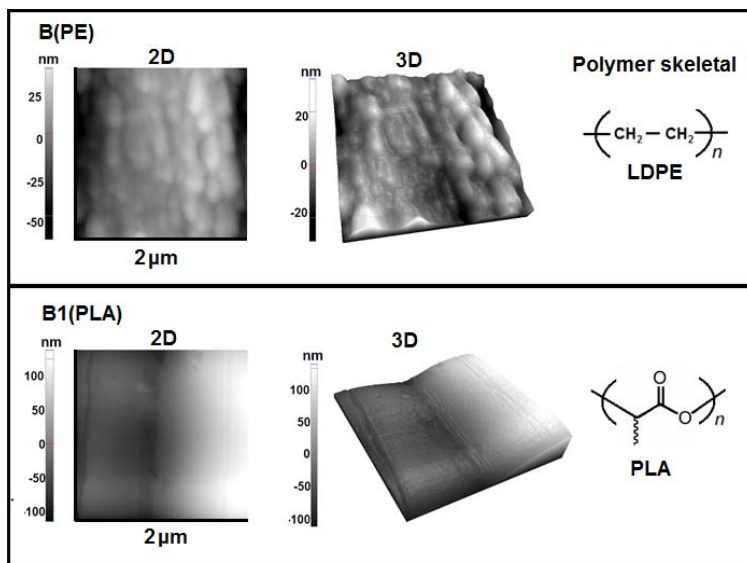


Figure 6. AFM images (2D and 3D) of LDPE-coated and PLA-coated board.

Thermogravimetric (TG) analysis was employed to investigate the degradation temperature of the different polymers and polymer-coated papers and boards. This was done in order to investigate whether these materials could be used as substrates in thin-film depositions. The TG analysis employed on the majority of the polymeric materials confirmed that the materials tested did not degrade thermally at the temperatures used in the low-temperature ALD experiments, i.e. below approximately 150 °C.

The resultant TG curves in air and in nitrogen atmospheres are presented in Figure 7. The polymeric materials behaved quite similarly. Degradation occurred at a slightly higher temperature in nitrogen atmosphere compared to air. The first endothermic step, water removal, began at room temperature and continued at higher temperatures. The materials decomposed in a single step at temperatures ranging from 300 to 450 °C. Decomposition in nitrogen was not completed for PEN and PET at 450 °C. The final step, carbon combustion, was highly exothermic. This was naturally observed only in air, i.e. in the presence of oxygen.

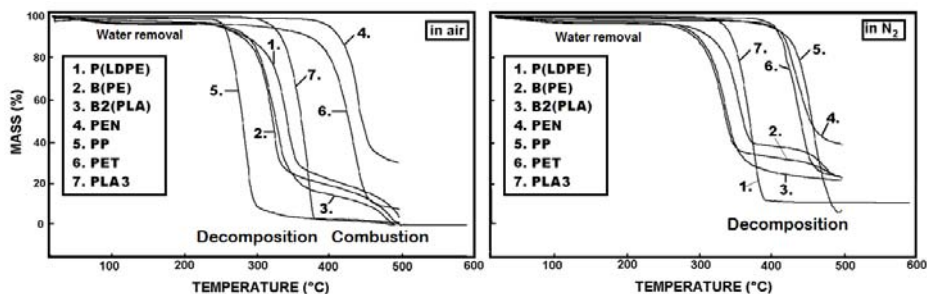


Figure 7. TG curves recorded for polymeric materials in air and nitrogen atmospheres.

6.1.2 Comparison of barrier properties obtained by different thin-film deposition techniques

It is evident based on earlier studies [63–65,68,77,100–102] that ALD-grown Al_2O_3 coating significantly improves the oxygen and water vapour barrier properties of various conventional i.e. petroleum-based polymer films. In this study, however, the scope was on bio-based substrates. It was observed that although the barrier properties were improved with Al_2O_3 coatings fabricated by all of the compared thin-film deposition techniques, with the thinnest coatings (25 nm), the improvement was the largest with the ALD technique (Table 4). This is mainly due to the nature of the ALD process. The other thin-film deposition techniques leave defects and pinholes in the Al_2O_3 coating but the ALD technique produces pinhole-free coatings even on porous materials in a highly controlled manner.

Table 4. Comparison of deposition techniques for the production of efficient barrier coatings.

OTR ($\text{cm}^3/\text{m}^2/10^5 \text{ Pa/day}$)				
Sample	ALD	MS	EBE	SG
B1(PLA) uncoated	420 ± 10	420 ± 10	420 ± 10	420 ± 10
B1(PLA) + 25 nm Al_2O_3	20 ± 3	75, 245*	150 ± 10	460 ± 10
B1(PLA) + 50 nm Al_2O_3	60 ± 5	25, 145*	300 ± 140	400 ± 10
B1(PLA) + 100 nm Al_2O_3	200 ± 40	65 ± 1	210 ± 15	370 ± 10
B1(PLA) + 50 nm Al	-	26 ± 1	-	-
WVTR ($\text{g}/\text{m}^2/\text{day}$)				
B1(PLA) uncoated	64.9 ± 1.6	64.9 ± 1.6	64.9 ± 1.6	64.9 ± 1.6
B1(PLA) + 25 nm Al_2O_3	1.4 ± 0.2	11.0 ± 0.5	25.9 ± 2.7	62.5 ± 1.0
B1(PLA) + 50 nm Al_2O_3	1.8 ± 0.5	0.5 ± 0.1	21.8 ± 4.2	62.3 ± 1.9
B1(PLA) + 100 nm Al_2O_3	29.1 ± 5.1	1.9 ± 0.6	21.6 ± 7.1	62.0 ± 0.6
B1(PLA) + 50 nm Al	-	1.3 ± 0.5	-	-

*For samples coated with 25 nm or 50 nm thick MS- Al_2O_3 layers the standard deviation for OTR could not be calculated due to high variation in the values obtained.

Based on the results, a thin Al_2O_3 coating had a positive effect on both the OTR and WVTR values. Most impressively, when coating B1(PLA) with a 25-nm-thick Al_2O_3 layer by means of ALD, both the OTR ($20 \text{ cm}^3/\text{m}^2/10^5 \text{ Pa/day}$) and WVTR ($1.4 \text{ g}/\text{m}^2/\text{day}$) values were excellent. In terms of oxygen barrier properties, this sample performed better than an equivalent sample coated with 50 nm thick metallic aluminium using the MS technique ($26 \text{ cm}^3/\text{m}^2/10^5 \text{ Pa/day}$). The results imply that a 50-nm or thicker ALD-grown layer cracks more readily than a 25-nm-thick layer. These results justify the use of 50 nm or thinner ALD-grown Al_2O_3 coatings in further studies.

6.2 ALD growth process for Al_2O_3 coatings on polymeric materials

A second task related to thin-film deposition was to optimize the Al_2O_3 process by means of ALD for a range of non-biodegradable and bio-based temperature-sensitive substrates. The main focus was nevertheless on bio-based substrates. In the preliminary experiments, the ALD process parameters, i.e. deposition temperature (80, 100 or 130 °C) and choice of oxygen source (H_2O or O_3), were

investigated. Interestingly, the growth per cycle (GPC) values for the H₂O and O₃ processes were found to be nearly identical, i.e. 0.1 nm/cycle (as measured for films grown on silicon substrates). This disagrees somewhat with the findings of Elliot *et al.* [91], who report lower GPC values for the TMA-O₃ process compared to the TMA-H₂O process. It seems that here the O₃ gas might have been wet; note that the H₂O present may act as a catalyst for the reactions during the TMA-O₃ process, increasing the GPC value. According to Elliot *et al.* [91], the combination of both O₃ and H₂O could increase GPC closer to the GPC value of films fabricated using H₂O alone as the oxygen source. It should be emphasized that due to the different surface chemistries of different polymers, the actual growth rates may deviate from that determined for Al₂O₃ coating on silicon wafer [63,132].

The results obtained by ellipsometry indicate that for relatively smooth polymer films with low anisotropy, the thickness of the ALD-grown Al₂O₃ coating is close to the thickness determined on silicon wafer. However, other studies have shown that when coating polymers with ALD-grown Al₂O₃ layers, a nucleation period occurs within the first layers due to an insufficient amount of surface groups to initiate growth [133]. For example, polyethylene is a saturated hydrocarbon that lacks the typical chemical functional groups, such as hydroxyl species, that are necessary to initiate the growth of an inorganic film.

The growth of Al₂O₃ coatings on polymeric substrates was investigated by ICP-AES, XPS and SEM. The ICP-AES analyses were carried out to determine the amount of aluminium in the ALD-grown Al₂O₃ layers deposited on B(PE) and B1(PLA) using TMA and H₂O as precursors. Due to different surface roughness values, the substrates accommodate different amounts of Al₂O₃ during the ALD process. During Al₂O₃ depositions aimed at 25, 50 and 100 nm thickness, the B1(PLA) substrate was found to accommodate 96, 377 and 637 mg/m² and the B(PE) substrate 128, 836 and 858 mg/m² of aluminium, respectively. One explanation could be that when comparing to the smoother B1(PLA), B(PE) has a larger specific surface area and, accordingly, a larger number of surface sites to accommodate a larger number of molecules during ALD deposition (see Figure 6). The results are in agreement with the finding that the final thickness of the ALD-grown Al₂O₃ coating somewhat varies from the thickness determined with silicon wafer [63,132]. Another explanation could be the different nucleation periods in the beginning of the Al₂O₃ growth on different polymers due to the indiffusion of precursors into polymers [133].

6. Results and discussion

The XPS analyses performed on samples with 25 nm thick Al_2O_3 coatings fabricated using TMA and H_2O as precursors were based on surface distribution of elements [134–137], and they were employed to evaluate the surface coverage of the Al_2O_3 coating. The XPS data confirmed that the substrate had been covered quite effectively with a homogenous layer of Al_2O_3 within the XPS detection depth range (2–10 nm). Even highly porous surfaces such as pigment-coated paper P(PIG) were covered with a uniform layer of Al_2O_3 . The SEM images confirmed the data from the XPS analyses, showing that the deposited Al_2O_3 layers were homogeneous in thickness also in the substrate pores. This was also achieved with very thick Al_2O_3 layers on highly porous paper samples. Figure 8 shows a cross-sectional SEM image from uncoated paper P(UNC) with a 900-nm-thick Al_2O_3 coating. The figure also shows a top surface image from pigment coated paper P(PIG) with a Al_2O_3 coating aiming at 900 nm thickness. The thickness of this Al_2O_3 layer was found to vary from 980–1050 nm.

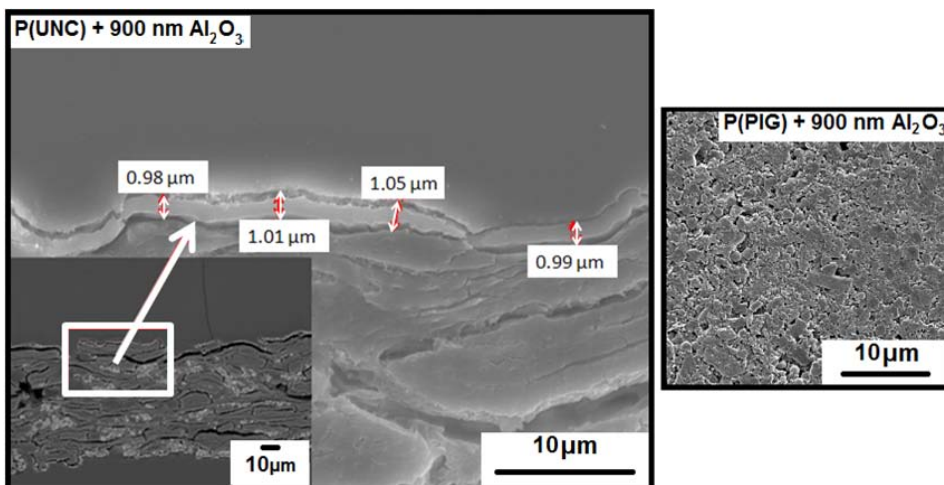


Figure 8. Images from P(UNC) and P(PIG) samples coated with 900 nm Al_2O_3 layers.

Surface coverage with Al_2O_3 was also demonstrated with nanofibrillated cellulose (NFC) fibres. The structure of NFC film resembles a fibre network. It was observed that a 25-nm-thick Al_2O_3 layer grown using the TMA- H_2O process could coat individual fibres. Figure 9 shows nanofibrillated fibres fully coated with Al_2O_3 . The cohesiveness of the Al_2O_3 coating was verified by determining the elements of the sample surface by energy dispersive spectroscopy (SEM-EDS). The smallest observed fibre thickness was approximately 50 nm with the curve radius from the fibre ends being approximately 25 nm. The ability to uniformly coat single fibres opens the potential for new applications in the area of filter development. Such materials are currently of great interest because of the combination of controlled integration of organic fibres and inorganic thin-film [138].

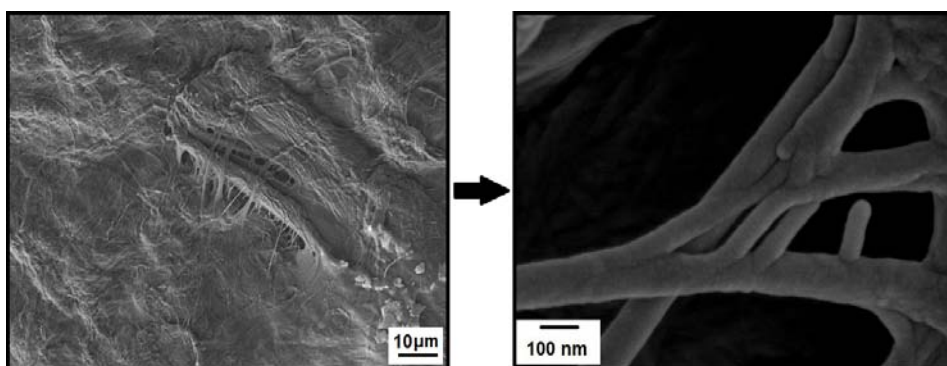


Figure 9. SEM image (*left*) with magnification (*right*) of Al_2O_3 -coated NFC fibre network possibly suitable for use in the area of filter development.

6.3 Barrier properties of ALD- Al_2O_3 coatings on biopolymeric materials

The task here was to study the improvement in the oxygen and water vapour barrier properties of mainly commercial biopolymeric materials brought about by ALD- Al_2O_3 coatings. In addition, non-commercial biopolymeric materials were used as substrate materials in order to widen the scope of investigation of potential ALD-coated materials. Because of the covalent bonding, the adhesion of metal precursor, such as TMA, to the substrate should be good even if the substrate lacks typical chemical functional groups such as hydroxyl (-OH) species [139,140]. Typically biopolymers have functional surface groups which

6. Results and discussion

can improve the adhesion between the substrate and the Al₂O₃ layer. This makes biopolymeric materials interesting substrates for ALD coatings.

In preliminary experiments conducted for process optimization purposes, two PLA-coated board samples, B1(PLA) and B2(PLA), were investigated. The deposition parameters considered were deposition temperature (80, 100 or 130 °C) and choice of oxygen source (H₂O or O₃). The results from the OTR and WVTR experiments with variously grown Al₂O₃ coatings are shown in Table 5. The deposited amount was 250 cycles aiming for a 25-nm-thick Al₂O₃ coating. To optimize the thickness, some B1(PLA) samples were also deposited with 100 cycles aiming for 10 nm. The variables investigated were temperature, oxygen source and film thickness. The results are given as average ± standard deviation of two to three parallel measurements.

Table 5. Comparison of different process parameters' (temperature, number of deposited cycles and oxidant) influence on barrier properties.

Sample	OTR (cm ³ /m ² /10 ⁵ Pa/day)	WVTR (g/m ² /day)
B1(PLA) uncoated	420 ± 10	65 ± 2
B1(PLA) + 25 nm Al ₂ O ₃ by O ₃ (100 °C)	12 ± 1	5 ± 2
B1(PLA) + 25 nm Al ₂ O ₃ by H ₂ O (100 °C)	20 ± 3	1 ± 0.2
B1(PLA) + 25 nm Al ₂ O ₃ by H ₂ O (130 °C)	107 ± 12	3 ± 2
B1(PLA) + 10 nm Al ₂ O ₃ by H ₂ O (100 °C)	48 ± 5	11 ± 3
B2(PLA) uncoated	400 ± 9	75 ± 2
B2(PLA) + 25 nm Al ₂ O ₃ by O ₃ (100 °C)	2 ± 0.2	1 ± 0.2
B2(PLA) + 25 nm Al ₂ O ₃ by O ₃ (80 °C)	3 ± 1	7 ± 2
B2(PLA) + 25 nm Al ₂ O ₃ by H ₂ O (80 °C)	6 ± 1	3 ± 1

Independent of the deposition parameters used, the 25-nm-thick ALD-Al₂O₃ coating remarkably improved both the oxygen and water vapour barrier properties of the PLA-coated board samples. For example, it was found with B1(PLA) that after 250 ALD cycles of TMA-O₃ carried out at 100 °C the OTR value improved from 420 to 12 cm³/m²/10⁵Pa/day and WVTR from 65 to 5 g/m²/day. The improvement was from 420 to 20 cm³/m²/10⁵ Pa/day and from 65 to 1 g/m²/day when using H₂O instead of O₃. The 10 nm layer was found to be too thin to form a sufficient barrier layer on B1(PLA). One explanation could be that for Al₂O₃ coatings this thin, the indiffusion of precursors into polymers

during the nucleation period could affect more on the film growth than i.e. with 25 nm thick Al₂O₃ coatings [133].

With O₃, somewhat better oxygen barrier properties may be achieved for bio-based substrates than in the case of the TMA-H₂O process. In the case of B2(PLA), similar improvements were noticed at 80 °C. The OTR value improved from 6 to 3 cm³/m²/10⁵Pa/day after 250 deposition cycles made using O₃ instead of H₂O.

The choice of deposition temperature (in the temperature range 80–100 °C) may not be crucially important. However, 130 °C was noticed to enhance the oxygen barrier properties significantly less than lower temperatures, indicating that 130 °C is too high a deposition temperature for these substrates. Although here, the deposition temperature (80–100 °C) was not the most effecting factor on the water vapour barrier properties, there are studies showing that the deposition temperature has a considerable impact on the topography, morphology as well as the adhesion to the Al₂O₃ coating of the polymeric substrates [141]. The increased crystallinity of the polymers caused by the higher temperature can cause brittleness for polymer structures which could then lead to cracking of the polymer layer impairing the barrier properties. The use of even lower deposition temperature than 80 °C could prevent the curling effect due to polymer shrinkage and could cause most improved barrier properties. In addition, the better adhesion between the polymer surface and the Al₂O₃ coating could be obtained by using lower deposition temperatures due to lower mobility of polymer chains during and after the deposition. In the study by Lahtinen *et al.* [141], polymers became brittle and the surfaces suffered considerable alterations in the process due to the process temperature on 100 °C influencing on the barrier performance. This led to easier routes for water vapour and oxygen to pass through the structures. The use of lower reactor temperatures could prevent cracking and enhance the barrier performance in terms of more controlled surface topography and polymer morphology.

It should be noted that the minimum detectable WVTR with the cup method is ~1 g/m²/day, meaning that even with a perfect barrier the result would probably be the same. Thus the barrier may be better than this but the standard deviation may also be higher.

Furthermore, both of the processes, TMA-H₂O and TMA-O₃, seem to work well, at least for PLA-coated boards. As seen in Table 5, the OTR values achieved are somewhat better in the case of the TMA-O₃ process, whereas the opposite seems to be true for the WVTR values. During the water pulses,

6. Results and discussion

absorbed H₂O may cause the polymer to swell, which should not be the case with O₃. Hence, with the exception of the most sensitive materials which might not withstand the strong oxidation power of O₃, the TMA-O₃ process can be considered a highly potential alternative for depositing Al₂O₃ coatings on biopolymers.

The moisture within the polymer chains of the substrate material should also be considered. This is especially the case with natural polymers, as these substrates tend to contain absorbed moisture. Removal of this moisture could enhance barrier properties because absorbed water can act as a plasticizer, thus deteriorating the material's barrier properties. The possible benefit of substrate moisture removal prior to ALD-Al₂O₃ deposition was investigated by keeping a B1(PLA) sample in a heated (100 °C) ALD reactor chamber overnight before coating it with Al₂O₃ at 100 °C using the TMA-H₂O process. The overnight thermal treatment resulted in a slight improvement in the OTR value: the value decreased from 20 to 8 cm³/m²/10⁵ Pa/day. However, the effect on the WVTR value was the opposite: it increased from 1 to 7 g/m²/day. This could be due to the different interactions that water vapour and oxygen induce in polymers [33,34]. Thus polymer swelling, plasticizing and possible morphological changes – in addition to film defects – could have different influences on the OTR than on the WVTR.

The removal of the moisture within the polymer chains reduced the plasticization effect of the water in the polymer, making the sample brittle.

The oxygen and water vapour barrier results achieved for a variety of biopolymer substrates with a 25-nm-thick Al₂O₃ layer deposited by the TMA-H₂O process are summarized in Figure 10. Note that H₂O was used as the oxygen source instead of O₃ to ensure that the results would not be distorted by the possible harmful effects of O₃ in the case of the most sensitive biopolymer film substrates. The depositions were made at 80 or 100 °C depending on the expected temperature tolerance of the substrate material. From Figure 10, it can be concluded that ALD-Al₂O₃-coated PLA2, pectin, NFC, B1(PLA) and B(GGM) samples are highly promising oxygen barriers with OTR values already at the commercial oxygen barrier level for dry food applications. Besides being a good oxygen barrier, the Al₂O₃-coated B1(PLA) sample is also a highly promising water vapour barrier.

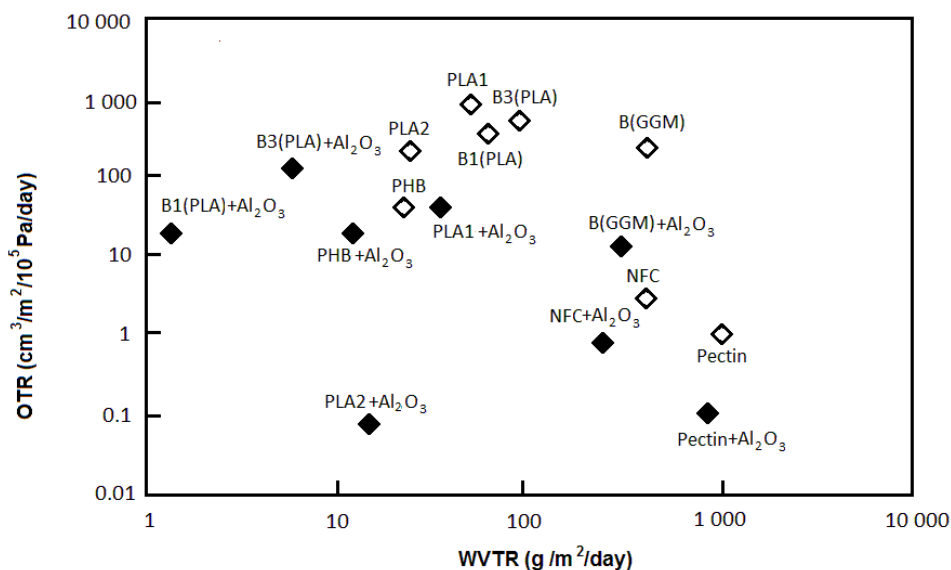


Figure 10. Best barrier results of bio-based materials achieved by coating substrates with a 25-nm-thick Al₂O₃ layer using the ALD process.

In addition to results presented in the Figure 10, similar Al₂O₃ coatings have been employed to a fibre-based substrate that has been coated with 15 g/m² petroleum-based low-density polyethylene. It was noticed that for this substrate a thicker Al₂O₃ coating was needed to improve to properties considerably. The results from the barrier measurements showed that a 50-nm-thick Al₂O₃ coating decreased the OTR value from 7900 to 2700 cm³/m²/10⁵ Pa/day. The WVTR value was decreased from 7.0 to 2.0 g/m²/day.

With the cup method, the WVTR measurement of pristine petroleum-based polymer films, such as LDPE, PEN or PET is difficult because these materials are already good water vapour barriers even without the Al₂O₃ coating. The improvement in WVTR by the Al₂O₃ coating remains often unrecognized due to the high detection limit. However, the OTR values of petroleum-based polymer films, such as 30 µm thick PP and 50 µm thick PET films, have been measured. The results showed that a 25-nm-thick Al₂O₃ coating decreased the OTR value of PP from 1250 to 170 cm³/m²/10⁵ Pa/day and PET from 24 to 11 cm³/m²/10⁵ Pa/day (Publication II).

With some polymeric substrates a temperature of even 80 °C may be too high to produce the best barrier properties [141,142]. This may also be the case with

some biopolymeric substrates and, as a result, the development of ALD processes at temperatures closer to 50 °C is essential.

Although the scope of the research here was oxygen and water vapour barrier properties, the results open up the potential for new applications in addition to dry food and pharmaceuticals. Similar coatings on non-biodegradable polymers have been shown to also reduce the permeability of other gases, such as CO₂ [142].

6.4 Influence of pre-treatments and pre-coating layers on barrier properties

6.4.1 Enhanced surface polarity by corona treatment

Corona pre-treatment was employed to improve the surface properties of the polymeric materials prior to the ALD process. The possible effect of increased surface polarity on barrier properties was studied. The effect of corona treatment on surface polarity is considered to alter during time [143]. In the case of polymer films or coatings for packages, the treatment is therefore usually employed at the production line. The treatment was consequently investigated over a seven-day period to determine its potential long-lasting impact. The effect of pre-treatments was greater on B(PE) than on B1(PLA). With the corona treatment, the contact angle value of B(PE) decreased from 90 to 67° and remained at this level for seven days.

The increased hydrophilicity also improved the oxygen and water vapour barrier properties after the ALD-grown Al₂O₃ layer. The effect could be a result of improved bonding and more even growth of the first ALD-grown layers on the polymeric substrate surface. The OTR of the plain B(PE) decreased from 7900 to 5700 cm³/m²/10⁵ Pa/day and the WVTR from 7.0 to 6.2 g/m²/day with the corona treatment. When B(PE) was coated with an Al₂O₃ layer, the values did not drop significantly. The values were 6700 cm³/m²/10⁵ Pa/day in the case of OTR and 6.9 g/m²/day and in the case of WVTR. However, when these samples were corona-treated prior to ALD, the barrier level was improved and the OTR was 1400 cm³/m²/10⁵ Pa/day and the WVTR 6.1 g/m²/day. After the corona treatment, the standard deviations of the OTR and WVTR seemed to decrease in many cases, implying that the treatment would lead to more uniform barrier properties probably due to more uniform ALD-grown layers.

Corona treatment caused the surface of B1(PLA) to become more hydrophilic, decreasing the contact angle value from 71 to 62°. After seven days the influence was minor and the contact angle was measured at 67°. The change was minor for B1(PLA) probably due to polar groups already existing on the surface of PLA. The barrier properties of plain and Al₂O₃-coated substrates with and without corona pre-treatment are presented in Table 6.

Table 6. OTR and WVTR values of plain and ALD-Al₂O₃ coated (25–50 nm) B1(PLA) substrates with and without corona treatment.

Sample	OTR (cm ³ /m ² /10 ⁵ Pa/day)		WVTR (g/m ² /day)	
	Untreated	Corona treated	Untreated	Corona treated
B1(PLA)	420 ± 10	330 ± 1	65 ± 1.6	61 ± 0.4
B1(PLA) + 25 nm	20 ± 3	17 ± 5	1.4 ± 0.2	5.7 ± 3.8
B1(PLA) + 50 nm	60 ± 5	80 ± 50	1.8 ± 0.5	14 ± 5.9

The best OTR values were achieved with a 25-nm Al₂O₃ layer on top of a corona pre-treated substrate. The influence of corona treatment was minor on the barrier properties of B1(PLA), probably due to the minor increase in surface polarity of the pristine substrates. The initial Al₂O₃ layers and subsequent Al₂O₃ layers have different functions. While the first layers influence the adhesion, the further layers serve to increase the film's rigidity. No further improvement in barrier performance was achieved by a 50-nm Al₂O₃ layer, which may be due to the cracking behaviour of thick ALD films. The corona pre-treatment did not improve the WVTR value. The increased surface polarity may aid the adhesion of polar H₂O molecules to the surface and thus the permeation through the material decreasing water vapour barrier properties. On the other hand, a more uniform layer provides a better oxygen barrier.

6.4.2 Enhanced polymer crystallinity by thermal treatment

Thermal pre-treatment of polymeric materials prior to the ALD process could increase crystallinity, which could in turn have an effect on barrier properties by altering the surface chemistry and topography of the material. Here, B3(PLA) was used as the substrate material. Topography measurements by AFM indicated that thermal treatment caused the substrate surface to become smoother. The average roughness (R_a) values measured from 5*5 μm² images decreased from

6. Results and discussion

110 to 27 nm already with the shortest thermal treatment time (4 minutes). The R_a value was not significantly different with longer thermal treatments (9 or 16 minutes).

The effect of thermal treatment on B3(PLA) is presented in Figure 11 as phase AFM images. Surface roughness as such has probably little effect on barrier properties if this is insignificant compared to the overall thickness of the barrier layer. However, surface irregularities may affect the initial wetting of the polymer by liquids, and irregularities of specific size can cause condensation and cluster formation of gaseous permeants, which may affect the dynamics of mass transfer. The amount of spherulites increased with increased thermal treatment time. The shortest thermal treatment (4 minutes) had only a small impairing effect on the oxygen barrier properties of the plain B3(PLA) substrates. The increased crystallinity of treated for 9 and 16 minutes seemed to create discontinuation points between the spherulites, which were noticed to destroy the oxygen barrier properties. WAXS analysis revealed that the crystallinity of B3(PLA) grew with increasing treatment time.

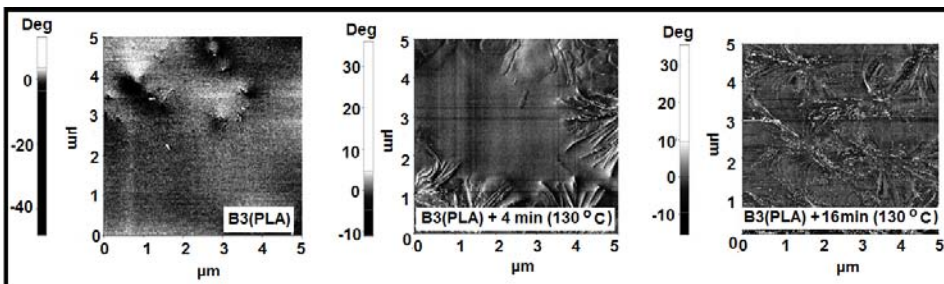


Figure 11. AFM phase images of plain B3(PLA) substrate and B3(PLA) after 4 and 16 minutes of thermal treatment for smoothed polymer surface.

Although the influence of thermal treatments on the morphology of the substrates was significant, the influence on improving barrier properties of the Al_2O_3 -coated samples was minor. The most significant improvement in OTR values was realized when the 4-minute thermally-treated sample was coated with a 25-nm ALD-grown Al_2O_3 film. The OTR value decreased from 650 to 40 $\text{cm}^3/\text{m}^2/10^5 \text{ Pa}/\text{day}$. The coating of 9- and 16-minute treated samples with the Al_2O_3 film did not improve the oxygen barrier properties. On the contrary to the OTR values, the WVTR value of plain B3(PLA) substrates was improved with all of the treatment times, and most with the 16-minute thermal treatment,

from 98 to 76 g/m²/day. The Al₂O₃ coating decreased the value to 11 g/m²/day. With 4- and 9-minute thermally-treated samples, the WVTR values were 88 and 78 g/m²/day prior to ALD, respectively. The WVTR values dropped to 3.0 and 3.2 g/m²/day, respectively, with the Al₂O₃ coating. The results indicated that the Al₂O₃ coating dominates water vapour barrier properties more than changes in crystallinity of the polymeric substrates. In addition, the oxygen barrier seems to be more sensitive to resulting coating defects than water vapor barrier. The WVTR is affected by the overall properties of the barrier layers.

6.4.3 Epoxy-SG layer as a pre-barrier for Al₂O₃-coated biopolymeric substrates

Besides pre-treatments, the barrier properties of polymeric materials can be improved by pre-blocking the biggest pinholes in the polymeric material by applying a coarser coating method than ALD. Despite the promising results achieved by coating the biopolymeric materials with the ALD-grown Al₂O₃ layer, further improvements are still desired. A pre-barrier layer fabricated using a coarser deposition method could close the larger pinholes on the surface of a porous substrate, making it denser and thus a more favourable surface on which to grow Al₂O₃ barrier layers.

The effect of a sol-gel (SG) coating as an intermediate layer between the substrate and the ALD-Al₂O₃ coating was studied using B2(PLA) as a substrate. Figure 12 shows the surfaces of plain, epoxy-SG-coated and epoxy-SG+Al₂O₃-coated B2(PLA) substrates. The observed average roughness (R_a) values are also given. As can be seen in Figure 12, the epoxy-SG coating decreases the R_a value making the surface of the substrate smoother, while an Al₂O₃ coating on epoxy-SG-coated B2(PLA) makes the surface smoother still. The total decrease in R_a was from 54 to 15 nm.

6. Results and discussion

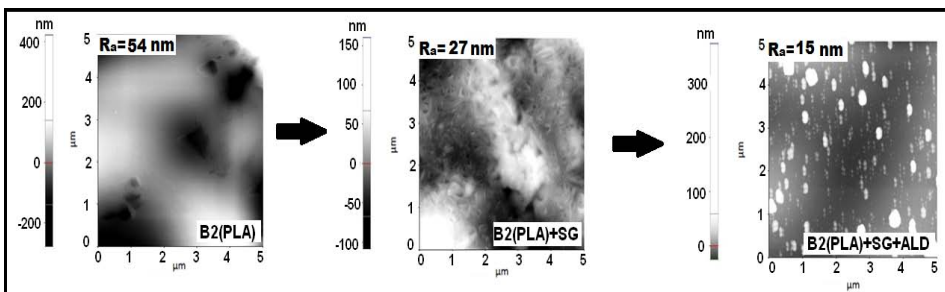


Figure 12. AFM surface images of plain B2(PLA) with SG coating and with a multilayer structure consisting of SG and Al_2O_3 layers.

The contact angle (CA) and surface energy (γ_s) values for plain, epoxy-SG-coated and epoxy-SG-+ Al_2O_3 -coated B2(PLA) samples are presented in Table 7 together with the barrier results. The intermediate layer decreases the CA value, indicating a more hydrophilic surface. The CA value drops even further with an additional Al_2O_3 coating. The barrier results show a moderate positive effect of epoxy-SG coating on barrier properties. Only after the SG-coated B2(PLA) was further coated with Al_2O_3 were the considerably low OTR and WVTR values of $2 \text{ cm}^3/\text{m}^2/10^5 \text{ Pa/day}$ and $2 \text{ g/m}^2/\text{day}$, respectively, attained. Most importantly, these values are lower than those achieved for B2(PLA) with the ALD- Al_2O_3 coating only, i.e. $6 \text{ cm}^3/\text{m}^2/10^5 \text{ Pa/day}$ and $3 \text{ g/m}^2/\text{day}$, respectively. Table 7 presents the impact of epoxy-SG coating on the CA and on the surface energy values, showing also the OTR and WVTR values. The total surface energy value (γ_s) is the sum of the dispersive (γ^d) and polar (γ^p) components.

Table 7. Contact angle and surface energy values together with the OTR and WVTR values, showing the impact of epoxy-SG pre-coating.

Sample	CA(°)	γ_s (γ^p) (mNm^{-1})	OTR ($\text{cm}^3/\text{m}^2/10^5$ Pa/day)	WVTR ($\text{g/m}^2/\text{day}$)
B2(PLA)	71 ± 2	45.6 (7.4)	400 ± 9	75 ± 2
B2(PLA) + epoxy-SG	58 ± 2	53.8 (13.2)	310 ± 2	44 ± 2
B2(PLA) + epoxy-SG + 25 nm Al_2O_3	52 ± 1	54.9 (18.0)	2 ± 1	2 ± 1

6.4.4 Polyelectrolyte multilayer film as a pre-coating for Al_2O_3 -coated biopolymeric substrates

In addition to pre-blocking the biggest pinholes prior to the ALD process, pre-coatings can also be utilized to alter the surface topography. Here, the effect of pre-coating the polymer film with a PEM film to improve barrier properties was investigated by using PLA1 as a substrate material. The PEM film was made by alternating depositions of sodium alginate (ALG) (M_v 280 000 g/mol) and chitosan (CHI) (M_v 170 000 g/mol), leaving CHI as the outermost layer. The PEM-coated PLA1 film was further coated with a 25-nm-thick ALD-grown Al_2O_3 layer. Figure 13 presents the targeted three-layer structure.

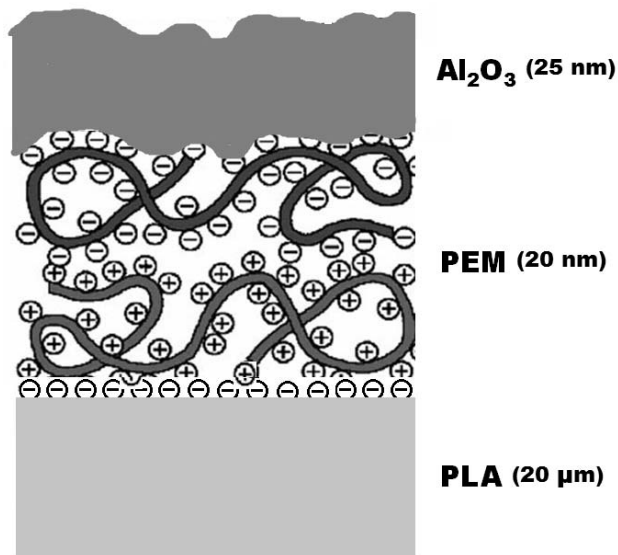


Figure 13. Schematic illustration of the multilayer structure of PEM- and Al_2O_3 -coated film, modified from that of Decher [120].

The average thickness of the film formed from ALG and CHI was 20 nm. The PEM coating alone did not improve the water vapour barrier properties of the substrate. In contrast, the WVTR value was increased from 53 to 106 $\text{g/m}^2/\text{day}$ after PEM coating. This is apparently due to the dipping process in the LbL method, which causes the hygroscopic biopolymers to swell in water solutions. However, after the Al_2O_3 coating had been applied on PEM-coated PLA1, the WVTR was improved to 25 $\text{g/m}^2/\text{day}$. When applying only the Al_2O_3 coating,

6. Results and discussion

the WVTR was 33 g/m²/day. PEM coating combined with Al₂O₃ coating was found to be a suitable and cost-efficient means of producing bio-based water vapour barrier coatings. The WVTR and contact angle values of variously-coated PLA1 films are presented in Table 8.

Table 8. Water vapour transmission rate (WVTR) and contact angle (CA) values for plain and variously coated PLA1 samples.

Sample	WVTR (g/m ² /day)	CA (°)
PLA	53 ± 4	73 ± 2
PLA + PEM	106 ± 7	76 ± 4
PLA + 25 nm Al ₂ O ₃	33 ± 6	48 ± 1
PLA + PEM + 25 nm Al ₂ O ₃	25 ± 9	98 ± 4

From Table 8, the water vapour transmission rates seem to correlate with the wettability properties of the Al₂O₃-coated samples such that the larger the CA, the lower the WVTR value. Polar H₂O molecules are apparently less readily adsorbed on the less polar surface. The contact angle value of the plain PLA1 film was 73°. The PEM coating alone did not change the contact angle value considerably. However, when the PEM-coated PLA1 film was further coated with an Al₂O₃ layer, the contact angle value increased to 98° thus making the surface more hydrophobic. Conversely, when the PLA1 film was coated only with the Al₂O₃ layer, the contact angle value was found to decrease to 48°, making the surface rather more hydrophilic. This result was expected, due to the intrinsically hydrophilic nature of Al₂O₃ surfaces [144].

Based on the above (Table 8), the PEM intermediate layer seems to influence the hydrophobicity of the Al₂O₃ surface. The precise reason for this remains to be determined by future studies. However, parallel behaviour (i.e. a CA value of 128°) was recently observed with a thermally-grown Al₂O₃ coating with a relatively rough surface [145]. It is known that certain special surface topologies can even produce superhydrophobic states on intrinsically hydrophilic surfaces [146]. The LbL dipping process may alter the surface of the PLA1 film and increase its roughness.

Figure 14 shows some SEM images of the plain and variously coated PLA1 films. The plain PLA1 substrate appears to be smooth with small patterns caused by the sputtered Pt. Nonconductive samples tend to charge when scanned by the electron beam causing possible scanning faults. They are therefore usually

sputtered with a thin coating of electrically-conducting material, such as Pt. The PEM-film-coated PLA1 substrate seems to have nanopores throughout the film. After further coating with a 25-nm-thick Al_2O_3 layer the surface seems to be uniformly coated with the Al_2O_3 layer.

As can be seen, the PLA1 film is a highly smooth substrate, presumably due to the commercial production method of the film. Some surface patterning can be observed, deriving from the sputtered Pt. Once the PLA1 film is coated with a PEM film, a surface structure with small pores (10–30 nm in diameter) appears on the entire surface of the film. After subsequent deposition of the 25-nm-thick Al_2O_3 layer, the nanostructured surface appears to be uniformly coated with Al_2O_3 , such that the smallest pores are filled, yet the surface still presents some surface structure.

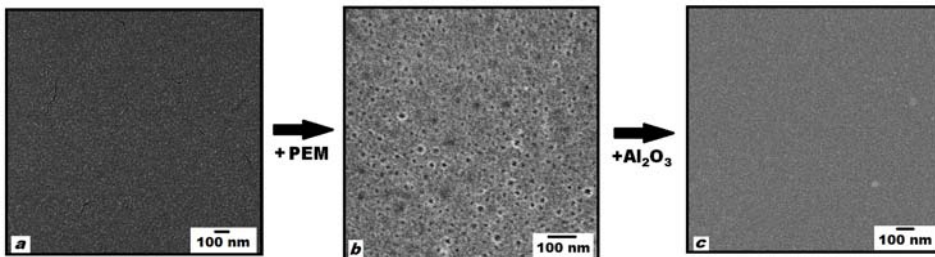


Figure 14. SEM images for plain (a) and variously coated PLA1 films (b–c).

7. Conclusions

The objective of the present work was to investigate the suitability of ALD-grown Al_2O_3 layers as barrier coatings for bio-based packaging materials. The focus was to determine whether ALD is the most feasible thin-film deposition technique for the production of high-quality barrier coatings on polymeric materials. Thereafter, the task was to clarify whether the ALD process could be performed in the temperature range of 80–130 °C on biopolymeric materials known to be temperature-sensitive. The ALD process parameters (oxygen source, deposition temperature, and film thickness) were optimized, which enabled the investigation of the oxygen and water vapour barrier properties of thin ALD-grown Al_2O_3 coatings on polymer films and polymer-coated papers and boards. An additional objective of this study was to improve the barrier properties of ALD-coated materials by employing treatments and coatings on the substrates prior to the ALD process.

By utilizing ALD-grown Al_2O_3 coatings with thicknesses of 10–50 nm, the oxygen and water vapour barrier properties of biopolymeric materials could be significantly improved. The barrier ability was achieved without the use of conventional aluminium film, thus achieving total biodegradability due to the thinness of the Al_2O_3 layer. The ALD-grown Al_2O_3 layer required to provide sufficient barrier properties is so thin that it should not affect the biodegradability of the substrate material.

The developed coatings with excellent gas and water vapour permeation resistance offer a new means of manufacturing biodegradable, thin, light and airtight packaging materials. The oxygen and water vapour barrier levels achieved here with the Al_2O_3 coatings grown onto biopolymeric materials reached the level required in commercial packaging applications for dry food and pharmaceuticals. Other thin film methods can also produce thin Al_2O_3 coatings; however, their gas and water vapour permeability is higher and the material is

stiffer and breaks easily. With these competing methods, comparable permeation resistance is possible only if thicker films are used.

Although a number of additional substrate pre-treatments and pre-coatings can be employed prior to the ALD process, the overall improvement in barrier properties gained by ALD-grown Al_2O_3 layers seems sufficient. However, such pre-treatments and pre-barrier coatings could make the materials and processes in some cases more cost-efficient at the industrial scale.

With some polymeric substrates, a deposition temperature of even 80 °C may be too high to achieve the most desirable barrier properties. This highlights the need for future research to develop efficient ALD processes at temperatures as low as 50 °C. In addition to corona and thermal pre-treatments, other pre-treatments such as plasma and flame spray treatments need to be investigated in future to clarify the overall potential of various pre-treatments to improve the barrier properties. As regards the characterization of Al_2O_3 coatings on biopolymers, cross-cut imaging of 25 nm thick or thinner Al_2O_3 layers has proven challenging due to the sensitive nature of the substrates. These imaging difficulties need to be overcome in order to be able to truly determine Al_2O_3 layer growth with respect to different substrate types.

The fabrication of nanolaminates wholly from several metal oxides or by utilizing molecular layer deposition (MLD) at low temperature for barrier purposes requires investigation in future. The resulting novel structures have the potential to provide improved flexibility as well as good barrier properties combined. By using the ALD process, different functions can be integrated in the packaging material, such as antimicrobial properties. As regards production of packages, the behaviour of Al_2O_3 layers during processes, such as sealing, greasing and laminating, is another significant area for future research.

References

1. K. Khwaldia, E. Arab-Tehrany, S. Desobry, *CRFSFS* **9** (2010) 82.
2. T. Suntola, *Mater. Sci. Rep.* **4** (1989) 261.
3. M. Ritala, M. Leskelä, J.-P. Dekker, C. Mutsaers, P.J. Soininen, J. Skarp, *Chem. Vap. Depos.* **5** (1999) 7.
4. K. Lahtinen, P. Maydannik, P. Johansson, T. Kääriäinen, D. C. Cameron, J. Kuusipalo, *Surf. Coat. Technol.* **205** (2011) 3916.
5. J. Yudovsky, *US patent application*, No. US2004/0067641 A1 (2004).
6. D. Levy, *US patent application* No. US2007/0238311 A1 (2007).
7. A. Erlat, E. Breitung, *PCT patent application* No. WO2008/057625 A2 (2008).
8. C. Bastioli, *Starch-Strärke* **53** (2001) 351.
9. G. Mensitieri, E. Di Maio, G.G. Buonocore, I. Nedi, M. Oliviero, L. Sansone, S. Iannace, *Trends Food Sci. Tech.* **22** (2011) 72.
10. Y. Ikada, H. Tsuji, *Macromol. Rapid Commun.* **21** (2000) 117.
11. B.L. Seal, T.C. Otero, A. Panitch, *Mater. Sci. Eng.* **R34** (2001) 147.
12. C. Andersson, *Packag. Technol. Sci.* **21** (2008) 339.
13. J. Kuusipalo, K. Lahtinen, *Tappi J.* **7** (2008) 8.
14. G. Scott, *Polym. Deg. Stab.* **68** (2000) 1.
15. G.L. Robertson, *Food Packaging Principles and Practice*, Marcel Dekker Inc., New York, United States of America, 1993, pp. 622–662.
16. A. Leppänen-Turkula, *Converted paper and paperboard as packaging materials*, in: *Paper and Paperboard Converting*, Papermaking Science and Technology, Book 12, (Ed. A. Savolainen), Fapet Oy, Helsinki, Finland, 1998, pp. 270–280.
17. C.J. Weber, *Biobased Packaging Materials for the Food Industry – Status and Perspectives*, The Royal Veterinary and Agricultural University, Frederiksberg, Denmark, 2000.
18. R. Coles, *Introduction*, in: *Food Packaging Technology*, (Eds. R. Coles, D. McDowell, M.J. Kirwan) Blackwell Publishing Ltd., CRC Press LLC: Boca Raton, FL, 2003, pp. 1–31.

19. R.J. Hill, *Film, transparent glass on plastic food packaging materials*, in: *The Wiley Encyclopedia of Packaging Technology, 2nd Ed.*, (Eds. A.L. Brody, K.S. Marsh), A Wiley-Interscience Publication, New York, 1997, pp. 445–448.
20. A. Savolainen, J. Kuusipalo, E. Laiho, T. Penttinen, *Extrusion coating and product applications*, in: *Paper and Paperboard Converting*, (Ed. A. Savolainen), Fapet Oy, Helsinki Finland, 1998, pp.123–1187.
21. J. Lange, Y. Wyser, *Packag. Technol. Sci.* **16** (2003) 149.
22. A. Sorrentino, M. Tortora, V.J. Vittoria, *Polymer Sci. B* **44** (2006) 265.
23. M. Stading, Å. Rindlav-Westling, P. Gatenholm, *Carbohydr. Polym.* **45** (2001) 209.
24. J.J. de Vlieger, *Green plastic for food packaging*, in: *Novel Food Packaging Techniques*, (Ed. R. Ahvenainen). Woodhead Publishing Ltd.: Cambridge, England, 2003, pp. 519–534.
25. S. Despond, N. Espuche, N. Cartier, A. Domand, *J. Appl. Polym. Sci.* **98** (2005) 704.
26. Y. Leterrier, *Prog. Mater. Sci.* **48** (2003) 1.
27. R.J. Hernandez, R. Gavara, *Pira International reviews of packaging: Plastic Packaging, Methods for studying Mass Transfer Interactions*, Pira International, Surrey, UK 1999, pp. 1–32.
28. B. Aurela, T. Ohra-aho, L. Söderhjelm, *Packag. Technol. Sci.* **14** (2001) 71.
29. H. Brown, J. Williams, *Packaged product quality and shelf life*, in *Food Packaging Technology*, (Eds. R. Coles, D. McDowell, M.J. Kirwan) Blackwell Publishing Ltd., CRC Press LLC: Boca Raton, FL, 2003, pp. 65–94.
30. K.S. Miller, J.M. Krochta, *Trends Food Sci. Technol.* **8** (1997) 228.
31. M.S. Hedenqvist, U.W. Gedde, *Polymer* **40** (1999) 2381.
32. J. E. Ritums, M.S. Hedenqvist, G. Bergman, T. Prodan, I. Emri, *Polym. Eng. Sci.* **45** (2005) 1194.
33. M. Chainey, *Transport phenomena in polymer films*, in: *Handbook of polymer science and technology, Vol. 4 Composites and specialty applications*, Marcel Dekker, 1989, pp. 499–540.
34. R.J. Hernandez, J.R. Giacini, A.L. Baner, *J. Plast. Film Sheet.* **2** (1986) 187.

35. F. Johansson, *Food and packaging interactions affecting food quality*, Doctoral dissertation Chalmers University of Technology, Gothenburg, Sweden, 1996.
36. D. Shires, *Developments in barrier technology*, Pira International, UK, 1993, pp. 13–19.
37. R.J. Ashley, *Permeability and plastics packaging*, in: *Polymer Permeability*, (Ed. J. Comyn), Elsevier Applied Science London, UK, 1985, pp. 269–308.
38. ASTM D 3985 *Standard Test Method for Oxygen Gas Transmission Rate through Plastic Film and Sheeting Using a Coulometric Sensor*, ASTM International: West Conshohocken, PA.
39. ASTM E 96 *Standard Test Methods for Water Vapor Transmission of Materials*, ASTM International: West, Conshohocken, PA.
40. DIN 53122-1 *Bestimmung der Wasserdampfdurchlässigkeit*, DIN Deutsches Institut für Normung e.V., Berlin, Germany.
41. ISO 2528 *Sheet Materials – Determination of Water Vapor Transmission Rate – Gravimetric (Dish) Method*, International Organization for Standardization: Geneva, Switzerland.
42. TAPPI T 448 *Water Vapor Transmission Rate of Sheet Materials at Standard Temperature and Humidity*, TAPPI Press, Atlanta, GA.
43. TAPPI T 464 *Water Vapor Transmission Rate of Paper and Paperboard at High Temperature and Humidity*, TAPPI Press, Atlanta, GA.
44. A. Gennadios, C.L. Weller, C.H. Gooding, *J. Food Eng.* **21** (1994) 395.
45. T. Kimpimäki, A. Savolainen, *Barrier dispersion coating of paper and board*, in: *Surface Application of Paper Chemicals*, (Eds. J. Brander, I. Thorn) Blackie Academic & Professional, Chapman & Hall, London, UK, 1997, pp. 208–228.
46. A. Grüninger, Ph.R. von Rohr, *Thin Solid Films* **459** (2004) 308.
47. P.A. Premkumar, S.A. Starostin, M. Creatore, H. de Vries, R.M.J. Paffen, P.M. Koenraad, M.C.M. van de Sanden, *Plasma Process. Polym.* **7** (2010) 635.
48. A.S. Da Silva-Sobrinho, G. Czeremuszkina, M. Latreche, G. Dennler, M.R. Wertheimer, *Surf. Coat. Technol.* **119** (1999) 1204.
49. A.S. Da Silva-Sobrinho, G. Czeremuszkina, M. Latreche, G. Dennler, M.R. Wertheimer, *J. Vac. Sci. Technol. A* **18** (2000) 149.

50. M. Yanaka, B.M. Henry, A.P. Roberts, C.R.M. Grovenor, G.A.D. Briggs, A.P. Sutton, T. Miyamoto, Y. Tsukahara, N. Takeda, R.J. Charter, *Thin Solid Films* **397** (2001) 176.
51. M. Hanika, W. Peukert, H.C. Langowski, *Chem. Ing. Tech.* **74** (2002) 984.
52. K. Mueller, H. Weisser, *Packag. Technol. Sci.* **15** (2002) 29.
53. A.P. Roberts, B.M. Henry, A.P. Sutton, C.R.M. Grovenor, G.A.D. Briggs, T. Miyamoto, A. Kano, Y. Tsukahara, M. Yanaka, *J. Membr. Sci.* **208** (2002) 75.
54. K. Saitoh, R.S. Kumar, S. Chua, A. Masuda, H. Matsumura, *Thin Solid Films* **516** (2008) 607.
55. L. Körner, A. Sonnenfeld, P. Rudolf von Rohr, *Thin Solid Films* **518** (2010) 4840.
56. S.B. Jin, Y.J. Kim, Y.S. Choi, I. S. Choi, J.G. Han, *Thin Solid Films* **518** (2010) 6385.
57. K.M. Vaeth, K.F. Jensen, *Chem. Mater.* **12** (2000) 1305.
58. A.G. Erlat, B.M. Henry, J.J. Ingram, D.B. Mountain, A. McGuigan, R.P. Howson, C.R.M. Grovenor, G.A.D. Briggs, Y. Tsukahara, *Thin Solid Films* **388** (2001) 78.
59. B.M. Henry, F. Dinelli, K.-Y. Zhao, C.R.M. Grovenor, O.V. Kosolov, G.A.D. Briggs, A.P. Roberts, R.S. Kumar, R.P. Howson, *Thin Solid Films* **355–356** (1999) 500.
60. J. Fahlteich, M. Fahland, W. Schönberger, N. Schiller, *Thin Solid Films* **517** (2009) 3075.
61. T. Hanada, T. Negishi, I. Shiroishi, T.I Shiro, *Thin Solid Films* **518** (2010) 3089.
62. G.-H. Lee, J. Yun, S. Lee, Y. Jeong, J.-H. Jung, S.-H. Cho, *Thin Solid Films* **518** (2010) 3075.
63. J.D. Ferguson, A.W. Weimer, S.M. George, *Chem. Mater.* **16** (2004) 5602.
64. M.D. Groner, S.M. George, R.S. McLean, P.F. Carcia, *Appl. Phys. Lett.* **88** (2006) 051907.
65. A.A. Dameron, S.D. Davidson, B.B. Burton, P.F. Carcia, R.S. McLean, S.M. George, *J. Phys. Chem. C* **112** (2008) 4573.
66. E. Langereis, M. Creatore, S.B.S. Heil, M.C.M. van de Sanden, W.M.M. Kessels, *Appl. Phys. Lett.* **89** (2006) 081915.

67. S. Ambers-Schwab, M. Hoffmann, H. Bader, M. Gessler, *J. Sol-Gel Sci. Techn.* **1/2** (1998) 141.
68. P.F. Carcia, R.S. McLean, M.H. Reilly, M.D. Groner, S.M. George, *Appl. Phys. Lett.* **89** (2006) 031915.
69. C.J. Brinker, G.W. Scherer, *Sol-Gel Science: The Physics and Chemistry of Sol-Gel Processing*, Academic Press Inc., New York, 1990.
70. L.L. Hench, J.K. West, *Chem Rev.* **90** (1990) 33.
71. C.-M. Chan, *Polymer surface modification and characterization*, Carl Hanser Verlag, Munich Vienna New York, 1994, pp. 35–76.
72. E.S. Vlahov, T.I. Donchev, A.Y. Spasov, K. Dorr, K.A. Nenkov, A. Handstein, S. Pignard, H. Vincent, *Vacuum* **69** (2003) 149.
73. D.F. Shriver, P.W. Atkins, *Inorganic Chemistry, 4. Ed.*, Oxford University Press, New York, 2006.
74. A.A. Trakton, *Coating technology hand book, 3rd edition*, Taylor & Francis Group, 2006.
75. M. Tuominen, K. Lahtinen, *Conventional and novel coating methods, in: Paper and Paperboard Converting* (Ed. J. Kuusipalo), Fapet Oy, Helsinki Finland, 2008, pp. 167–185.
76. L. Graff, R.E. Williford, P.E. Burrows, *J. Appl. Phys.* **96** (2004) 1840.
77. S.H.K. Park, J. Oh, C.S. Hwang, J.I. Lee, Y.S. Yang, H.Y. Chu, *Electrochem. Solid-State Lett.* **8** (2005) H21.
78. M. Knez, K. Nielsch, L. Niinistö, *Adv. Mater.* **19** (2007) 3425.
79. R.L. Puurunen, *Chem. Vap. Depos.* **9** (2003) 249.
80. R.L. Puurunen, *J. Appl. Phys.* **97** (2005) 121301.
81. T. Suntola, J. Antson, *US Patent No 4,058,430* (1977).
82. S.M. George, *Chem. Rev.* **110** (2010) 111.
83. G.S. Higashi, C-G. Fleming, *Appl. Phys. Lett.* **55** (1989) 1963.
84. A.C. Dillon, A.W. Ott, J.D. Way, S.M. George, *Surf. Sci.* **322** (1995) 230.
85. S.M. George, A.W. Ott, J.W. Klaus, *J. Phys Chem.* **100** (1996) 13121.

86. A.W. Ott, J.W. Klaus, J.M. Johnson, S.M. George, *Thin Solid Films* **292** (1997) 135.
87. R. Matero, A. Rahtu, M. Ritala, M. Leskelä, T. Sajavaara, *Thin Solid Films* **368** (2000) 1.
88. S. Jakcshik, U. Schroeder, T. Hecht, D. Krueger, G. Dollinger, A. Bergmaier, C. Luhmann, J.W. Bartha, *Appl. Surf. Sci.* **211** (2003) 352.
89. S.-C. Ha, E. Choi, S.-H. Kim, J.S. Roh, *Thin Solid Films* **476** (2005) 252.
90. G.D. Wilk, R.M. Wallace, J.M. Anthony, *J. Appl. Phys.* **89** (2001) 5243.
91. S.D. Elliot, G. Scarel, C. Wiemer, M. Fanciulli, G. Pavia, *Chem. Mater.* **18** (2006) 3764.
92. J. Kim, K. Chakrabarti, J. Lee, K.-Y. Oh, C. Lee, *Mater. Chem. Phys.* **78** (2003) 733.
93. O.R. Wulf, *The thermal decomposition of ozone*, PhD thesis, California Institute of Technology, Pasadena, CA, 1926.
94. J.B. Kim, D.R. Kwon, K. Chakrabarti, C. Lee, K.Y. Oh, J.H. Lee, *J. Appl. Phys.* **92** (2002) 6739.
95. R.L. Puurunen, *Chem. Vap. Depos.* **9** (2003) 327.
96. G. Prechtel, A. Kersch, G. Schulze Icking-Konert, W. Jacobs, T. Hecht, H. Boubekeur, U. Schroeder, Tech. Dig.-Int. Electron Devices Meet., (2003) 245.
97. S.K. Kim, C.S. Hwang, *J. Appl. Phys.* **96** (2004) 2323.
98. D.N. Goldstein, J.A. McCormick, S.M. George, *J. Phys. Chem. C* **112** (2008) 19530.
99. M. Rose, J. Niinistö, I. Endler, J.W. Bartha, P. Kcher, M. Ritala, *ACS Appl. Mater. Interfaces* **2** (2010) 347.
100. R. Cooper, H.P. Upadhyaya, T.K. Minton, M.R. Berman, X. Du, S.M. George, *Thin Solid Films* **516** (2008) 4036.
101. Y. Zhang, J. A. Bertrand, R. Yang, S. M. George, Y.C. Lee, *Thin Solid Films* **517** (2009) 3269.
102. P.F. Carcia, R.S. McLean, S. Hegedus, *Solar Energy Mater. Solar Cells* **94** (2010) 2375.

103. T.O. Kääriäinen, P. Maydannik, D.C. Cameron, K. Lahtinen, P. Johansson, J. Kuusipalo, *Thin Solid Films* **519** (2011) 3146.
104. C. Charton, N. Schiller, M. Fahland, A. Holländer, A. Wedel, K. Noller, *Thin Solid Films* **502** (2006) 99.
105. B.B. Burton, M.P. Boleslawski, A.T. Desombre, S.M. George, *Chem. Mater.* **20** (2008) 7031.
106. Z.A. Sechrist, F.H. Fabreguette, O. Heintz, T.M. Phung, D.C. Johnson, S.M. George, *Chem. Mater.* **17** (2005) 3475.
107. C.A. Wilson, J.A. McCormick, A.S. Cavanagh, D.N. Goldstein, A.W. Weimer, S.M. George, *Thin Solid Films* **516** (2008) 6175.
108. D. Josell, J.E. Bonevich, T.P. Moffat, T. Aaltonen, M. Ritala, M. Leskelä, *Electrochem. Solid-State Lett.* **9** (2006) C48.
109. G. Beyer, A. Satta, J. Schuhmacher, K. Maex, W. Besling, O. Kilpelä, H. Sprey, G. Tempel, *Microelectron. Eng.* **64** (2002) 233.
110. P. Alen, M. Ritala, K. Arstila, J. Keinonen, M. Leskelä, *Thin Solid Films* **491** (2005) 235.
111. B.B. Burton, A.R. Lavoie, S.M. George, *J. Electrochem. Soc.* **155** (2008) D508.
112. S. Cho, K. Lee, P. Song, H. Jeon, Y. Kim, *Jpn. J. Appl. Phys.* **46** (2007) 4085.
113. A.A. Dameron, D. Seghete, B.B. Burton, S.D. Davidson, A.S. Cavanagh, J.A. Bertrand, S.M. George, *Chem. Mater.* **20** (2008) 3315.
114. M. Pykönen, H. Sundqvist, J. Järnström, O.-V. Kaukonen, M. Tuominen, J. Lahti, J. Peltonen, P. Fardim, M. Toivakka, *Appl. Surf. Sci.* **255** (2008) 3217.
115. Y. Qin, M. Rubino, R. Auras, L.T. Lim, *J. Appl. Polym. Sci.* **110** (2008) 1509.
116. K. Lahtinen, K. Nättinen, J. Vartiainen, *Polym-Plast. Tech. Eng.* **48** (2009) 561.
117. K. Lahtinen, S. Kotkamo, T. Koskinen, S. Auvinen, J. Kuusipalo, *Packag. Technol. Sci.* **22** (2009) 451.
118. R. Edwards, *Polymers, Laminations & Coatings Conference Proceedings*, Boston, MA., Sep. 4–7, 1990, p. 595.
119. H. Tsuji, R. Okino, H. Daimon, K. Fujie K, *J. Appl Polym Sci* **99** (2006) 2245.
120. G. Decher, *Science* **277** (1997) 1232.

121. M. Salomäki, P. Tervasmäki, S. Areva, J. Kankare, *Langmuir* **20** (2004) 3679.
122. B. Bhushan, *Introduction, Measurements techniques and applications, in: Handbook of Micro/Nanotribology, 2nd Ed.*, (Ed. B. Bhushan) CRC Press, Boca Raton, FL, 1999.
123. Q. Zhong, D. Inniss, K. Kjoller, V.B. Elings, *Surf. Sci. Lett.* **290** (1993) L688.
124. A.P. Quist, J. Ahlbom, C.T. Reimann, B.U.R. Sundqvist, *Nucl. Instrum. Methods B* **88** (1994) 164.
125. T. Kallio, *Interfacial interactions and fouling in paper machines*, PhD thesis, Helsinki University of Technology, 1997.
126. I. Perrissin-Fabert, G. Peix, D. Babot, *Meas. Sci. Technol.* **15** (2004) 889.
127. R.L. Cleland, *Biopolymers* **23** (1984) 647.
128. C. Rochas, M. Rinaudo, S. Laundry, *Carbohydr. Polym.* **12** (1990) 255.
129. A. Martinsen, G. Skjåk-Bræk, O. Smidsrod, F. Zanetti, S. Paoletti, *Carbohydr. Polym.* **15** (1991) 171.
130. M. Rinaudo, M. Milas, P.L. Dung, *Int. J. Biol. Macromol.* **15** (1993) 281.
131. T.E. Emereeva, T.O. Bykova, *Carbohydr. Polym.* **36** (1998) 319.
132. X.H. Liang, L.F. Hakim, G.D. Zhan, J.A. McCormick, S.M. George, A.W. Weimer, J.A. Spencer, K.J. Buechler, J. Blackson, C.J. Wood, J.R. Dorgan, *J. Am. Ceram. Soc.* **90** (2007) 57.
133. C.A. Wilson, R.K. Grubbs, S.M. George, *Chem. Mater.* **17** (2005) 5625.
134. S. Tougaard, A. Ignatiev, *Surf.Sci.* **129** (1983) 355.
135. L.-S. Johansson, J. Juhanaja, *Thin Solid Films* **238** (1994) 242.
136. S. Tougaard, *Surf. Interface Anal.* **26** (1998) 249.
137. L.-S. Johansson, J. Campbell, K. Koljonen, M. Kleen, J. Buchert, *Surf. Interface Anal.* **36** (2004) 706.
138. J.S. Jur, J.C. Spagnola, K. Lee, B. Gong, Q. Peng, G.N. Parsons, *Langmuir* **26** (2010) 8239.
139. T.O. Kääriäinen, D.C. Cameron, M. Tantari, *Plasma Process. Polym.* **6** (2009) 631.

140. D.C. Miller, R.R. Foster, Y. Zhang, S.-H. Jen, J.A. Bertrand, Z. Lu, D. Seghete, J.L. O'Patchen, R. Yang, Y.-C. Lee, S.M. George, M.L. Dunn, *J. Appl. Phys.* **105** (2009) 093527.
141. K. Lahtinen, P. Maydannik, P. Johansson, T. Kääriäinen, D. C. Cameron, J. Kuusipalo, *Surf. Coat. Technol.* **205** (2011) 3916.
142. M.D. Groner, F.H. Fabreguette, J.W. Elam, S.M. George, *Chem. Mater.* **16** (2004) 639.
143. M. Pascual, R. Balart, L. Sánchez, O. Fenollar, O. Calvo, *J. Mater. Sci.* **43** (2008) 4901.
144. D.S. Finch, T. Oreskovic, K. Ramadurai, C.F. Herrmann, S.M. George, R.L. Mahajan, *J. Biomed. Mater. Res. A* **87** (2008) 100.
145. J.E Samad, J..A. Nychka, *Bioinsp. Biomim.* **6** (2011) 016004.
146. J-L. Liu, X-Q. Feng, G. Wang, S-W. Yu, *J. Phys.:Condens. Matter* **19** (2007) 356002.

PUBLICATION I

**Comparison of some coating
techniques to fabricate barrier
layers on packaging materials**

In: Thin Solid Films 518 (2010),
pp. 5463–5466.

Reprinted with permission from the publisher.



Comparison of some coating techniques to fabricate barrier layers on packaging materials

Terhi Hirvikorpi^a, Mika Vähä-Nissi^{a,*}, Ali Harlin^a, Maarit Karppinen^b

^a VTT Technical Research Centre of Finland, Biologinkuja 7, Espoo, P.O. Box 1000, FI-02044 VTT, Finland

^b Laboratory of Inorganic Chemistry, Department of Chemistry, Aalto University School of Science and Technology, Kemistintie 1, P.O. Box 16100, FI-00076 AALTO, Finland

ARTICLE INFO

Article history:

Received 17 September 2009
Received in revised form 26 February 2010
Accepted 6 April 2010
Available online 14 April 2010

Keywords:

Barrier coating
Atomic layer deposition
Electron beam evaporation
Magnetron sputtering
Sol-gel
Aluminum oxide

ABSTRACT

Atomic layer deposition (ALD), electron beam evaporation, magnetron sputtering and a sol-gel method were used to deposit thin aluminum oxide coatings onto two different fiber-based packaging materials of commercial board grades coated with synthetic and biodegradable polymers. Significant decreases in both the water vapor and oxygen permeation rates were observed. With each technique the barrier performance was improved. However, among the techniques tested ALD was found to be most suitable. Our results moreover revealed that biodegradable polylactic acid-coated paperboard with a 25-nm thick layer of aluminum oxide grown by ALD on top of it showed promising barrier characteristics against water vapor and oxygen.

© 2010 Elsevier B.V. All rights reserved.

1. Introduction

Fiber-based packaging materials have many advantages over their plastic competitors, such as sustainability, recyclability and stiffness/weight ratio [1]. However, poor barrier properties and sensitivity towards moisture are the main challenges for their extended use. In order to improve the barrier properties packaging materials are often coated with polymers or laminated with other materials such as aluminum foils and plastic films. Most of the studies have concerned polyethylene (PE), accompanied mainly by ethyl vinyl alcohol and poly(ethylene terephthalate) [1]. In recent years environmental aspects have become important and considerable efforts have been made to replace fossil-based raw materials by environmentally friendly, biodegradable or recyclable materials from natural sources.

The general permeation process through non-porous materials includes collision with the polymer surface and sorption on the high permeant concentration side, diffusion through the material and finally desorption of the permeant on the low concentration side. Mass transfer properties of polymer films define the permeation process. Diffusion, solubility and permeability are among the parameters used to describe the mass transfer for a specific material/permeant combination [2,3]. Permeability is an important parameter, which measures the overall transfer rate through a polymer film [2].

When considering polymer-coated paperboards, the water vapor transmission rate (WVTR) is affected by e.g. the coating weight of the polymer as well as the temperature and humidity of surroundings [4]. The common synthetic moisture barrier polymers include low- and high-density polyethylenes, polypropylene and polyethylene terephthalate [5]. Other polymers with moisture barrier properties include cyclo-olefin copolymers, liquid-crystal polymers and nanocomposites [6,7]. Hygroscopic materials, such as many biopolymers, typically lose their barrier properties at high relative humidity. This is due to absorption of water and swelling of the polymer which results in a more porous or open structure [8]. Therefore, efforts have been made to improve the water vapor and oxygen barrier properties by coating such materials by e.g. thin glass-like SiO_x coatings [6,9].

Atomic layer deposition (ALD) is a surface controlled layer-by-layer process based on self-terminating gas-solid reactions and is uniquely suited to produce high-performance gas diffusion barrier coatings on porous materials as it allows preparation of dense and pin-hole-free inorganic films that are uniform in thickness even deep inside pores, trenches and cavities of various dimensions. In our previous work [10] we demonstrated that a thin layer of Al₂O₃ deposited by the ALD technique is an efficient way to improve the barrier properties of sensitive packaging materials such as various uncoated papers, polymer-coated papers and boards and plain polymer films. The suitability of ALD to produce high-performance barriers has also been studied elsewhere [11–13]. Especially Al₂O₃ depositions have been used to produce gas diffusion barriers on polymers. One of the problems of coating barrier layers on packaging materials is poor flexibility. Liang et al. previously reported an

* Corresponding author. Tel.: +358 40 5308 472; fax: +358 20 722 7026.

E-mail addresses: terhi.hirvikorpi@vtt.fi (T. Hirvikorpi), mika.vaha-nissi@vtt.fi (M. Vähä-Nissi), ali.harlin@vtt.fi (A. Harlin), maarit.karppinen@tkk.fi (M. Karppinen).

alternative method of barrier membrane fabrication by ALD [14]. Membranes made from polymer/ceramic nanocomposite were fabricated by extruding ALD- Al_2O_3 coated micron-sized high-density polyethylene particles. According to Liang et al., the difficulty seems to be the interface between the polymer and the ALD- Al_2O_3 layer. Due to the different surface properties of these materials voids are formed during extrusion. Parallel results have been reported also elsewhere [15–20]. There is a need to upgrade the existing packaging materials, and thin inorganic coatings are an interesting way to create high-performance materials for food packages.

Despite of its obvious advantages, ALD is in its current form a time consuming and relatively expensive process. In this work the aim was to clarify whether the ALD technique could be replaced with other techniques and still produce as efficient barriers toward gases as with the ALD technique. For the comparative techniques, magnetron sputtering (MS), electron beam evaporation (EBE) and a sol-gel (SG) method were chosen, as they have been in general employed to produce coatings with relatively good or excellent barrier properties [6,21,22].

2. Experimental details

Commercial-grade paperboards (provided by Stora Enso Oyj) with synthetic low-density polyethylene (LDPE) and biopolymer polylactic acid (PLA) coatings on one side as summarized in Table 1 were used as test substrates. The substrates were ca. $10 \times 10 \text{ cm}^2$ in size. On these substrates Al_2O_3 coatings aiming at thicknesses of 25, 50 and 100 nm were deposited at temperatures below 100°C by means of the four comparative thin-film techniques tested, i.e. ALD, MS, EBE and SG. The processes employed are well established and accordingly the actual thicknesses of the Al_2O_3 layers are believed to deviate at most by few nanometers from the target values.

The ALD- Al_2O_3 depositions of 250, 500 and 1000 cycles were carried out in a Picosun SUNALE™ reactor at 100°C reaction temperature. Depositions were made on silicon wafers and paperboard samples. Trimethylaluminum (TMA, electronic grade purity, SAFC Hitech) and water were used as precursors. High purity nitrogen (99.9999% N_2) was used as carrier and purge gas. The precursors were evaporated at near room temperature and a deposition sequence was: 0.2 s TMA pulse, 4 s purge, 0.1 s water pulse, and 15 s purge. The operating pressure was 500–1000 Pa. The resultant film growth rates and actual film thicknesses on the polymer-coated boards could not be directly measured. Instead, we estimated the film thicknesses based on the growth rate determined to be 0.094 nm/cycle with a Nanospec AFT4150 reflectometer for films grown with the same TMA- H_2O ALD process on a silicon wafer Si(100). It should however be emphasized that because of the different polarities and functional groups of the PE and PLA surfaces the actual growth rates on our polymer-coated board substrates may somewhat deviate from that determined for the ALD- Al_2O_3 coating on flat silicon wafer [23,24]. Although the aim was to deposit only on the polymer-coated side, film growth also on the uncoated side could not be totally prevented.

The MS- Al_2O_3 films were deposited using a Sloan SL1800 magnetron sputtering deposition system. One single rectangular aluminum target was used. The sputtering gases were Ar and O^{2-} ,

the latter being the reactive gas for oxide film formation. Stoichiometry of the film was controlled using in-situ optical emission monitor feedback from the target emission lines [25]. Pulsed DC power was applied to the aluminum target at a frequency of 150 kHz and a pulse off time of 1000 ns. The target was operated in the controlled current mode, fixed at 3 A. The background pressure in the chamber was $0.2\text{--}2.6 \times 10^{-4}$ Pa and the sputtering pressure during the Al_2O_3 deposition was around 0.28 Pa. The thicknesses of the deposited films were measured from Si(100) reference samples by spectroscopic ellipsometry. The temperature of the substrate was monitored by means of temperature-sensitive tapes attached to the substrate surface to assure that it remained below 100°C during the depositions. For comparison, pure aluminum films with a thickness of 50 nm were also grown by the MS technique on both substrate materials. This was made because as a thicker film, metallic Al is considered to be a high-performance barrier.

The equipment used in the EBE- Al_2O_3 depositions was a UHV-class electron beam gun evaporator. The distance from the Al_2O_3 source was approximately 30 cm. Before the depositions the chamber was flushed with dry N_2 gas in order to improve the pumping efficiency. The chamber was pumped into pressure of $0.1\text{--}1 \times 10^{-5}$ Pa. After this the electron beam of 200–250 W was focused on the Al_2O_3 source with a voltage of 6.55 kV. The area of the electron beam was 3–6 mm^2 . The deposition rate was 0.3–0.5 nm/min.

For the SG- Al_2O_3 depositions the substrates were pretreated with plasma in order to clean the surface before the depositions. The SG solution was a mixture of water and alcohol and it was catalyzed with acid. Aluminum alkoxide was used as a precursor. The SG solution was sprayed on the substrate and hardened in an oven. The temperature of the oven was kept below 100°C . It should be noted that pure Al_2O_3 depositions are not possible with the SG technique but traces of organic molecules will be always present in the film due to the precursor solution. The thicknesses of the SG- Al_2O_3 layers deposited on Si(100) substrates were measured with the spectrophotometric modeling method described by Ylilammi and Ranta-aho [26]. The reflectance spectra for thickness modeling were recorded with a Hitachi U-2000 spectrophotometer in the 190–1100 nm wavelength range and modeling was performed with the Thinfilm program.

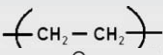
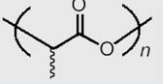
Images were taken of the uncoated substrates with an atomic force microscope (AFM; Park Systems XE-100) in order to clear their surface morphologies. Inductively coupled plasma atomic emission spectroscopy (ICP-AES) analyses were carried out in order to determine the amount of aluminum in the ALD- Al_2O_3 deposited samples. Test pieces of the substrates before and after each ALD treatment were ignited and dissolved in an alkali metal melt. The results are expressed as mg/m^2 . Two to three parallel analyses from every sample were performed.

All the samples together with the uncoated substrate materials used were characterized for their oxygen transmission rate (OTR) expressed as $\text{cm}^3/\text{m}^2/10^5 \text{ Pa/day}$ and water vapor transmission rate (WVTR) expressed as $\text{g/m}^2/\text{day}$. The OTR measurements were carried out using humid gases with Mocon OXTRAN equipment such that the Al_2O_3 -deposited side of the sample faced the carrier gas stream. The measurements were performed at room temperature (23°C) and at 50–60% relative humidity. Two to three parallel samples were measured. The WVTR measurements were carried out for five parallel samples according to the modified gravimetric methods ISO 2528:1995 and SCAN P 22:68. The test conditions were 23°C and 75% relative humidity.

3. Results and discussion

Fig. 1 presents AFM images of the two uncoated substrate materials, B(PE) and B(PLA). The surface of B(PLA) appears to be smoother than that of B(PE). This might be due to its larger polymer-coating weight (35 g/m^2) in comparison to that for B(PE) (15 g/m^2),

Table 1
Commercial substrates used in the deposition tests.

Code	Description	Skeletal of the polymer
B(PE)	Low-density polyethylene (LDPE) coated (15 g/m^2) board	
B(PLA)	Polylactic acid (PLA) polymer-coated (35 g/m^2) board	

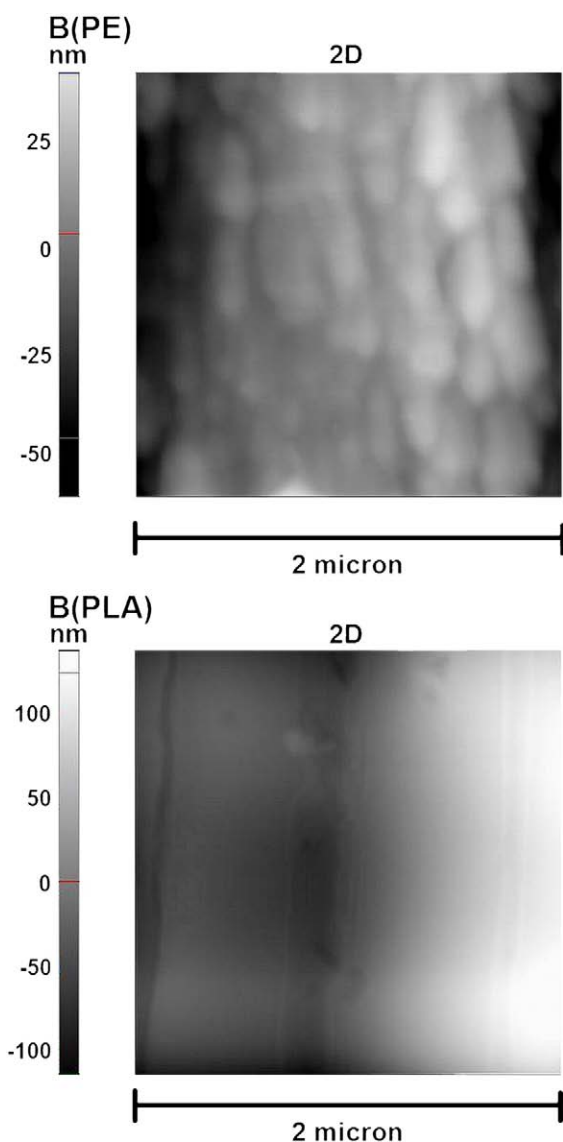


Fig. 1. AFM images of PE-coated paperboard (B(PE)) and PLA-coated paperboard (B(PLA)) substrate materials.

see Table 1. Another explanation could be the different chill roll surface patterns used in extrusion coating of the paperboard.

Due to their different surface roughness, the two substrate materials apparently accommodate different amounts of Al_2O_3 during parallel ALD treatments. In Table 2, ICP-AES results for the Al contents (expressed in mg/m^2) in the various ALD- Al_2O_3 treated B(PE) and B(PLA) samples are summarized. The results are given as average \pm standard deviation of two to three parallel analyses. It can be seen from Table 2 that the Al content increases with increasing number or ALD cycles or increasing Al_2O_3 -film thickness. Compared to the smoother B(PLA) substrate, the B(PE) substrate has larger specific

Table 2
ICP-AES results for the Al content in ALD- Al_2O_3 coated B(PE) and B(PLA) samples. The results are given as average \pm standard deviation of two to three parallel analyses.

	Al content (mg/m^2)	
	B(PE)	B(PLA)
25 nm ALD- Al_2O_3	260 \pm 3	96 \pm 0.2
50 nm ALD- Al_2O_3	650 \pm 260	380 \pm 150
100 nm ALD- Al_2O_3	860 \pm 200	495 \pm 78

surface area and accordingly larger concentration of surface sites to accommodate larger amounts of TMA and water molecules upon the ALD depositions. The results show, however, that the standard deviations with the thicker (50 and 100 nm) films are greater than those with the thinner (25 nm) films. The porosity and the variances in porosity within pristine substrate materials may explain this. This may partly be also due to the different polarities of the polymer surfaces leading to different nucleation periods needed for the ALD- Al_2O_3 film growth as explained elsewhere [23,24].

Results from the oxygen transmission rate (OTR) and water vapor transmission rate (WVTR) measurements are presented in Tables 3 and 4, respectively. Based on the results the positive effect of a thin Al_2O_3 layer on both the OTR and WVTR values is evident. The oxygen barrier performance of B(PLA) remains better than that of B(PE) independent of the thickness of the Al_2O_3 layer and the deposition technique employed. Tables 3 and 4 also reveal that the ALD technique is the best among the coating techniques investigated. Most impressively, when coating B(PLA) with a 25-nm thick Al_2O_3 layer by means of ALD, both the OTR (21 $\text{cm}^3/\text{m}^2/10^5$ Pa/day) and WVTR (1.4 $\text{g}/\text{m}^2/\text{day}$) values are excellent. In terms of the oxygen barrier property this sample is even better than the one coated with metallic aluminum by means of the MS technique (26 $\text{cm}^3/\text{m}^2/10^5$ Pa/day).

The barrier performances of B(PE) and B(PLA) coated with Al_2O_3 by different techniques were found quite different. This could be due to the different ability of different techniques to form high-quality conformal films under the chosen deposition conditions. ALD is the only technique where the substrate is most perfectly and conformally coated from all sides. The probability of a pin-hole extending through the thin film or the whole material is smaller when the film is constructed of layer-by-layer deposited Al_2O_3 coating compared to a single deposition. In addition, the moisture being removed from the board during the deposition may affect the processes utilizing lower pressures, such as the MS technique.

The barrier properties of the pristine substrates were different making the reference level very different for these two substrates. Nevertheless, based on the results from OTR and WVTR measurements it seems to be so that when the substrate is rough a thicker Al_2O_3 layer is needed to block the diffusion of oxygen and water molecules. If the substrate is smooth a thinner Al_2O_3 barrier layer is enough; an excessively thick Al_2O_3 layer on top of a smooth substrate may be rather prone to cracking, which in turn impairs the barrier properties. It should also be emphasized that the two substrate materials used possess different surface chemistries. There are significantly fewer

Table 3

Oxygen transmission rates of uncoated, Al_2O_3 -coated and Al-coated B(PE) and B(PLA) samples. The results are given as average \pm standard deviation of two to three parallel measurements.

Deposition technique	OTR ($\text{cm}^3/\text{m}^2/10^5$ Pa/day)			
	ALD	MS	EBE	SG
B(PE) uncoated	7900 \pm 1600	7900 \pm 1600	7900 \pm 1600	7900 \pm 1600
B(PE) + 25 nm Al_2O_3	6700 \pm 2500	>10 000 ^a	3900 \pm 1900	8300 \pm 2400
B(PE) + 50 nm Al_2O_3	2700 \pm 400	>10 000 ^a	5200 \pm 400	7400 \pm 3600
B(PE) + 100 nm Al_2O_3	2300 \pm 100	>10 000; 645 ^b	3300 \pm 600	8400 \pm 2200
B(PE) + 50 nm Al	–	>10 000 ^a	–	–
B(PLA) uncoated	420 \pm 10	420 \pm 10	420 \pm 10	420 \pm 10
B(PLA) + 25 nm Al_2O_3	20 \pm 3	160 \pm 120	150 \pm 10	460 \pm 10
B(PLA) + 50 nm Al_2O_3	60 \pm 5	85 \pm 85	300 \pm 140	400 \pm 10
B(PLA) + 100 nm Al_2O_3	200 \pm 40	65 \pm 0.5	210 \pm 15	370 \pm 10
B(PLA) + 50 nm Al	–	26 \pm 1	–	–

^a The reliable detection limit with this OTR equipment is 10 000 $\text{cm}^3/\text{m}^2/10^5$ Pa/day.

^b Great variation between parallel samples, average could not be reliably calculated.

Table 4

Water vapor transmission rates of uncoated, Al₂O₃-coated and Al-coated B(PE) and P(PLA) samples. The results are given as average ± standard deviation of five parallel measurements.

Deposition technique	WVTR (g/m ² /day)			
	ALD	MS	EBE	SG
B(PE) uncoated	7.0 ± 0.9	7.0 ± 0.9	7.0 ± 0.9	7.0 ± 0.9
B(PE) + 25 nm Al ₂ O ₃	6.9 ± 0.1	3.5 ± 1.0	5.7 ± 1.2	9.2 ± 3.3
B(PE) + 50 nm Al ₂ O ₃	2.0 ± 0.5	2.4 ± 0.9	3.9 ± 0.3	6.8 ± 0.5
B(PE) + 100 nm Al ₂ O ₃	2.0 ± 0.5	2.8 ± 1.3	3.7 ± 0.3	6.4 ± 0.6
B(PE) + 50 nm Al	–	2.0 ± 1.2	–	–
B(PLA) uncoated	64.9 ± 1.6	64.9 ± 1.6	64.9 ± 1.6	64.9 ± 1.6
B(PLA) + 25 nm Al ₂ O ₃	1.4 ± 0.2	11.0 ± 5.0	25.9 ± 2.7	62.5 ± 1.0
B(PLA) + 50 nm Al ₂ O ₃	1.8 ± 0.5	0.5 ± 0.1	21.8 ± 4.2	62.3 ± 1.9
B(PLA) + 100 nm Al ₂ O ₃	29.1 ± 5.1	1.9 ± 0.6	21.6 ± 7.1	62.0 ± 0.6
B(PLA) + 50 nm Al	–	1.3 ± 0.5	–	–

functional groups on the surface of B(PE) compared to the functional OH[−] groups on the surface of B(PLA). The lack of functional groups at surface may lead to poor bonding between the polymer surface and the Al₂O₃ layer. The lack of functional groups may also lead to cracking after the Al₂O₃ layer has been deposited.

The paperboard itself and even more significantly the polymer coating on top of it have an effect on the barrier performance of the final Al₂O₃-coated sample. Among the two polymers (at least in pure form), the melting point and the glass transition temperature are higher for PLA than for LDPE, making PLA more stable under the presently employed deposition conditions. At elevated deposition temperatures (around 100 °C) the polymer chains of LDPE start to move which may create pores and result in poor film growth. As a general observation from the OTR and WPTR values given in Tables 3 and 4, it is clear that with both the substrate materials the relation between the Al₂O₃-layer thickness and the gas barrier performance was not completely linear. The results for e.g. MS-Al₂O₃ treatments showed a very irregular behavior. This is at least partly due to the fact that the substrate is somewhat sensitive to the treatment conditions and thus the barrier performance varies accordingly. Although the ALD-Al₂O₃ layer deposited at 100 °C should be amorphous, the Al₂O₃ layer has also an effect on the cracking behavior as partial crystallization of the polymer coating on the substrate may cause interfacial tension between the Al₂O₃ layer and the polymer coating. This means that in practice a thicker inorganic film does not necessarily lead to improved barrier properties. This was in particular clear with the ALD-grown films, as even very thin films grown by the ALD technique are known to be highly conformal, dense and pin-hole free. Here, among the ALD-treated samples the best results were gained for samples with a 25-nm or 50-nm (but not 100-nm) thick ALD-Al₂O₃ coating. For the MS-grown films the film thickness had to be approximately doubled to achieve the same barrier level, see Tables 3 and 4. The growth circumstances were not optimized to these substrates during the depositions which may lead to better barrier results in the future.

When compared to the OTR and WVTR results in our previous studies [10] the results in this paper are better. This is due to several factors; the quality of the substrate materials may differ between different manufacturing lots. The tests indicate that the materials used in this study were better barriers as such. The other plausible explanation for the different barrier performance could be that in this study we used TMA with higher purity and 20 °C higher deposition temperatures. These could influence on the quality and conformality of the ALD-Al₂O₃ coating.

4. Conclusions

Thin (25–100 nm) layers of Al₂O₃ were grown at low temperatures on two types of polymer-coated paperboards by means of four

different thin film deposition techniques, i.e. atomic layer deposition (ALD), magnetron sputtering (MS), electron beam evaporation (EBE) and a sol-gel (SG) method. The aim of the work was to compare the different deposition techniques for their capability to produce high-quality gas barrier layers on top of commercial paperboard packaging materials. Despite the substrate material and the deposition technique employed, the gas barrier properties were significantly improved once the packaging material was coated with a thin layer of Al₂O₃. Among the four deposition techniques investigated, the best results were obtained with the ALD technique, followed by the MS technique. ALD technique was best among these techniques because the ALD-grown Al₂O₃ layers were most dense and the deposition conditions were most suitable for these sensitive materials in the ALD reactor. Films grown by ALD are typically highly conformal, dense and pin-hole free and therefore even nanometer-scale films are thick enough to work as efficient gas barriers. Paperboard coated with polylactic acid (PLA) polymer and a 25-nm thick ALD-grown Al₂O₃ layer was found as a highly promising barrier against oxygen and water vapor.

Acknowledgements

The authors thank Picosun Oy for fabricating the ALD deposited samples, Millidyne Oy for the SG deposited samples, LUT (ASTRA unit) for the MS deposited samples and Savonia University of Applied Sciences for the work with the EBE technique. Harry Helén from University of Helsinki is thanked for measuring the oxygen transmission rates, Metsäliitto Group, Myllykoski Corporation, Stora Enso Oyj and UPM-Kymmene Oyj for their funding and Stora Enso Oyj also for providing the substrates.

References

- [1] C. Andersson, Packag. Technol. Sci. 21 (2008) 339.
- [2] F. Johansson, Doctoral dissertation Chalmers University of Technology, Gothenburg, Sweden, 1996.
- [3] M. Chainey, Transport phenomena in polymer films, Composites and specialty applications, Handbook of polymer science and technology, Vol. 4, Marcel Dekker, 1989, pp. 499–540.
- [4] J. Kuusipalo, K. Lahtinen, TAPPI J. 7 (2008) 8.
- [5] A. Savolainen, Paper and Paperboard Converting, Fapet Oy, Helsinki Finland, 1998, p. 123.
- [6] J. Lange, Y. Wyser, Packag. Technol. Sci. 16 (2003) 149.
- [7] A. Sorrentino, M. Tortora, V.J. Vittoria, Polym. Sci. B 44 (2006) 265.
- [8] M. Stading, Å. Rindlav-Westling, P. Gatensholm, Carbohydr. Polym. 45 (2001) 209.
- [9] Y. Leterrier, Prog. Mater. Sci. 48 (2003) 1.
- [10] T. Hirvikorpi, M. Vähä-Nissi, T. Mustonen, E. Iiskola, M. Karppinen, Thin Solid Films 518 (2010) 2654.
- [11] M.D. Groner, S.M. George, R.S. McLean, P.F. Garcia, Appl. Phys. Lett. 88 (2006) 051907.
- [12] P.F. Garcia, R.S. McLean, M.H. Reilly, M.D. Groner, S.M. George, Appl. Phys. Lett. 89 (2006) 031915.
- [13] S.H.K. Park, J. Oh, C.S. Hwang, J.I. Lee, Y.S. Yang, H.Y. Chu, Electrochem. Solid State Lett. 8 (2005) H21.
- [14] X.H. Liang, D.M. King, M.D. Groner, J.H. Blackson, J.D. Harris, S.M. George, A.W. Weimer, J. Membr. Sci. 322 (2008) 105.
- [15] T.T. Moore, W.J. Koros, J. Mol. Struct. 739 (2005) 87.
- [16] R. Mahajan, W.J. Koros, Ind. Eng. Chem. Res. 39 (2000) 2692.
- [17] R. Mahajan, W.J. Koros, Polym. Eng. Sci. 42 (2002) 1420.
- [18] R. Mahajan, W.J. Koros, Polym. Eng. Sci. 42 (2002) 1432.
- [19] R. Mahajan, R. Burns, M. Schaeffer, W.J. Koros, J. Appl. Polym. Sci. 86 (2002) 881.
- [20] T.T. Moore, R. Mahajan, D.Q. Vu, W.J. Koros, AIChE J. 50 (2004) 311.
- [21] J. Kuusipalo (Ed.), Paper and Paperboard Converting, Fapet Oy, Helsinki Finland, 2008, p. 174.
- [22] S. Ambers-Schwab, M. Hoffmann, H. Bader, M. Gessler, J. Sol-Gel Sci. Technol. 1 (2) (1998) 141.
- [23] J.D. Ferguson, A.W. Weimer, S.M. George, Chem. Mater. 16 (2004) 5602.
- [24] X.H. Liang, L.F. Hakim, G.D. Zhan, J.A. McCormick, S.M. George, A.W. Weimer, J.A. Spencer, K.J. Buechler, J. Blackson, C.J. Wood, J.R. Dorgan, J. Am. Ceram. Soc. 90 (2007) 57.
- [25] Z. Pang, M. Boumerzoug, R.V. Kruzelecky, P. Mascher, J.G. Simmons, D.A. Thompson, J. Vac. Sci. Technol. A 12 (1994) 83.
- [26] M. Yililampi, T. Ranta-Aho, Thin Solid Films 232 (1993) 56.

PUBLICATION II

**Atomic layer deposited aluminum
oxide barrier coatings for
packaging materials**

In: Thin Solid Films 518 (2010),
pp. 2654–2658.

Reprinted with permission from the publisher.



Atomic layer deposited aluminum oxide barrier coatings for packaging materials

Terhi Hirvikorpi ^{a,1}, Mika Vähä-Nissi ^{a,*}, Tuomas Mustonen ^{a,1}, Eero Iiskola ^a, Maarit Karppinen ^b

^a Oy Keskuslaboratorio – Centrallaboratorium Ab (KCL), P.O. Box 70, FI-02151 Espoo, Finland

^b Laboratory of Inorganic Chemistry, Department of Chemistry, Helsinki University of Technology, P.O. Box 6100, FI-02015 TKK, Finland

ARTICLE INFO

Article history:

Received 20 April 2009

Received in revised form 6 August 2009

Accepted 11 August 2009

Available online 12 October 2009

Keywords:

Atomic layer deposition
Aluminum oxide
Diffusion barriers
Biodegradable polymers
Polymers
Packaging material

ABSTRACT

Thin aluminum oxide coatings have been deposited at a low temperature of 80 °C on various uncoated papers, polymer-coated papers and boards and plain polymer films using the atomic layer deposition (ALD) technique. The work demonstrates that such ALD-grown Al₂O₃ coatings efficiently enhance the gas-diffusion barrier performance of the studied porous and non-porous materials towards oxygen, water vapor and aromas.

© 2009 Elsevier B.V. All rights reserved.

1. Introduction

Various future distribution channels and the key role of packaging in ensuring the quality and safety of a wide variety of food items will increase the need for better packaging materials. Here the paper and board industry has to compete with the plastics industry for the market share. Fiber-based packages have advantages over their plastic competitors, such as sustainability, recyclability and stiffness/weight ratio. However, poor barrier properties and sensitivity towards moisture are some of the main challenges of the fiber-based materials. On the other hand, oil-based barrier coatings create problems for recycling. Development of biomaterials to replace the currently used oil-based ones is under way thus improving the competitiveness of fiber-based packaging materials and enabling enhanced packaging solutions [1]. There is a clear need to upgrade the existing materials and thin inorganic coatings are an interesting way to create high-performance materials for food packages.

Here we demonstrate significantly enhanced barrier properties towards oxygen, water vapor and aromas for various polymer-coated papers and paperboards as achieved by coating them with a thin conformal aluminum oxide layer grown by the atomic layer deposition (ALD) technique. ALD is a surface controlled layer-by-layer process based on self-terminating gas–solid reactions and is uniquely suited to

produce high-performance gas-diffusion barrier coatings on porous materials as it allows preparation of dense and pinhole-free inorganic films that are uniform in thickness even deep inside pores, trenches and cavities of various dimensions. The other advantages of ALD include low impurity content and mild deposition conditions in terms of temperature and pressure. There is a wide range of ALD-grown materials and commercial applications, from catalysts to electroluminescent displays in microelectronics and beyond [2–4].

The ALD technique has been used to produce gas-diffusion barriers on polymers [5–7]. Water-vapor transmission rates of the order of 1×10^{-3} g/m²/day were reported for less than 25-nm thick Al₂O₃ depositions on polymers [5]. In addition, Park et al. [7] reported a water-vapor transmission rate value of 0.03 g/m²/day at 38 °C and 100% relative humidity for an ALD-grown Al₂O₃ barrier that was 30 nm thick and deposited on both sides of a poly(ethersulfone) substrate, whereas Garcia et al. [6] showed that a 25-nm thick ALD-Al₂O₃ barrier films on poly(ethylene naphthalate) substrates can have a water-vapor transmission rate less than 1×10^{-5} g/m²/day. These results are, however, only partly comparable with our results because some of our substrates are biodegradable. Our aim was to study biodegradable and recyclable substrates and compare the results to those obtained for conventional synthetic polymer substrates used as gas-diffusion barriers. There are no previous studies concerning less than 100-nm thick ALD-grown Al₂O₃ layers on biodegradable polymers or fiber-based substrates coated with synthetic or biopolymers.

2. Experimental details

A variety of uncoated papers, polymer-coated boards and papers, and plain polymer films as summarized in Table 1 were used as

* Corresponding author. VTT Tekniikantie 2, Espoo, P.O. Box 1000, FI-02044 VTT Finland. Tel.: +358 40 5308 472; fax: +358 9 464 305.

E-mail addresses: terhi.hirvikorpi@vtt.fi (T. Hirvikorpi), mika.vaha-nissi@vtt.fi (M. Vähä-Nissi), tuomas.mustonen@vtt.fi (T. Mustonen), eero.iiskola@kcl.fi (E. Iiskola), maarit.karppinen@tkk.fi (M. Karppinen).

¹ VTT Technical Research Centre of Finland, Tekniikantie 2, Espoo, P.O. Box 1000, FI-02044 VTT Finland.

Table 1
Commercial substrates used in the ALD- Al_2O_3 deposition tests.

Code	Description
P(PIG)	Pigment-coated and calendered high gloss paper 60 g/m ²
P(LDPE)	Polyethylene (LDPE) coated paper
P(UNC)	Commercial uncoated copy paper 80 g/m ²
B(PE)	Polyethylene-coated (15 g/m ²) board
B(PLA)	Poly(lactic acid (PLA) coated (35 g/m ²) board
PEN	Polyethylene naphthalene (PEN) film, 50 μm
PP	Polypropylene film, 30 μm
PET	Polyester (PET) film, 50 μm
PLA	PLA film, 25 μm

substrates for the Al_2O_3 depositions. Al_2O_3 coatings of different thicknesses (of 5, 25, 50, 100 and 900 nm) were deposited at 80 °C using a commercial ALD TFS 500 reactor manufactured by Beneq Ltd., Finland. Trimethylaluminum (TMA, Sigma-Aldrich, 98% purity) and water were used as precursors for aluminum and oxygen, respectively. The precursors were introduced in the reactor in alternate pulses, separated by an inert N_2 gas pulse such that one ALD cycle comprised the following four process steps: (i) TMA pulse, (ii) N_2 purge pulse, (iii) water pulse, and (iv) N_2 purge pulse [8]. The substrates were ca. 10 cm*10 cm in size, and they were coated on one side only. This was achieved by taping the substrate on the sides so that the gas flow could only reach one side of the substrate. The targeted coating thicknesses were produced according to the TFS 500 reactor process parameters based on the thicknesses determined for Al_2O_3 films on a silicon wafer by means of ellipsometry with an accuracy of ± 0.5 nm.

Thermogravimetric (TG) analysis was performed for all substrate materials except P(PIG) and P(UNC) to reveal the thermal behavior and the limitations of different polymer coatings to be used as substrates in ALD depositions. The TG experiments were performed in both air and nitrogen atmospheres with a heating rate of 10 °C/min.

Selected samples, *i.e.* P(UNC), P(PIG), B(PE) and B(PLA), were characterized with X-ray photoelectron spectroscopy (XPS; KRATOS AXIS 165) for the surface chemistry and surface distributions and by scanning electron microscopy (SEM; Hitachi S-3400 N VP-SEM, operating voltage 15 keV) for the microstructure. In the XPS analysis monochromatic Al K α (12.5 kV, 8 mA) radiation at 100 W was used. Wide binding energy range spectra (0–1100 eV) were recorded using 80 eV pass energy and 1 eV step. The high-resolution spectra of C 1s and O 1s regions were also recorded, using 20 eV pass energy and 0.1 eV. The area measured was approximately 1 mm² while the analysis varies from 2 to 10 nm, depending on the element and on the sample material. Also an atomic force microscopy (AFM; Nanoscope III a Multimode scanning probe microscope, Digital Instruments Inc.) image from the PEN film (PEN) was taken to demonstrate the topography of the ALD-treated sample surface.

The oxygen transmission rates (OTR) were measured using humid gases with a Mocon OXTRAN equipment and expressed as cm³/m²/10⁵ Pa/day. The measurements were performed at 23 °C and at 50–60% relative humidity. The water-vapor transmission rates (WVTR) were measured from flat samples according to the modified gravimetric methods ISO 2528:1995 and SCAN P 22:68 and were expressed as g/m²/day. The test conditions were 23 °C and 75% relative humidity. KCL AromaBar equipment was used for evaluating the aroma barrier properties. Details of the test cell and the method used have been described elsewhere [9].

3. Results and discussion

3.1. Thermal stability of the biopolymer-coated substrate materials

Thermogravimetric analyses were performed both in air and nitrogen atmospheres to reveal the thermal behavior and the limitations of different polymers and polymer-coated papers and boards to be used

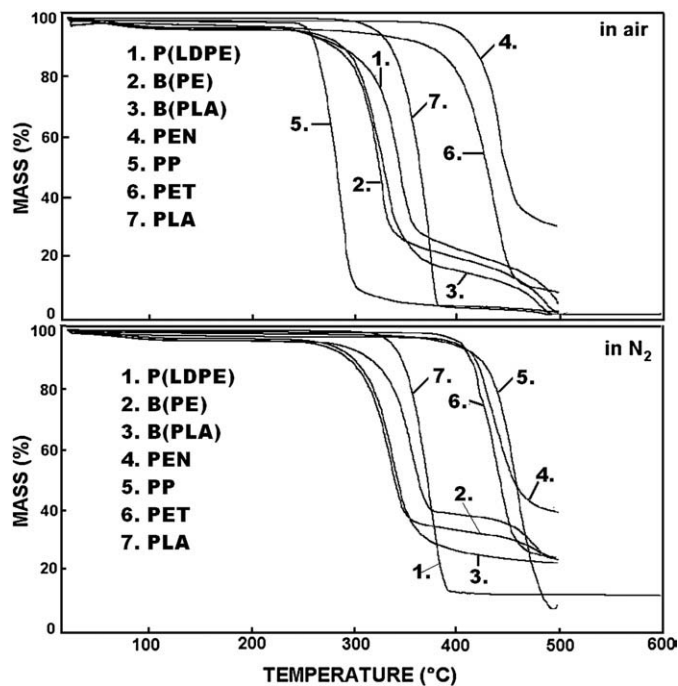


Fig. 1. TG curves recorded for seven different substrate materials in air and nitrogen atmospheres.

as substrates in the ALD depositions. The resultant TG curves are presented in Fig. 1. All the substrate materials investigated were found to behave quite similarly. No significant water removal occurred at low temperatures, instead the materials decomposed in an essentially single, sharp step at temperatures ranging from 300 to 450 °C. Except for PEN and PET, decomposition was practically complete by 450 °C in air, whereas in nitrogen the decomposition was more incomplete and shifted to higher temperatures. Most importantly, the TG measurements confirmed that the materials tested do not degrade thermally at temperatures employed in low-temperature ALD experiments, *i.e.* below ~150 °C.

3.2. Characterization of the Al_2O_3 coatings

XPS provides two independent means of surface coverage analysis. In the conventional approach, quantitative analysis based on XPS peak

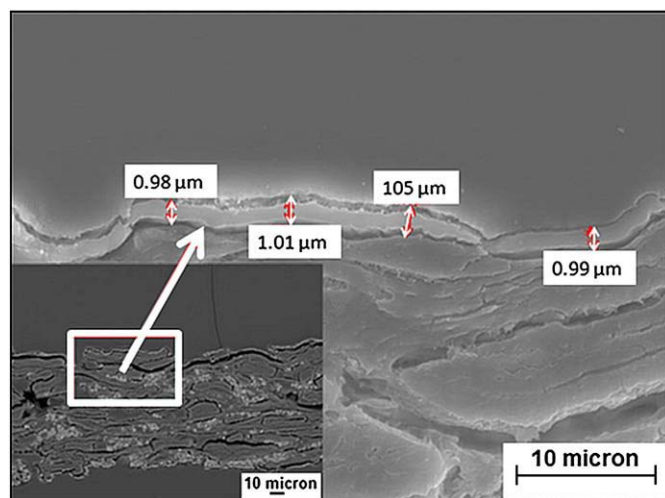


Fig. 2. A cross-cut SEM image from a paper sample P(UNC) with a 900-nm thick ALD-grown layer of Al_2O_3 on top of it.

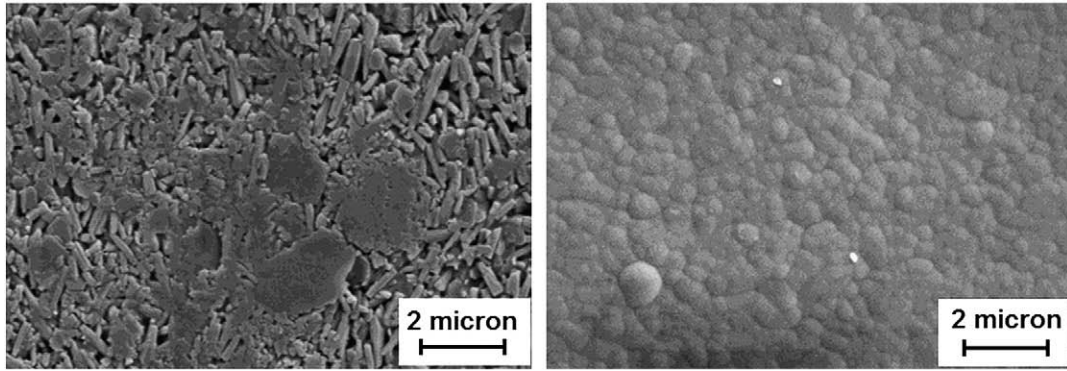


Fig. 3. SEM images of pigment-coated paper surface of P(PIG) as such (left) and with a 900-nm thick ALD-grown Al_2O_3 layer on top of it (right).

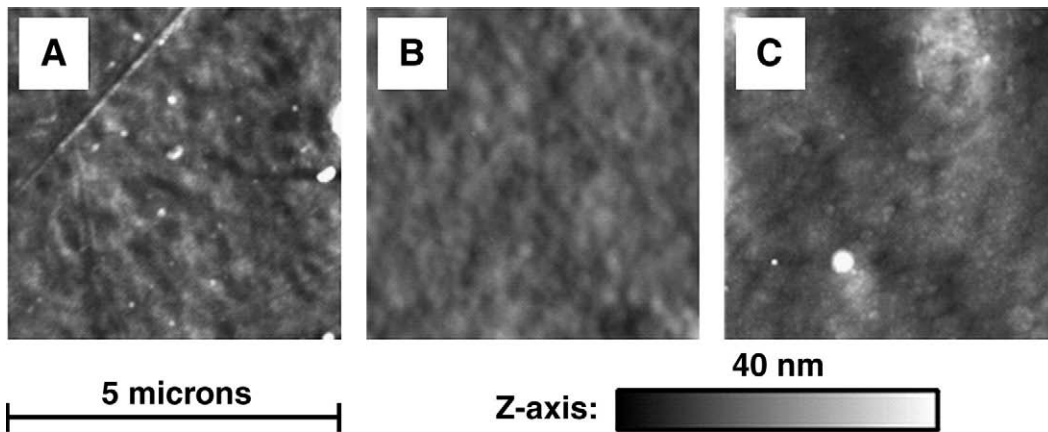


Fig. 4. AFM topographic images of A) a pure polyethylene naphthalene film (PEN) with B) a 100-nm thick and C) a 900-nm thick ALD-grown Al_2O_3 layer on top of it.

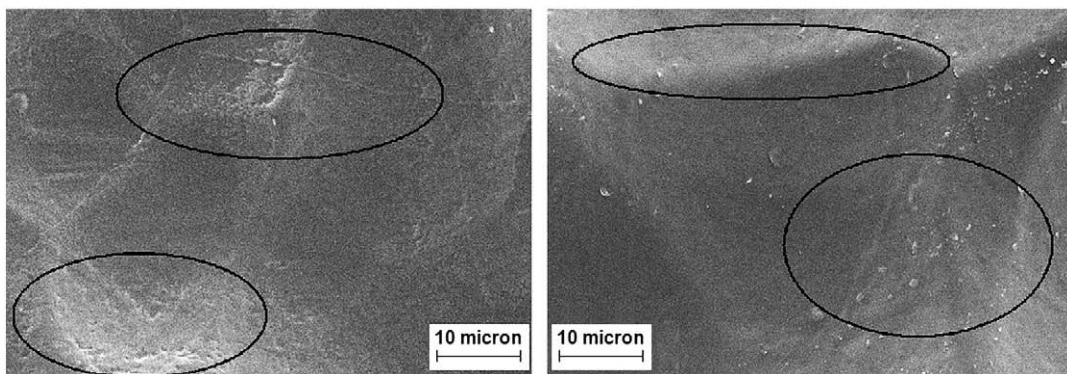


Fig. 5. SEM images of polyethylene-coated board B(PE) (left) and poly(lactic acid)-coated board B(PLA) (right) with a 20-nm thick ALD-grown Al_2O_3 layer on top of it.

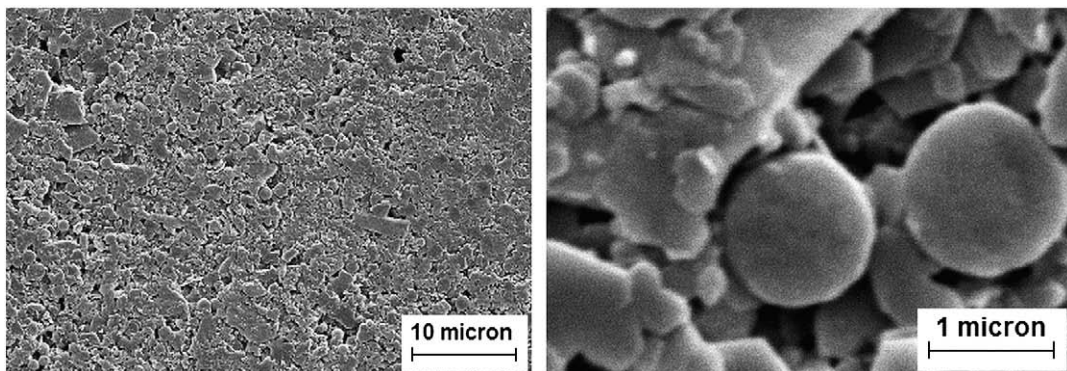


Fig. 6. SEM images of coated paper P(PIG) with magnification from the deposited 900-nm layer of Al_2O_3 .

intensities is used. In addition to this, surface depth distributions may be evaluated from the spectral backgrounds tailing each peak, according to the approach formulated by Tougaard et al. [10–13]. This latter method is especially well suited for thin film studies, because it differentiates homogeneous films from films with loopholes, and because it gives information of surface coverage up to three times the inelastic mean free path (IMFP) of the photoelectron signal studied.

Here, the XPS analyses were performed on samples with a 25-nm thick aluminum oxide coating, in order to evaluate the chemistry and the coverage of the ALD-deposited coating. In the case of even, 25-nm thick surface film, the sample should behave as a semi-infinite bulk material. This means that there should be no signal from the substrate, neither as peaks nor as changes in the spectral background. Thus, XPS data of a uniform surface film should be similar to the respective bulk material (including peaks and the spectral backgrounds tailing them).

In this case, coverage analysis using elements was not optimal, since the surface contamination (unavoidable in air-exposed metal oxide surfaces) and substrate both contained carbon. However, the carbon signal detected was chemically similar to typical surface contamination (but differed markedly from substrates). Furthermore, there was no inelastic background tailing the carbon signal, indicating that the carbon observed originated just from the outmost surface and not from the bulk. In addition to these, the spectral background shapes of aluminum and oxygen were both indicative of uniform, homogeneous depth distributions.

Put together, XPS data confirmed that the substrates *i.e.* P(PIG), B(PE) and B(PLA), had been covered quite efficiently by a homogenous ALD layer of Al₂O₃, within the detection depth of XPS (2–10 nm).

SEM images were taken to inspect the cross cuts and surfaces of the Al₂O₃-coated samples. In Fig. 2, a cross-cut SEM image taken from a paper sample P(UNC) with a 900-nm ALD-grown layer of Al₂O₃ on top of it is shown. The deposited Al₂O₃ layer is readily observed and found to be highly conformal and homogeneous in thickness. With porous surfaces, such as the surface of our uncoated paper sample P(UNC), Al₂O₃ enters also into the pores of the paper.

Fig. 3 shows SEM images of a pigment-coated paper P(PIG) before and after the deposition of a 900-nm thick Al₂O₃ layer. The initial topography of the substrate surface has no substantial effect on the resultant Al₂O₃ surface. That is, the barrier layer is nearly complete as it fills or overlays the pores. Very similar surface structures have been observed also for other materials studied here.

Fig. 4 presents AFM images of a pure polyethylene naphthalene film and the same film with 100-nm and 900-nm thick Al₂O₃ layers on top of it. The surface looks rather similar to the pigment-coated paper surface with a similar Al₂O₃ coating (Fig. 3). Both pigment-coated paper and PEN surfaces with a thick Al₂O₃ coating appear granular. The surface of a pure PEN film shows also a fine structure in the nm scale (rms roughness 4.5 nm). A 100-nm thick Al₂O₃ layer (rms 2.94 nm) cannot totally hide the surface features, but with a 900-nm thick layer (rms 4.89 nm) the granularity is obvious. The granular surfaces could be due to the uneven surface properties and hydrophobicity of the substrate. Our hypothesis is that the unevenness and hydrophobicity influence the water pulse in the ALD cycle. The chemical variations of the polymer as well as the variations in crystallinity of the polymer may cause the ALD-Al₂O₃ layer

Table 2

Oxygen transmission rates (cm³/m²/10⁵ Pa/day) of non-coated and Al₂O₃-coated (with various Al₂O₃-layer thicknesses) samples.

Code	Non-coated	25 nm	50 nm	100 nm
P(PIG)	>20,000	>20,000	>20,000	>20,000
B(PE)	>20,000	6650	818	3700
B(PLA)	3150	49	121	513
PP	1250	170	109	103
PET	24	11	12	10
PLA	315	44	32	57

Table 3

Water-vapor transmission rates (g/m²/day) of non-coated and 50-nm Al₂O₃-coated samples.

Code	Non-coated	50 nm
P(LDPE)	5.4	3.1
B(PE)	8.5	4.6
B(PLA)	131	14
PEN	0.9	0.6
PLA	93	3.3

to grow unevenly. Pretreatment procedures could solve both of these problems.

The polyethylene-coated and polylactic acid-coated board samples, B(PE) and B(PLA), in Fig. 5 are coated with a 20-nm thick Al₂O₃ layer. Small structural features (marked in the figure) can be observed in the sample surfaces in the SEM images. The sample surfaces seem to be grainy. The polymer surface is probably partly heterogeneous. This may have an influence on the growth of the Al₂O₃ layer, especially in the beginning of the ALD process. In addition, if the sample is highly porous, thin Al₂O₃ layers cannot totally fill the pores, as indicated in Fig. 6 for the coated paper P(PIG).

3.3. Barrier properties

Oxygen transmission rates were measured by positioning the Al₂O₃-coated side of the sample facing the carrier gas stream. The thus obtained OTR values are presented in Table 2. From Table 2, it is clearly seen that the ALD-Al₂O₃ treatment has improved the oxygen barrier properties of the materials tested here. However, the OTR value does not change linearly with the thickness of the deposited Al₂O₃ layer. In the cases of the polymer-coated paper and board substrates, B(PE) and B(PLA), and the plain polylactic acid film sample PLA, a higher OTR value is obtained for a 100-nm thick Al₂O₃ coating than for the thinner layers. For the polypropylene film substrate PP, on the other hand, the OTR value decreases with increasing thickness of the Al₂O₃ layer. With the polyester film substrate PET the thinnest Al₂O₃ layer seems to improve the barrier properties as much as the thicker layers. The varying responses could be due to *e.g.* differences between the surface roughnesses of the polymers. An excessively thick layer may cause cracking, which in turn impairs the barrier properties. The OTR value for the pigment-coated paper P(PIG) remains very high, even for the Al₂O₃-layer thickness of 100 nm. In this case the substrate surface contained cracks and the pores were probably not filled with a thick ALD-Al₂O₃ layer.

The water-vapor transmission rate measurements were carried out for substrates coated with a 50-nm thick Al₂O₃ layer, and for each material three parallel samples were measured. The WVTR results are presented in Table 3. Similarly to the OTR values, the positive effect of a thin Al₂O₃ layer on the WVTR value is evident. Especially the polylactic acid-coated board and the polylactic acid film samples B(PLA) and PLA are found to experience a significant improvement in the WVTR as achieved through the ALD-grown Al₂O₃ layer.

The aroma barrier properties were measured only for one substrate material, polyethylene-coated paper P(LDPE). Results are shown in Table 4. Although the diffusion coefficient decreases more

Table 4

Diffusion coefficients (10⁻¹⁵m²/s) for different aromas measured for the P(LDPE) sample before and after coating it with a 50-nm Al₂O₃ layer.

Code	coated	50 nm
Isoamyl acetate	9.1	3.6
D-Limonene	15.8	8.7
cis-3-hexenol	7.6	3.6
r-Carvone	9.9	5.2

than 50% of the original value the aroma barrier properties are considered to be of medium level only. The improvement is not as dramatic as expected. This result is in line with the results from the WVTR measurements for the same substrate material.

4. Conclusions

Aluminum oxide films with thicknesses ranging from few nanometers to one-micron scale were grown using the ALD technique at low temperature on polymer films and on papers and boards coated with polymers. XPS and SEM results indicated that even the thinnest films provided a good coverage over the surface features of the various porous and non-porous substrate materials investigated. However, there were also signs of some graininess in nanometer scale which may be a disturbance. Even without being optimized, the barrier properties of the substrate materials studied were improved significantly – especially for oxygen and water-vapor diffusion – upon coating the materials with a thin ALD-deposited layer of Al_2O_3 .

Acknowledgements

The authors thank Beneq Ltd. for fabricating the ALD-deposited samples, Harry Helen from the University of Helsinki for measuring the oxygen transmission rates, Monika Österberg from the Helsinki

University of Technology for carrying out the AFM experiments, Leena-Sisko Johansson from the Helsinki University of Technology for carrying out the XPS experiments and Jari Malm from the Helsinki University of Technology for helping with the TG experiments.

References

- [1] C. Andersson, Packag. Technol. Sci. 21 (2008) 339.
- [2] M. Ritala, M. Leskelä, in: H.S. Nalwa (Ed.), Handbook of Thin Film Materials, Academic Press, San Diego, 2002, 103 p.
- [3] M. Leskelä, M. Kemell, K. Kukli, V. Pore, E. Santala, M. Ritala, J. Lu, Mater. Sci. Eng. C 27 (2007) 1504.
- [4] R.L. Puurunen, J. Appl. Phys. 97 (2005) 121301.
- [5] M.D. Groner, S.M. George, R.S. McLean, P.F. Carcia, Appl. Phys. Lett. 88 (2006) 051907.
- [6] P.F. Carcia, R.S. McLean, M.H. Reilly, M.D. Groner, S.M. George, Appl. Phys. Lett. 89 (2006) 031915.
- [7] S.H.K. Park, J. Oh, C.S. Hwang, J.I. Lee, Y.S. Yang, H.Y. Chu, Electrochem. Solid-State Lett. 8 (2005) H21.
- [8] A.W. Ott, J.W. Klaus, J.M. Johnson, S.M. George, Thin Solid Films 292 (1997) 135.
- [9] M. Vähä-Nissi, T. Hjelt, M. Jokio, R. Kokkonen, J. Kukkonen, A. Mikkelsen, Packag. Technol. Sci. 21 (2007) 425.
- [10] S. Tougaard, A. Ignatiev, Surf. Sci. 129 (1983) 355.
- [11] L.-S. Johansson, J. Juhanoja, Thin Solid Films 238 (1994) 242.
- [12] S. Tougaard, Surf. Interface Anal. 26 (1998) 249.
- [13] L.-S. Johansson, J. Campbell, K. Koljonen, M. Kleen, J. Buchert, Surf. Interface Anal. 36 (2004) 706.

PUBLICATION III

**Thin Al₂O₃ barrier coatings onto
temperature-sensitive packaging
materials by atomic layer deposition**

In: Surface and Coatings Technology 205 (2011),
pp. 5088–5092.

Copyright 2011, with permission from Elsevier.



Thin Al₂O₃ barrier coatings onto temperature-sensitive packaging materials by atomic layer deposition

Terhi Hirvikorpi^a, Mika Vähä-Nissi^{a,*}, Juha Nikkola^b, Ali Harlin^a, Maarit Karppinen^c

^a VTT Technical Research Centre of Finland, Biologinkuja 7, Espoo, P.O. Box 1000, FI-02044 VTT, Finland

^b VTT Technical Research Centre of Finland, P.O. Box 1300, FI-33101 Tampere, Finland

^c Aalto University, School of Chemical Technology, Department of Chemistry, Laboratory of Inorganic Chemistry, P.O. Box 16100, FI-00076 AALTO, Finland

ARTICLE INFO

Article history:

Received 11 March 2011

Accepted in revised form 15 May 2011

Available online 23 May 2011

Keywords:

Atomic layer deposition

Barrier

Packaging material

Recyclability

Aluminum oxide

Biopolymer

ABSTRACT

Thin (25 nm) and highly uniform Al₂O₃ coatings have been deposited at relatively low temperature of 80 and 100 °C onto various bio-based polymeric materials employing the atomic layer deposition (ALD) technique. The work demonstrates that the ALD-grown Al₂O₃ coating significantly enhances the oxygen and water vapor barrier performance of these materials. Promising barrier properties were revealed for polylactide-coated board, hemicellulose-coated board as well as various biopolymer (polylactide, pectin and nano-fibrillated cellulose) films.

© 2011 Elsevier B.V. All rights reserved.

1. Introduction

Growing environmental concerns related to the use of synthetic polymers in the packaging industry have led to the need for new, especially bio-based, materials in such applications [1]. Currently synthetic polymers are widely used in packaging applications because of their relatively low cost and high performance. Bio-based packaging materials would have many advantages over their plastic competitors, such as sustainability and recyclability [2]. However, the sensitivity towards moisture restricts their extended use. One way to improve the water-sensitivity is to apply a surface coating.

“Barrier property” refers to a material's capability to resist the diffusion of a specific species (molecule, atom or ion) into and through the material. To be a good gas and vapor barrier, the material needs to be pore-free. When considering polymer-coated boards, the water vapor transmission rate (WVTR) is affected by e.g. the coating weight of the polymer as well as the temperature and humidity of the surroundings [3, 4]. The common polymers used in packages include low- and high-density polyethylene, polypropylene and polyethylene terephthalate [5]. Hygroscopic materials, such as many biopolymers, typically lose their barrier properties at high relative humidity due to water absorption [6]. There have been some efforts to improve the

water vapor and oxygen barrier properties of polymer coatings with e.g. SiO_x layers [7]. Based on our recent studies [8–11] and studies by others [12–14], a thin Al₂O₃ coating layer grown by the atomic layer deposition (ALD) technique could work as a high-quality pore-free barrier film. The ALD technique is a surface-controlled layer-by-layer deposition process based on self-limiting gas-solid reactions [15]. It is well suited to produce inorganic gas barrier coatings on various materials.

Because of the covalent bonding, the adhesion of ALD-grown Al₂O₃ layer with the substrate is commonly excellent [16, 17]. Biopolymers typically have functional surface groups improving the bonding between the substrate and the Al₂O₃ layer. This makes biopolymeric materials, in our opinion, even more interesting substrates to create efficient gas and moisture barrier materials when combined with a thin Al₂O₃ coating than regular oil-based polymers, such as polyethylene, polypropylene or polyethylene terephthalate, for instance.

The ALD film growth characteristics on oil-based polymers have been previously studied by others [18–21]. Metal oxide films were found to grow on the native substrate surface. The basis for the initial film growth and nucleation was the hydroxyl groups on the polymer [15, 22]. The Al₂O₃ growth mechanism on porous polymeric substrates was demonstrated to occur through the adsorption of the trimethylaluminum (TMA) precursor onto the surface or by absorption into the porous material leading to the formation of Al₂O₃ clusters and further on to the linear film growth rate after the nucleation period [19]. The same mechanism has been demonstrated for many polymers. However, the initiation period differs depending on the polymer [18].

* Corresponding author.

E-mail addresses: Terhi.Hirvikorpi@vtt.fi (T. Hirvikorpi), mika.vaha-nissi@vtt.fi (M. Vähä-Nissi), juha.nikkola@vtt.fi (J. Nikkola), Ali.Harlin@vtt.fi (A. Harlin), maarit.karppinen@tkk.fi (M. Karppinen).

Here we demonstrate that ALD is indeed a promising technique to fabricate thin Al_2O_3 barrier layers on bio-based temperature-sensitive packaging materials. We moreover show that the barrier properties can be further improved by coating the materials with a pre-barrier layer prior to the ALD- Al_2O_3 coating.

2. Material and methods

The packaging materials investigated were commercial boards (provided by Stora Enso Oyj) coated with bio-based polylactide (PLA). In addition, several different biopolymer films were investigated. The materials tested are presented in Table 1. From our previous thermogravimetric study performed for most of the present substrate materials [8], we may conclude that the materials do not degrade thermally at temperatures employed in our low-temperature ALD- Al_2O_3 process.

The ALD- Al_2O_3 depositions were carried out at 80 or 100 °C in a Picosun SUNALE™ reactor on substrates that were ca. $10 \times 10 \text{ cm}^2$ in size. Trimethylaluminum (TMA, electronic grade purity, SAFC Hitech) and H_2O or O_3 were used as precursors. Ozone was produced by feeding oxygen gas (99.9999%) into the reactor through an ozone generator (In USA Inc., model AC 2025). The concentration of ozone was ca. 8% and the gas flow rate during the pulse was about 200 sccm (standard cubic centimeters per minute). High purity nitrogen (99.9999% N_2) was used as a carrier and purge gas. The operating pressure was 1–2 kPa. The precursor pulsing sequence was: 0.1 s TMA pulse, 6 s N_2 purge, 0.1 s H_2O or O_3 pulse, and 6 s N_2 purge, and the number of ALD cycles was adjusted according to the targeted Al_2O_3 coating thickness of 25 nm (selected based on our previous works) [9–11]. The actual thicknesses of the Al_2O_3 films could not be directly measured. Instead, we estimated the thicknesses based on the growth rate determined to be appr. 0.1 nm/cycle with a Nanospec AFT4150 reflectometer from films grown on a Si(100) wafer. This was done for the TMA- H_2O process at both temperatures and for the TMA- O_3 process at 100 °C. Because of the different surface chemistries of different polymers, the actual thickness may somewhat deviate from that determined for the Al_2O_3 -coated silicon wafer [20, 23]. It should also be mentioned that even though the aim was to deposit only on the polymer-coated side, film growth also on the uncoated side could not be totally prevented.

We also considered the possibility to coat the substrate material with a pre-barrier layer prior to the ALD- Al_2O_3 coating to block the largest pinholes in the porous substrates. For these experiments B2(PLA) substrates were used. Epoxy-based hybrid coatings with targeted coating weight of 2 g/m^2 were fabricated by a sol-gel (SG) method using 3-(trimethoxysilyl)propyl glycidyl (from Sigma-Aldrich) as an epoxy source, ethanol as a solvent and water to initiate the hydrolysis and condensation reactions. The coatings were sprayed on corona-treated substrates and dried at 120 °C for 10 min. The corona treatment unit (ET1 from Vetaphone) with treatment time of 60 s was used for better wetting and adhesion properties between the coating and the

substrate. The SG-coated substrates were further coated with an Al_2O_3 layer at 80 °C using TMA and H_2O as precursors.

The Al_2O_3 -coated samples were characterized by scanning electron microscopy (SEM; Hitachi S-3400 N VP-SEM, operating voltage 15 keV) for the microstructure. Prior to the imaging the samples were sputter-coated with Pt. The surface topography was analyzed with atomic force microscopy (AFM: Park Systems XE-100 equipment with cantilever 905-ACTA) using a non-contact “tapping” mode.

Contact angle (CA) and surface energy (SE) measurements (KSV CAM 200 Optical Contact Angle Meter) were carried out for some of the samples in a controlled atmosphere (relative humidity 50%, temperature 23 °C) with three to eight parallel measurements and expressed as degrees (°). The CA value was determined using water as solvent. For the SE measurements, water and di-iodomethane were used as solvents. The CA values of solvents were calculated at the time of 1 s from the moment the drop contacts. The SE values were calculated from the CA data by using the OWRK (ext. Fowkes) theory and expressed as mN/m.

For all the samples, the oxygen and water vapor transmission rate (OTR, WVTR) values were determined. The OTR values expressed as $\text{cm}^3/\text{m}^2/10^5\text{Pa}/\text{day}$ were measured (Systech M8001 and Mocon Oxtran 2/20) from two to three parallel samples using humid gases at 23 °C and in 50% relative humidity. The WVTR values were measured from three to five parallel samples according to the modified gravimetric methods ISO 2528:1995 and SCAN P 22:68 and were expressed as $\text{g}/\text{m}^2/\text{day}$ in conditions of 23 °C and 75% relative humidity.

3. Results and discussion

Our first task was to optimize the ALD- Al_2O_3 process for temperature-sensitive bio-based substrates. In these preliminary experiments two PLA-coated board samples, B1(PLA) and B2(PLA), were investigated and the deposition parameters considered were the deposition temperature (80 or 100 °C) and the choice of the oxygen source (H_2O or O_3). Interestingly, the growth per cycle (GPC) values for the H_2O and O_3 processes were found to be nearly identical, i.e. 0.1 nm/cycle (as measured for films grown on silicon substrates). This somewhat disagrees with the work by Elliot et al. [22] reporting somewhat lower GPC values for the TMA- O_3 process compared to the TMA- H_2O process. It seems that in our case the O_3 gas might have been somewhat wet; note that the H_2O present may act as a catalyst for the reactions during the TMA- O_3 process, increasing the GPC value.

The results from the OTR and WVTR experiments for the B1(PLA) and B2(PLA) samples with differently grown Al_2O_3 coatings are shown in Table 2. Independent of the deposition parameters used, the 25-nm thick ALD- Al_2O_3 coating remarkably improves both the oxygen and water vapor barrier properties of our PLA-coated board samples. Previous studies have shown that the deposition temperature may have some impact on the surface topography and morphology as well on the adhesion of Al_2O_3 coating in the case of polymeric substrates [24]. Higher deposition temperature may increase crystallinity of the polymers and cause brittleness for polymer structures which could

Table 1
Packaging materials employed as substrates.

Code	Description
B1(PLA)	Poly lactide-coated board; PLA 35 g/m^2 , board 310 g/m^2
B2(PLA)	Poly lactide-coated board; PLA 35 g/m^2 , board 210 g/m^2
B3(PLA)	Poly lactide-coated board; PLA 27 g/m^2 , board 210 g/m^2
PLA1	Poly lactide film, $20 \mu\text{m}$
PLA2	Poly lactide film, $75 \mu\text{m}$
NFC	Nano-fibrillated cellulose film; NFC; appr. 60 g/m^2
B(GGM)	Galactoclugomannan-coated board; GGM appr. 9 g/m^2 , board 200 g/m^2 pigment coated
PHB	Polyhydroxy butyrate film, $180 \mu\text{m}$
Pectin	Pectin film made by solution casting, $160 \mu\text{m}$

Table 2

OTR and WVTR values for plain and variously ALD- Al_2O_3 -coated B1(PLA) and B2(PLA) samples. The ALD parameters investigated were the deposition temperature (80 or 100 °C) and the choice of the oxygen source (H_2O or O_3).

Sample	OTR ($\text{cm}^3/\text{m}^2/10^5 \text{ Pa}/\text{day}$)	WVTR ($\text{g}/\text{m}^2/\text{day}$)
B1(PLA) uncoated	420 ± 10	65 ± 2
B1(PLA) + Al_2O_3 by H_2O (100 °C)	20 ± 3	1 ± 0.2
B1(PLA) + Al_2O_3 by O_3 (100 °C)	12 ± 1	5 ± 2
B2(PLA) uncoated	400 ± 9	75 ± 2
B2(PLA) + Al_2O_3 by H_2O (80 °C)	6 ± 1	3 ± 1
B2(PLA) + Al_2O_3 by O_3 (80 °C)	3 ± 1	7 ± 2
B2(PLA) + Al_2O_3 by O_3 (100 °C)	2 ± 0.2	1 ± 0.2

then lead to cracking of the polymer layer impairing the barrier properties. Here however, the choice of the deposition temperature (in the range investigated, i.e. 80–100 °C) may not be crucially important. In some cases even lower deposition temperatures might be advantageous. For extremely temperature-sensitive biopolymeric substrates the low deposition temperature could prevent the curling effect due to polymer shrinkage. Moreover, Lahtinen et al. [24], demonstrated that by using lower deposition temperatures it was possible to achieve better adhesion between the polymer surface and the Al₂O₃ coating.

Also, both the processes, TMA-H₂O and TMA-O₃, apparently work well at least for the PLA-coated boards. This could be due to the different fabrication methods of the pristine substrates. From Table 2, the OTR values achieved are somewhat better in the case of the TMA-O₃ process, while the opposite seems to be true for the WVTR values. During the water pulse, the absorbed H₂O may cause the polymer to swell, which should not be the case with O₃. OTR is generally regarded as more sensitive towards coating defects than WVTR. Hence, the TMA-O₃ process can be considered a highly potential alternative for depositing Al₂O₃ coatings on biopolymers except for the most sensitive materials not standing the strong oxidation power of O₃.

We should also consider the moisture within the polymer chains of the substrate material. Bio-based substrates tend to contain absorbed moisture and the removal of it could enhance the barrier properties because absorbed water may act as a plasticizer impairing the barrier properties. The possible benefits of the removal of the substrate moisture prior to the ALD-Al₂O₃ deposition were investigated by keeping a B1(PLA) sample in a heated (100 °C) ALD reactor chamber overnight before coating it with Al₂O₃ at 100 °C using the TMA-H₂O process. The overnight heat-treatment resulted in a slight improvement in the OTR value: the value decreased from 20 to 8 cm³/m²/10⁵Pa/day. However, the effect on the WVTR value was just the opposite: it increased from 1 to 7 g/m²/day. The removal of the moisture within the polymer chains made the sample brittle.

The main scope of the present work was to investigate whether the excellent results obtained for the PLA-coated boards with ALD-grown Al₂O₃ coatings could be extended to other bio-based materials. The oxygen and water vapor barrier results achieved for a variety of biopolymer substrates with a 25 nm-thick Al₂O₃ layer deposited by the TMA-H₂O process are summarized in Fig. 1. Note that H₂O was used as the oxygen source instead of O₃ to be sure that the results would not be distorted by the possible harmful effects of O₃ in the case of the most sensitive biopolymer film substrates. The depositions

were performed at 80 or 100 °C depending on the expected temperature tolerance of the substrate material. From Fig. 1, it can be concluded that our ALD-Al₂O₃-coated PLA, pectin, NFC, B1(PLA) and B(GGM) samples are highly promising oxygen barriers with OTR values that are already close to the oxygen barrier level required for dry food applications. For example, for PLA1 and B1(PLA) the OTR values were improved from 702 to 43 cm³/m²/10⁵Pa/day and from 420 to 20 cm³/m²/10⁵Pa/day, respectively. Besides being a good oxygen barrier, the Al₂O₃-coated B1(PLA) sample is also a highly promising water vapor barrier as the WVTR value of it was improved from 65 to 1 g/m²/day.

The NFC film investigated here is a highly interesting fiber network for various potential applications. Besides enhancing the oxygen barrier of NFC, the ALD-Al₂O₃ coating works as a kind of protective layer for the nanofibers (Fig. 2). Such materials are in the very focus of current research interest as examples of the controlled material integration of organic fibers and inorganic thin films [25]. This type of uniform coatings on single fibers are believed to open up new application possibilities e.g. in the area of filter development.

Despite the promising results achieved so far for the ALD-Al₂O₃ coated bio-based materials here and in our earlier studies [8–11], further improvements are still desired. A pre-barrier layer could close the larger pinholes on the surface of porous substrate making it denser and probably smoother and thus more favorable surface for the Al₂O₃ barrier layers to be grown on. The effect of a sol-gel coating between the substrate and the top ALD-Al₂O₃ coating was studied using B2(PLA) as a substrate material. In Fig. 3, AFM surface and phase images for plain, SG-coated and SG + Al₂O₃-coated B2(PLA) are presented. The observed average roughness (R_a) values are also given. From Fig. 3, the SG coating decreases the R_a value making the surface of the substrate smoother. The ALD-Al₂O₃ layer on top of the SG coating makes the surface even smoother. The total decrease in R_a was from 54 to 15 nm.

We also determined the contact angle (CA) and surface energy (SE) values for plain, SG-coated and SG + Al₂O₃-coated B2(PLA), see Table 3. The SG coating decreases the CA value indicating a more hydrophilic surface. The CA value drops even further with the additional Al₂O₃ coating. In Table 3, also given are the OTR and WVTR values for the same samples. The results show a moderate positive effect of SG coating on the barrier properties of B2(PLA). Only after the SG-coated B2(PLA) was additionally coated with Al₂O₃, the appreciably low OTR and WVTR values of 2 cm³/m²/10⁵ Pa/day and 2 g/m²/day, respectively, were reached. Most importantly, these

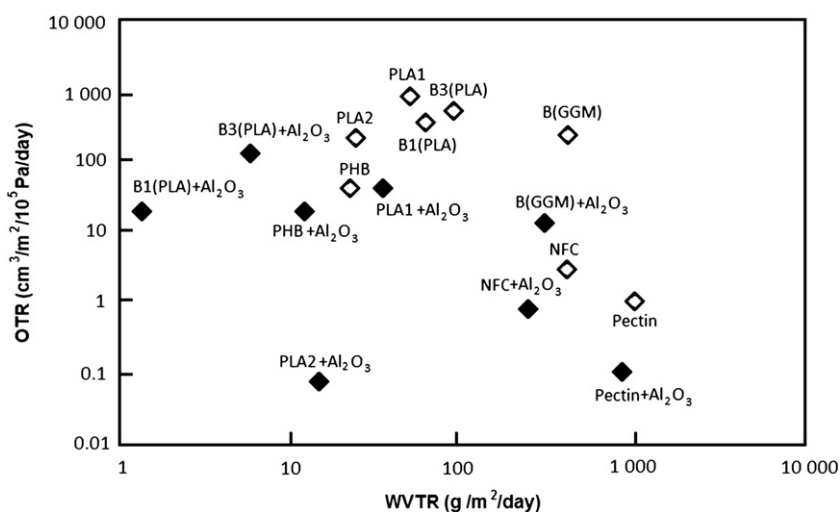


Fig. 1. Oxygen and water vapor barrier results achieved for various bio-based substrate materials (open markers) by means of a 25-nm thick ALD-Al₂O₃ coating (filled markers). The depositions were carried out at 80 or 100 °C using the TMA-H₂O process.

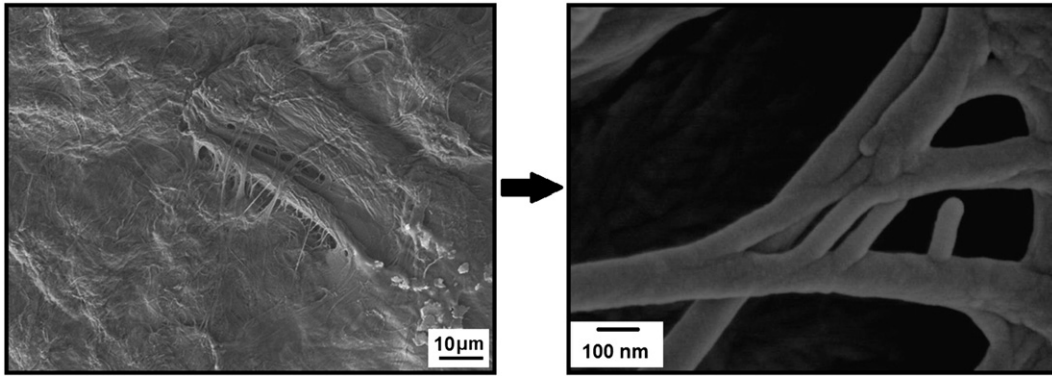


Fig. 2. SEM image (left image) with a magnification (right image) of NFC coated with a 25-nm thick Al_2O_3 layer, showing that the nano-fibrillated fibers are indeed uniformly coated with Al_2O_3 . The smallest observed fiber thickness is ca. 50 nm and the curve radius from the fiber ends is appr. 25 nm.

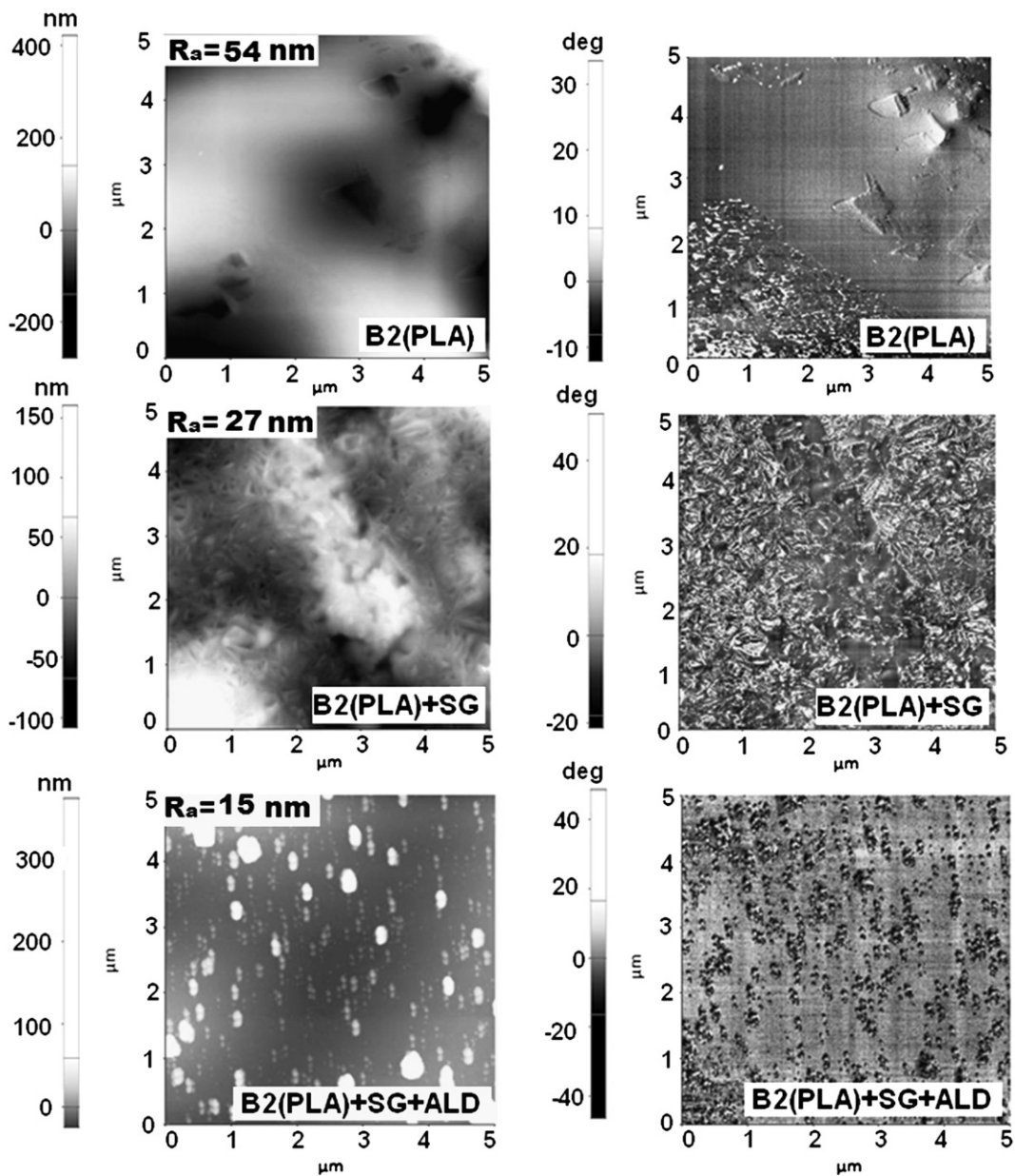


Fig. 3. AFM surface topography (left image) and phase (right image) images of plain, SG- and SG + Al_2O_3 -coated B2(PLA).

Table 3
Contact angle (CA), surface energy (SE), OTR and WVTR values for plain, SG-, SG + Al₂O₃-, and Al₂O₃-coated B2(PLA). The total value of surface energy (SE) is the sum of dispersive (SE_d) and polar (SE_p) components.

Sample	CA (°)	SE _p (mN/m)	SE _d (mN/m)	SE (mN/m)	OTR (cm ³ /m ² /10 ⁵ Pa/day)	WVTR (g/m ² /day)
B2(PLA) uncoated	71	7.4	38.2	45.6	400 ± 9	75 ± 2
B2(PLA) + SG	58	13.2	40.6	53.8	310 ± 2	44 ± 2
B2(PLA) + SG + Al ₂ O ₃	52	18.0	36.9	54.9	2 ± 1	2 ± 1
B2(PLA) + Al ₂ O ₃	–	–	–	–	6 ± 1	3 ± 1

values are lower than those achieved for B2(PLA) with the ALD-Al₂O₃ coating only, i.e. 6 cm³/m²/10⁵ Pa/day and 3 g/m²/day, respectively.

4. Conclusions

We have demonstrated that the oxygen and water vapor barrier properties of various bio-based boards and films are significantly enhanced by coating them with a 25-nm thick ALD-grown Al₂O₃ film. Through careful process optimization excellent barrier properties were reached for some of the bio-based materials investigated such that the materials satisfy the basic requirements set for commercial barrier materials for dry food or pharmaceutical packaging applications. Also shown was that there are means to improve the barrier properties further by cheap and easy-to-make coatings applied on the substrate surface prior to the top ALD-Al₂O₃ coating. In the future these materials could be produced with a continuous ALD process. There are already research tools and several patent applications concerning the development of the continuous ALD process.

Acknowledgements

The authors thank VTT and the Academy of Finland (No: 126528) for funding. Stora Enso Oyj and polymer film suppliers are thanked for providing the substrates. The facilities of Nanomicroscopy Center, Aalto University were also used during this research.

References

- [1] K. Khwaldia, E. Arab-Tehrany, S. Desobry, CRFSFS 1 (2010) 82–91.
- [2] C. Andersson, Packag. Technol. Sci. 2 (2008) 339–372.
- [3] J. Kuusipalo, K. Lahtinen, TAPPI J. 7 (2008) 8–15.
- [4] A. Savolainen, J. Kuusipalo, E. Laiho, T. Penttinen, in: A. Savolainen (Ed.), Paper and Paperboard Converting, Fapet Oy, Helsinki Finland, 1998, pp. 123–187.
- [5] J. Lange, Y. Wyser, Packag. Technol. Sci. 16 (2003) 149–158.
- [6] Y. Leterrier, Prog. Mater. Sci. 48 (2003) 1–55.
- [7] A. Sorrentino, M. Tortora, V.J. Vittoria, Polymer Sci. B 44 (2006) 265–274.
- [8] T. Hirvikorpi, M. Vähä-Nissi, T. Mustonen, E. Iiskola, M. Karppinen, Thin Solid Films 518 (2010) 2654–2658.
- [9] T. Hirvikorpi, M. Vähä-Nissi, A. Harlin, M. Karppinen, Thin Solid Films 518 (2010) 5463–5466.
- [10] T. Hirvikorpi, M. Vähä-Nissi, A. Harlin, J. Marles, V. Miikkulainen, M. Karppinen, Appl. Surf. Sci. 257 (2010) 736–740.
- [11] T. Hirvikorpi, M. Vähä-Nissi, J. Vartiainen, P. Penttilä, J. Nikkola, A. Harlin, R. Serimaa, M. Karppinen, J. Appl. Polymer Sci. (2011) in press.
- [12] M.D. Groner, S.M. George, R.S. McLean, P.F. Garcia, Appl. Phys. Lett. 88 (051907) (2006) 1–3.
- [13] P.F. Garcia, R.S. McLean, M.H. Reilly, M.D. Groner, S.M. George, Appl. Phys. Lett. 89 (031915) (2006) 1–3.
- [14] S.H.K. Park, J. Oh, C.S. Hwang, J.I. Lee, Y.S. Yang, H.Y. Chu, H.Y. Electrochem. Solid-State Lett. 8 (2005) H21–H23.
- [15] R.L. Puurunen, J. Appl. Phys. 97 (121301) (2005) 1–52.
- [16] T.O. Kääriäinen, D.C. Cameron, M. Tantari, Plasma Process. Polym. 6 (2009) 631–641.
- [17] D.C. Miller, R.R. Foster, Y. Zhang, S.-H. Jen, J.A. Bertrand, Z. Lu, D. Seghete, J.L. O'Patches, R. Yang, Y.-C. Lee, S.M. George, M.L. Dunn, J. Appl. Phys. 105 (2009) 093527–12.
- [18] M.D. Groner, F.H. Fabreguette, J.W. Elam, S.M. George, Chem. Mater. 16 (2004) 639–645.
- [19] C.A. Wilson, R.K. Grubbs, S.M. George, Chem. Mater. 17 (2005) 5625–5634.
- [20] J.D. Ferguson, A.W. Weimer, S.M. George, Chem. Mater. 16 (2004) 5602–5609.
- [21] C.A. Wilson, J.A. McCormick, A.S. Cavanagh, D.N. Goldstein, A.W. Weimer, S.M. George, Thin Solid Films 516 (2008) 6175–6185.
- [22] S.D. Elliot, G. Scarel, C. Wiemer, M. Fanciulli, G. Pavia, Chem. Mater. 18 (2006) 3764–3773.
- [23] X.H. Liang, L.F. Hakim, G.D. Zhan, J.A. McCormick, S.M. George, A.W. Weimer, J.A. Spencer, K.J. Buechler, J. Blackson, C.J. Wood, J.R. Dorgan, J. Am. Ceram. Soc. 90 (2007) 57–63.
- [24] K. Lahtinen, P. Maydannik, P. Johansson, T. Kääriäinen, D.C. Cameron, J. Kuusipalo, Surf. Coat. Technol. 205 (2011) 3916–3922.
- [25] J.S. Jur, J.C. Spagnola, K. Lee, B. Gong, Q. Peng, G.N. Parsons, Langmuir 26 (2010) 8239–8244.

PUBLICATION IV

**Effect of corona pre-treatment on the
performance of gas barrier layers
applied by atomic layer deposition
onto polymer-coated paperboard**

In: *Applied Surface Science* 257 (2010),
pp. 736–740.

Reprinted with permission from the publisher.



Effect of corona pre-treatment on the performance of gas barrier layers applied by atomic layer deposition onto polymer-coated paperboard

Terhi Hirvikorpi^a, Mika Vähä-Nissi^{a,*}, Ali Harlin^a, Jaana Marles^b,
Ville Miikkulainen^b, Maarit Karppinen^c

^a VTT Technical Research Centre of Finland, Biologinkuja 7, P.O. Box 1000, FI-02044 VTT Espoo, Finland

^b Picosun Oy, Tietotie 3, FI-02150 Espoo, Finland

^c Aalto University School of Technology and Science, Laboratory of Inorganic Chemistry, Kemistintie 1A, Espoo, P.O. Box 16100, 00076 Aalto, Finland

ARTICLE INFO

Article history:

Received 6 March 2010

Received in revised form 7 June 2010

Accepted 16 July 2010

Available online 24 July 2010

Keywords:

Atomic layer deposition

Corona

Barrier

Packaging material

Silicon oxide

Aluminum oxide

ABSTRACT

The effect of corona pre-treatment on the performance of Al₂O₃ and SiO₂ gas barrier layers applied by atomic layer deposition onto polymer-coated paperboards was studied. Both polyethylene and polylactide coated paperboards were corona treated prior to ALD. Corona treatment increased surface energies of the paperboard substrates, and this effect was still observed after several days. Al₂O₃ and SiO₂ films were grown on top of the polymer coatings at temperature of 100 °C using the atomic layer deposition (ALD) technique. For SiO₂ depositions a new precursor, bis(diethylamido) silane, was used. The positive effect of the corona pre-treatment on the barrier properties of the polymer-coated paperboards with the ALD-grown layers was more significant with polyethylene coated paperboard and with thin deposited layers (shorter ALD process). SiO₂ performed similarly to Al₂O₃ with the PE coated board when it comes to the oxygen barrier, while the performance of SiO₂ with the biopolymer-coated board was more moderate. The effect of corona pre-treatment was negligible or even negative with the biopolymer-coated board. The ALD film growth and the effect of corona treatment on different substrates require further investigation.

© 2010 Elsevier B.V. All rights reserved.

1. Introduction

The tightened requirements for the quality and safety of various food items have increased the need for better packaging materials. Fiber-based packaging materials have many advantages over their plastic competitors, such as sustainability, recyclability and stiffness/weight ratio [1]. However, poor barrier properties and sensitivity towards moisture are the main challenges for their extended use. Most of the studies have concerned polyethylene, ethyl vinyl alcohol and poly(ethylene terephthalate) but in recent years, owing to increased impact of environmental issues, the replacement of fossil-based raw materials with bio-based materials has become important.

Many biopolymers are hygroscopic materials, meaning that they will lose their barrier properties at high relative humidity. This is due to absorption of water and swelling of the polymer, which results in a more porous or open structure [2]. In order to prevent

the phenomenon, thin glass-like SiO_x coatings have been utilized to improve the gas barrier properties of moisture sensitive materials [3,4]. Furthermore, there is a need to upgrade the existing packaging materials, and thin inorganic coatings are an interesting way to create high performance materials for food packages.

Atomic layer deposition (ALD) technique is a surface controlled layer-by-layer thin film deposition process based on self-terminating gas–solid reactions. It is uniquely suited to produce high-performance gas-diffusion barrier coatings on porous materials as it allows preparation of dense and pinhole-free inorganic films that are uniform in thickness even deep inside pores, trenches and cavities of various dimensions. In our previous work thin Al₂O₃ coatings were deposited by the ALD technique at low temperature on various polymer-coated papers and boards and plain polymer films [5]. The work demonstrated that such ALD-grown Al₂O₃ coatings efficiently enhanced the gas-diffusion barrier performance of the studied materials towards oxygen, water vapor and aromas. We also have demonstrated that ALD is a recommended thin film deposition technique when making extremely thin (25 nm) barrier coatings from Al₂O₃ to temperature sensitive fiber-based materials [6].

Despite the promising results, improvement in barrier performance towards gases is still needed in order to create barrier coatings suitable for demanding packaging purposes. One route

* Corresponding author. Tel.: +358 40 5308 472; fax: +358 20 722 7026.

E-mail addresses: terhi.hirvikorpi@vtt.fi (T. Hirvikorpi), mika.vaha-nissi@vtt.fi (M. Vähä-Nissi), ali.harlin@vtt.fi (A. Harlin), jaana.marles@picosun.com (J. Marles), ville.miikkulainen@picosun.com (V. Miikkulainen), maarit.karppinen@tkk.fi (M. Karppinen).

towards improved barrier performance could be to pre-treat the substrate before the ALD. The surface chemistry of the substrate may affect the ALD deposition, especially the initial formation of the monolayers due to e.g. different amounts of hydrogen-bonded water on the surfaces. Based on our hypothesis, pre-treating the surface could even out the surface chemistry and enhance the uniformity of the ALD layer on polymeric coatings and thus improve the barrier properties, especially those obtained with thin ALD-grown coatings. Polymer films are often chemically inert, non-porous, and have low surface energy. This causes surfaces to be non-receptive to wetting and bonding with e.g. aqueous coatings. Corona treated films exhibit a higher surface energy crucial for producing high quality coated products.

Pre-treating substrates with corona discharge is a widely used method for polyolefin films [7]. Corona treatment is an electrical process which utilizes ionized air converting the substrate surface from non-polar to polar state. The surface is bombarded with ozone, oxygen and free radicals of oxygen and this enables the oxidation of the surface which increases the surface energy. Corona treatment has been found to increase oxygen content and carbon–oxygen functionalities on low-density polyethylene, while the effect on more polar ethylene methyl acrylate copolymer was marginal [8]. Due to the fact that there are significantly less polar functional groups on polyethylene (PE) than on polylactide (PLA) we assumed that the effect of corona treatment would be more profound with PE. In addition to oxidation, the effect of corona on the polymer surface can be due to cross-linking and removal of low molecular weight contaminants [8,9], changing surface micro-roughness and morphology [8–10], and formation of electret [8,11]. However, no significant changes in roughness values have been observed with corona treatment in earlier studies [12–14]. Changes in polymer morphology cannot be ruled out.

The aim of the present work was to study the influence of corona pre-treatment to the oxygen and water vapor barrier performance of polymer-coated boards additionally coated with Al_2O_3 and SiO_2 by the ALD. In SiO_2 depositions, a new precursor (bis(diethylamido) silane) was used. Use of this precursor has not been previously published in relation with barrier coatings. SiO_2 has been grown by the ALD using compounds such as $\text{Si}(\text{NCO})_4$, and $\text{N}(\text{C}_2\text{H}_5)_3$ as precursors [15]. Deposition of SiO_2 using SiCl_4 and H_2O as precursors has also been described [16], as well as dichloro silane (SiH_2Cl_2) and O_3 [17]. However, the problem with these precursors is the relatively high deposition temperatures which cannot be used with heat sensitive materials, such as polymer-coated boards.

2. Experimental details

Commercial paperboards with both synthetic low-density polyethylene (B(PE): board 210 g/m^2 ; coating 15 g/m^2) and bio-based polylactide (B(PLA); board 310 g/m^2 ; coating 35 g/m^2) coatings were used as substrates. The corona pre-treatment was performed at VTT with a corona treatment unit from Vetaphone (type: CP1C MKII, 2.0 kW, TF-415). The speed of the substrate was 500 mm/min and the power output of the corona treatment was 50 Wmin/m^2 . This is a widely used treatment unit for plastics [18].

ALD coatings were deposited at 100°C using a commercial SUNALE™ R-series reactor manufactured by Picosun Oy, Finland targeting at coating thicknesses of 25 and 50 nm. The general procedure of ALD- Al_2O_3 depositions has been reported previously elsewhere [6]. The ALD precursors for Al_2O_3 depositions were trimethylaluminum (TMA, SAFC Hitech, electronic grade purity) and water. High purity N_2 (99.9999%) was used as a carrier and purge gas. For Al_2O_3 depositions the precursor pulses lasted 0.1 s and the purges 5 s.

The procedure for SiO_2 depositions was based on the earlier study of Dussarrat et al. [19]. For SiO_2 depositions the precursors were bis(diethylamido) silane (SAFC Hitech, electronic grade purity) and ozone (20 vol%) produced from oxygen (99.9999%). Surface OH^- -groups have different reactivity towards Al_2O_3 and SiO_2 . In order to initiate the SiO_2 film growth, a thin ($\sim 2\text{ nm}$) layer of Al_2O_3 was first deposited from TMA and water. For Al_2O_3 depositions the precursor pulses lasted 0.1 s and the purges for 4 s, respectively. For SiO_2 depositions the precursor pulses lasted 1 s and the purges for 5 s.

The resultant film growth rates and actual film thicknesses on the polymer-coated boards could not be directly measured. Instead, the coating thicknesses were produced according to the reactor process parameters and compared to the thickness of Al_2O_3 and SiO_2 on a silicon wafer analyzed with a Nanospec AFT4150 reflectometer. The film growth rates for ALD were estimated to be ca 1.1 \AA/cycle for TMA- H_2O and silane- O_3 0.085 \AA/cycle . Due to the different polarities and functional groups of the PE and PLA surfaces the actual growth rates on the polymer-coated board substrates may somewhat deviate from those determined for the ALD coating on silicon wafer [20,21]. Although the aim was to deposit only the polymer-coated side of the substrate, film growth also on the uncoated side could not be totally prevented.

Contact angle (CA) and surface energy (SE) measurements were made directly after the corona pre-treatment and repeated 7 days after the pre-treatment. These measurements were carried out in order to study the decrease in surface energy during a certain time period. The measurements were made with KSV CAM 200 Optical Contact Angle Meter in a controlled atmosphere (RH 50%, temperature 23°C) and were expressed as $^\circ$ for contact angle and mN/m for surface energy. The probe liquids used were H_2O and di-iodomethane (CH_2I_2). Results are given as an average of three parallel measurements. The surface energy values, including dispersive and polar components, were calculated from the contact angle data using the OWRK (ext. Fowles) theory. The values of contact angles were calculated at the time of 1 s from the moment the drop contacts the surface.

The oxygen transmission rate (OTR) was measured from two to three parallel samples using humid gases at room temperature (23°C) with Systech M8001 and Mocon OXTRAN equipment and expressed as $\text{cm}^3/\text{m}^2/10^5\text{ Pa/day}$. The results from the two OTR equipments were roughly the same so the results from two different equipments may be compared. The water vapor transmission rate (WVTR) was measured from three to five parallel flat samples according to the modified gravimetric methods ISO 2528:1995 and SCAN P 22:68 and was expressed as $\text{g}/\text{m}^2/\text{day}$. Test conditions were 23°C and 75% relative humidity.

3. Results and discussion

3.1. Surface energies of the polymer-coated substrate materials

As described in our previous work [6], the surface topographies of the substrates B(PE) and B(PLA) vary greatly from each other. The surface of B(PLA) appears to be smoother than that of B(PE). This might be due to its larger polymer-coating weight (35 g/m^2) in comparison to that for B(PE) (15 g/m^2). Another explanation could be the different chill roll surface patterns used in extrusion coating of the paperboard. Due to their different surface roughness, the two substrate materials apparently accommodate different amounts of Al_2O_3 and SiO_2 during parallel ALD treatments. Compared to the smoother B(PLA) substrate, the B(PE) substrate has larger specific surface area and accordingly larger concentration of surface sites to accommodate larger amounts molecules upon the ALD depositions.

Table 1
Contact angle with water (CA) and surface energy (SE) values (γ^d , γ^p , γ^s) of pristine substrates directly after the corona pre-treatment and after 7 days from the pre-treatment.

Sample	Directly after pre-treatments				Seven days after pre-treatments			
	CA	γ^d	γ^p	γ^s	CA	γ^d	γ^p	γ^s
B(PE) untreated	90	36.7	3.8	40.5	90	36.7	3.8	40.5
B(PE) corona treated	67	43.5	7.6	51.0	71	41.2	6.4	47.7
B(PLA) untreated	71	40.1	7.7	47.8	71	40.1	7.7	47.8
B(PLA) corona treated	62	42.7	10.4	53.1	67	42.2	8.0	50.2

The results from the contact angle measurements with water and surface energy analyses are presented in Table 1. The total value of surface energy (γ^s) consists of dispersive (γ^d) and polar (γ^p) components. The latter measures the increase in polarity on the surface. The polar component is our main interest because it indicates the density of polar groups on the surface.

Results showed that the contact angle values of both B(PE) and B(PLA) changed after the corona pre-treatment making the surfaces more hydrophilic. The change was greater for B(PE) than for B(PLA). In addition, for B(PE) the contact angle remained approximately similar for 7 days. For B(PLA) the influence of corona pre-treatment was minor and after 7 days the contact angle with water was almost the same than before the pre-treatment. The surface energy values also increased when corona pre-treatment was applied. The results imply that the amount of polar groups at the surface increased. The effect was greater for B(PE) than for B(PLA). This can be explained by the different behavior of the chemical bonds in these polymers, PE and PLA, and the capability of the polymers to form additional oxygen containing functional surface groups. For both of the substrates the surface energy values remained at higher level after 7 days.

We also applied significantly lower corona treatment ($<10 \text{ Wmin/m}^2$) to the same samples with a smaller and simple corona unit, and Enercon Industries performed atmospheric plasma treatment to the samples with an optimized gas mixture. Plasma treatment is interesting due to lower tendency of the base polymer to degrade during the treatment without pin-holing and backside treatment. Plasma treatment also allows wider adjustment of surface properties by using different gases or gas mixtures. Unfortunately, no clear effect of these pre-treatments could be detected on contact angles or surface energy. The reason for the poor result with the plasma treatment could be the time delay of several days between the treatment and the measurement.

3.2. Barrier properties

Oxygen transmission rates (OTR) were measured in a way that the ALD deposited side of the sample faced the oxygen stream. The results are presented in Table 2.

Table 2
Oxygen transmission rates ($\text{cm}^3/\text{m}^2/10^5 \text{ Pa/day}$) of pure B(PE) and B(PLA) substrates and Al_2O_3 or SiO_2 coated substrates with and without of pre-treatment. The results are given as average \pm standard deviation of two to three parallel measurements.

Sample	Untreated	Corona treated
B(PE) uncoated	7900 \pm 1600	5700 \pm 140
B(PE) + 25 nm Al_2O_3	6700 \pm 2500	1400 \pm 70
B(PE) + 50 nm Al_2O_3	2700 \pm 400	1800 \pm 200
B(PE) + 25 nm SiO_2	5050 \pm 1300	2000 \pm 140
B(PE) + 50 nm SiO_2	2100 \pm 900	2500 \pm 140
B(PLA) uncoated	420 \pm 10	328 \pm 1.0
B(PLA) + 25 nm Al_2O_3	20 \pm 3	17 \pm 5
B(PLA) + 50 nm Al_2O_3	60 \pm 5	80 \pm 50
B(PLA) + 25 nm SiO_2	360 \pm 5	250 \pm 10
B(PLA) + 50 nm SiO_2	20 \pm 2	27 \pm 5

Corona treatment improved the oxygen barrier properties of the substrates as such probably due to the surface cross-linking caused by the relatively strong pre-treatment. Cross-linking of base polymer can also decrease diffusion of precursors into the polymer matrix. The influence of the corona treatment was greater for B(PE) than for B(PLA). Corona treatment seems also to lead to more even ALD-grown layers due to smaller standard deviation with corona pre-treated samples.

For B(PE), without the corona pre-treatment, the thicker (50 nm) Al_2O_3 layer, i.e. the longer ALD process, resulted in better barrier properties than the thinner (25 nm) layer, i.e. the shorter ALD process. However, the situation was different after corona treatment; better oxygen barrier properties were obtained already with 25 nm Al_2O_3 layers. For SiO_2 depositions, the barrier properties were most improved when a 50 nm SiO_2 layer was deposited onto substrate but after the corona pre-treatment the thinner (25 nm) layers resulted in larger improvement.

When B(PLA) was used as a substrate and Al_2O_3 layers were deposited on the substrate without corona pre-treatment, a 25 nm Al_2O_3 layer improved the properties more than a thicker (50 nm) layer. After the pre-treatment, the properties of the 25 nm Al_2O_3 layer remain practically at the same good level. The barrier performance did not improve further with the 50 nm Al_2O_3 layer, which could be due to the cracking behavior of thick ALD films [5]. However, for SiO_2 depositions, the barrier properties improved most when a 50 nm SiO_2 layer was deposited onto substrate and the properties were further improved after corona pre-treatment. For B(PE) and B(PLA), in general, the best barrier properties towards oxygen were obtained with a 25-nm Al_2O_3 layer on top of corona pre-treated substrates.

The WVTR results are presented in Table 3. The results show that the corona pre-treatment only slightly improved the water vapor barrier properties for both of the uncoated substrates. For B(PE), both with and without the corona pre-treatment, the 50 nm Al_2O_3 layers resulted in better barrier properties than the 25 nm Al_2O_3 layers. The values with and without corona pre-treatment are close to each other when taking into account the statistical scattering. With SiO_2 depositions on B(PE), the barrier properties were at the same level with both film thicknesses as with the Al_2O_3 layers. However, the corona treatment improved the WVTR of the

Table 3
Water vapor transmission rates ($\text{g}/\text{m}^2/\text{day}$) of pure B(PE) and B(PLA) substrates and Al_2O_3 or SiO_2 coated substrates with and without of pre-treatment. The results are given as average \pm standard deviation of three to five parallel measurements.

Sample	Untreated	Corona treated
B(PE) uncoated	7.0 \pm 0.9	6.2 \pm 0.4
B(PE) + 25 nm Al_2O_3	6.9 \pm 0.1	6.1 \pm 1.1
B(PE) + 50 nm Al_2O_3	2.0 \pm 0.5	4.6 \pm 1.6
B(PE) + 25 nm SiO_2	6.3 \pm 0.3	2.9 \pm 0.3
B(PE) + 50 nm SiO_2	6.5 \pm 1.0	7.0 \pm 0.4
B(PLA) uncoated	64.9 \pm 1.6	60.5 \pm 0.4
B(PLA) + 25 nm Al_2O_3	1.4 \pm 0.2	5.7 \pm 3.8
B(PLA) + 50 nm Al_2O_3	1.8 \pm 0.5	13.2 \pm 5.9
B(PLA) + 25 nm SiO_2	48.1 \pm 1.8	42.2 \pm 1.1
B(PLA) + 50 nm SiO_2	41.5 \pm 5.3	41.9 \pm 2.7

25 nm SiO₂ layer. This could be due to a more even Al₂O₃ layer under the SiO₂ layer. With B(PLA) the best WVTR was obtained with Al₂O₃ without the corona pre-treatment. Corona treatment impaired the WVTR, although the values were better than those obtained with SiO₂ on the same substrate. Similarly to the OTR, the WVTR of the 50 nm Al₂O₃ layer increased more than with the thinner layer. The negative effect of corona pre-treatment on the performance of B(PLA) could be due to uneven or too excessive treatment.

When Al₂O₃ was applied on B(PLA) without corona pre-treatment, the 25 nm Al₂O₃ layer improved the oxygen barrier properties more than the 50 nm layer. Corona treatment did not alter the situation. When SiO₂ was applied on B(PLA) without corona pre-treatment the barrier properties were slightly better with the thicker (50 nm) SiO₂ layer. After the pre-treatment, the properties of the 25 nm SiO₂ layer were improved, as the properties of the thicker layer remained the same. The cracking of thicker ALD layers may affect also the water vapor barrier [5]. The effect of corona treatment on water vapor barrier properties of the studied substrates were not as clear as it was for oxygen barrier properties for e.g. B(PE). It is evident that in order to clarify this, more investigation is needed. Among the two polymers (at least in pure form), the melting point and the glass transition temperature are higher for PLA than for LDPE, making PLA more stable under the presently employed deposition conditions. At elevated deposition temperatures (around 100 °C) the polymer chains of LDPE start to move which may result in a poor quality ALD-grown coating.

Neither the low corona nor the atmospheric plasma treatment had an unambiguous effect on the barrier properties. In the case of plasma treatment this might be due to the time delay of several days between the treatment and the ALD test.

The decrease in the barrier properties with increasing ALD layer thickness in some cases is in line with our initial studies [5]. The same phenomenon has been detected also with other thin deposition methods, such as vacuum sputtering [6]. The ALD film thickness must thus be optimized for each substrate and process parameters separately. The effect of corona treatment was assumed to be most obvious when aiming at thin ALD films due to the different initial film growth between untreated and treated polymer surfaces. This study utilized the ALD process with two different number of process cycles.

Due to the different polarities and type/density of functional groups of the untreated and treated polymer surfaces the nucleation and the initial film growth may somewhat deviate from each other and from that determined for the ALD-Al₂O₃ coating on silicon wafer [20–22]. The reason for the different properties between the untreated and corona treated and ALD deposited samples could thus be dissimilar film thickness and evenness of the grown film. Secondly, diffusion of precursors into and out of the polymer surface [22] is likely affected both by the polymer type and the pre-treatment, especially during the initial stages of film growth. Cross-linking of the polymer surface during corona treatment could decrease diffusion of precursors into the polymer, thus making the interface between the polymer and the ALD film sharper. The interface between e.g. polyethylene and Al₂O₃ has been found problematic in other studies [23]. In spite of a probably more uniform ALD film on the corona treated samples, the interfacial tension could become higher with thick ALD films causing cracking. Thirdly, corona treatment can increase the roughness of polymer surfaces. However, this is not very likely as stated earlier. Clearly, the ALD film growth on different substrates needs further investigation.

The results with e.g. PLA coated board would indicate that the SiO₂ film is more polar and the structure more open than the Al₂O₃ film. The open structure would explain the need for a thicker SiO₂ layer for improved oxygen barrier. However, even thick film of this

material cannot decrease water vapor barrier significantly due to possible swelling. The problem with SiO₂ ALD is in some cases formation of salt [22]. It is well known that oxygen and water vapor barrier properties do not necessary correlate. With a dense polar polymer, such as ethylene vinyl alcohol copolymer, oxygen barrier can be good when dry, but the polymer structure swells at humid conditions.

4. Conclusions

The effect of corona pre-treatment on the oxygen and water vapor barrier properties of Al₂O₃ or SiO₂ layers applied by the ALD technique onto polymer-coated paperboard was studied. Corona treatment was performed for polyethylene and polylactide coated boards. Al₂O₃ and SiO₂ layers were then successfully deposited at low temperature on these fiber-based substrates. For SiO₂ depositions a new precursor, bis(diethylamido) silane, was used. Substrates that had been corona surface treated exhibited a higher surface energy and the effect of the treatment lasted for several days at the substrate surface. The positive effect of the corona pre-treatment of the polymer-coated boards on the barrier properties after the ALD deposition was more significant with the polyethylene coated paperboard and with thin deposited layers, i.e. the short ALD process. This supports our hypothesis concerning more favorable substrate surface chemistry after corona pre-treatment, especially with thin deposited layers. In addition, cross-linking of polymer surface layer may decrease diffusion of precursors into the polymer matrix. These are more important than the less likely increase in surface roughness during the corona pre-treatment. SiO₂ performed similarly to Al₂O₃ with the PE coated board when it comes to the oxygen barrier, while performance of SiO₂ with the biopolymer-coated board was more moderate. Corona treatment also evened out the surface properties of some samples. However, the effect of corona pre-treatment was negligible or even negative on the water vapor barrier, especially with the polylactide coated board. Clearly, the ALD film growth and the effect of corona pre-treatment on different substrates need further investigation.

Acknowledgements

The authors thank VTT, Metsäliitto Group, Myllykoski Corporation, Stora Enso Oyj and UPM-Kymmene Oyj for their funding and Stora Enso Oyj for providing the paperboard samples. Enercon Industries is thanked for performing the atmospheric plasma treatment for the samples.

References

- [1] C. Andersson, New ways to enhance the functionality of paperboard by surface treatment—a review, *Packag. Technol. Sci.* 21 (2008) 339.
- [2] M. Stading, Å. Rindlav-Westling, P. Gatenholm, Humidity-induced structural transitions in amylase and amylopectin films, *Carbohydr. Polym.* 45 (2001) 209.
- [3] J. Lange, Y. Wyser, Recent innovations in barrier technologies for plastic packaging—a review, *Packag. Technol. Sci.* 16 (2003) 149.
- [4] Y. Leterrier, Durability of nanosized oxygen-barrier coatings on polymers, *Prog. Mater. Sci.* 48 (2003) 1.
- [5] T. Hirvikorpi, M. Vähä-Nissi, T. Mustonen, E. Iiskola, M. Karppinen, Atomic layer deposited aluminum oxide barrier coatings for packaging materials, *Thin Solid Films* 518 (2010) 2654.
- [6] T. Hirvikorpi, M. Vähä-Nissi, A. Harlin, M. Karppinen, Comparison of some coating techniques to fabricate barrier layers on packaging materials, *Thin Solid Films* 518 (2010) 5463.
- [7] J. Kuusipalo, *Paper and Paperboard Converting*, second ed., Finnish Paper Engineers' Association, Gummerus Oy, Jyväskylä, 2008.
- [8] J. Lahti, *Dry Toner-based Electrophotographic Printing on Extrusion Coated Paperboard*, Tampere University of Technology, Publication 523, Tampere, 2005.
- [9] Q.C. Sun, D.D. Dong, D. Zhang, L.C. Wadsworth, Corona treatment for polyethylene films, *TAPPI J.* 81 (8) (1998) 177–183.

- [10] D. Briggs, D.M. Brewis, M.B. Konieczko, X-ray photoelectron spectroscopy studies of polymer surfaces, *J. Mater. Sci.* 14 (1979) 1344–1348.
- [11] D.M. Brewis, *Surface Analysis and Pretreatment of Plastics and Metals*, Applied Science, Publishers Ltd., Essex, 1982.
- [12] M. Strobel, V. Jones, C.S. Lyons, M. Ulsh, M.J. Kushner, R. Dorai, M.C. Branch, A comparison of corona-treated and flame-treated polypropylene films, *Plasma Polym.* 8 (2003) 61.
- [13] L.-A. O'Hare, S. Leadley, B. Parbhoo, Surface physicochemistry of corona-discharge-treated polypropylene film, *Surf. Interf. Anal.* 33 (2002) 335.
- [14] E. Földes, A. Tóth, E. Kálmán, E. Fekete, Á. Tomasovszky-Bobák, Surface changes of corona-discharge-treated polyethylene films, *J. Appl. Polym. Sci.* 76 (2000) 1529.
- [15] K. Yamaguchi, S. Imai, N. Ishitobi, M. Takemoto, H. Miki, M. Matsumura, Atomic-layer chemical-vapor-deposition of silicon dioxide films with an extremely low hydrogen content, *Appl. Surf. Sci.* 130–132 (1998) 202.
- [16] J.W. Klaus, O. Sneh, A.W. Ott, S.M. George, Atomic layer deposition of SiO₂ using catalyzed and uncatalyzed self-limiting surface reactions, *Surf. Rev. Lett.* 6 (1999) 435.
- [17] J.-H. Lee, V.-J. Kim, C.-H. Han, S.-K. Rha, W.-J. Lee, C.-O. Park, Investigation of silicon oxide thin films prepared by atomic layer deposition using SiH₂Cl₂ and O₃ as the precursors, *Jpn. J. Appl. Phys.* 43 (2004) L328.
- [18] M. Pykönen, H. Sundqvist, J. Järnström, O.-V. Kaukoniemi, M. Tuominen, J. Lahti, J. Peltonen, P. Fardim, M. Toivakka, Effects of atmospheric plasma activation on surface properties of pigment-coated and surface-sized papers, *Appl. Surf. Sci.* 255 (2008) 3217.
- [19] C. Dussarrat, I. Suzuki, K. Yanagita, Extra low-temperature SiO₂ deposition using aminosilanes, in: 210th ECS Meeting Proceedings, 2006, p. 1.
- [20] J.D. Ferguson, A.W. Weimer, S.M. George, Atomic layer deposition of Al₂O₃ films on polyethylene particles, *Chem. Mater.* 16 (2004) 5602.
- [21] X.H. Liang, L.F. Hakim, G.D. Zhan, J.A. McCormick, S.M. George, A.W. Weimer, J.A. Spencer, K.J. Buechler, J. Blackson, C.J. Wood, J.R. Dorgan, Novel processing to produce polymer/ceramic nanocomposites by atomic layer deposition, *J. Am. Ceram. Soc.* 90 (2007) 57.
- [22] S.M. George, Atomic layer deposition: an overview, *Chem. Rev.* 110 (2010) 111–131.
- [23] X.H. Liang, D.M. King, M.D. Groner, J.H. Blackson, J.D. Harris, S.M. George, A.W. Weimer, Barrier properties of polymer/alumina nanocomposite membranes fabricated by atomic layer deposition, *J. Membr. Sci.* 322 (2008) 105.

PUBLICATION V

**Effect of heat-treatment on the
performance of gas barrier layers
applied by atomic layer deposition
onto polymer-coated paperboard**

In: Journal of Applied Polymer Science 122 (2011),
pp. 2221–2227.

Copyright 2011 Wiley Periodicals, Inc.
Reproduced with permission of John Wiley &
Sons Inc.

Effect of Heat-Treatment on the Performance of Gas Barrier Layers Applied by Atomic Layer Deposition onto Polymer-Coated Paperboard

Terhi Hirvikorpi,¹ Mika Vähä-Nissi,¹ Jari Vartiainen,¹ Paavo Penttilä,² Juha Nikkola,³ Ali Harlin,¹ Ritva Serimaa,² Maarit Karppinen⁴

¹VTT Technical Research Centre of Finland, P.O.Box 1000, FI-02044 VTT, Finland

²Division of Materials Physics, Department of Physics, University of Helsinki, P.O.Box 64, FI-00014, Finland

³VTT Technical Research Centre of Finland, P.O.Box 1300, FI-33101 Tampere, Finland

⁴Laboratory of Inorganic Chemistry, Aalto University School of Science and Technology, P.O.Box 16100, FI-00076 Aalto, Finland

Received 6 September 2010; accepted 8 February 2011

DOI 10.1002/app.34313

Published online 15 June 2011 in Wiley Online Library (wileyonlinelibrary.com).

ABSTRACT: The effect of heat treatment on the gas barrier of the polymer-coated board further coated with an Al₂O₃ layer by atomic layer deposition (ALD) was studied. Heat treatment below the melting point of the polymer followed by quenching at room temperature was used for the polylactide-coated board [B(PLA)], while over-the-melting-point treatment was utilized for the low-density polyethylene-coated board [B(PE)] followed by quenching at room temperature or in liquid nitrogen. Heat treatment of B(PLA) and B(PE) followed by quenching at room temperature improved the water vapor barrier. However, because of the changes in the polymer morphology,

quenching of B(PE) with liquid nitrogen impaired the same barrier. No improvement in oxygen barrier was observed explained by, e.g., the spherulitic structure of PLA and the discontinuities and possible short-chain amorphous material around the spherulites forming passages for oxygen molecules. This work emphasizes the importance of a homogeneous surface prior to the ALD growth Al₂O₃ barrier layer. © 2011 Wiley Periodicals, Inc. *J Appl Polym Sci* 122: 2221–2227, 2011

Key words: barrier; gas permeation; morphology; nanolayers; thin films

INTRODUCTION

The trend today is to develop sustainable and light-weight packaging materials, which are not interfering with the energy and material recovery schemes set for the packaging waste. Traditional packaging materials typically consist of layers of oil-based polymers and aluminum foil, which are difficult to sort out and recycle efficiently. Simultaneously, there is an increasing interest to develop new kinds of renewable solutions, and this opens up new application areas for fiber-based materials and biopolymers. Polylactide (PLA) is a biopolymer that can be synthesized from renewable resources, and is thus, environmentally and economically appropriate.¹ Properties such as biodegradability and good mechanical strength make PLA interesting raw-material for many recyclable products. In addition, PLA is an attractive material option for the traditional applications where common thermoplastics, such as low-density polyethylene (LDPE) are employed. Like many other biopolymers, PLA loses barrier properties in high humidity conditions because of absorp-

tion of water and swelling of the polymer. Previously thin SiO_x coatings have been employed to improve the barrier properties of these sensitive materials.^{2,3} Various kinds of thin inorganic coatings are often utilized to create high performance materials, e.g., food packages.

Atomic layer deposition (ALD) technique is a surface controlled layer-by-layer thin film deposition process based on self-terminating gas-solid reactions. It allows preparation of dense and pinhole-free inorganic films that are uniform in thickness.⁴ In our previous work thin Al₂O₃ and SiO₂ coatings have been successfully deposited by the ALD technique at low temperatures on various polymer-coated papers, boards, and plain polymer films.^{5–7} The work demonstrated that ALD is a feasible deposition technique when making extremely thin (25 nm) barrier coatings from Al₂O₃ onto such temperature-sensitive fiber-based materials.⁶ Despite the promising results, improvement in barrier performance toward gases is needed to create barrier coatings suitable for demanding packaging purposes. One route toward improved barrier performance is to pretreat the substrate before the inorganic ALD coatings. In our earlier studies,⁷ corona pretreatment slightly enhanced the oxygen barrier performance of thin Al₂O₃ layers on LDPE-coated board.

Correspondence to: M. Vähä-Nissi (mika.vaha-nissi@vtt.fi).

The effects of heat treatment on polyolefin-coated papers and PLA-coated boards have also been studied.^{8–10} Barrier properties of polymers are affected by the chemical structure, morphology, and surface properties.¹¹ In addition, the process used for forming the polymer influences the barrier properties. This is due to the redistributed crystalline and amorphous regions and the overall change in free volume of the polymer when the film is formed. To get good adhesion the polymer has to be applied at high melt temperatures followed by rapid quenching to avoid adhesion to the chill roll of the process equipment. This leads to a polymer layer with low density as molecules do not have time to pack efficiently. In extrusion coating, polymer crystallinity has been found to be inversely related to the difference between the melt temperature and the quenching temperature¹² leading sometimes to formation of a totally amorphous structure. This is the case with PLA coatings.^{8,10} Diffusion of gas permeants occurs through the amorphous regions, whereas crystalline regions are more or less impermeable. Water vapor transmission rate (WVTR) of PLA decreases with increasing crystallinity.¹³ This may be due to the fact that restricted amorphous regions have higher resistance to water vapor permeation compared with the free amorphous regions. Based on recent studies^{9,10} concerning PLA, the improved water vapor barrier after treatment at 130°C was due to the increase in crystallinity and the growth of spherulites.

Crystallization and formation of spherulites in polyethylenes have been studied elsewhere.^{14,15} In the work by Scheirs et al.¹⁵ the thermal oxidation during isothermal crystallization at 123°C decreased the size of the spherulites similarly to fast quenching. Short-chain material is usually deposited at the boundaries of the spherulites and edges of lamellae creating brittle areas. The over-melting-point heat treatment has also been shown to improve the barrier properties of polyethylene-coated paper.^{8,10} This was explained by increased level of crystallinity and spherulite size after quenching at room temperature. A dramatic improvement was observed in oxygen transmission rate after 5 min treatment at 210°C, while water vapor barrier was slightly impaired. Increased oxidation was accounted to be the reason for the increased water vapor permeation. The mobility of polymer chain is restricted in the crystalline region and also between such regions.¹⁶

The aim of this work was to study the effects of a heat treatment on the oxygen and water vapor barrier performance of polymer-coated boards additionally coated with a thin Al₂O₃ layer by the ALD technique. Our hypothesis was that an improvement achieved with such a heat treatment in an originally poor barrier property plays little role if the properties of the Al₂O₃ layer grown by the ALD technique

dominates. Indirectly the heat treatment could have significant effects on the surface chemistry and topography, and diffusion of ALD precursors into and out of the polymer.

EXPERIMENTAL

Commercial paperboards coated with synthetic LDPE (B(PE); board 210 g/m²; polymer coating 15 g/m²) and the same base board coated with bio-based PLA (B(PLA); coating 27 g/m²) were used as substrates for the Al₂O₃ depositions by ALD. Before the depositions the substrates were heat-treated in a convection oven. The test conditions were chosen based on the previous works.^{8–10} For B(PE) the temperature of the oven was 170°C or 200°C, and 130°C for B(PLA). For B(PE) the heat-treatment lasted for 5 min after which the samples were quenched at room temperature (23°C) or dipped into liquid nitrogen. With B(PLA) the treatment lasted for 4, 9, or 16 min followed by quenching at room temperature. The times used for inserting and removing the samples into and from the oven were approximately constant throughout the test series.

Plain and heat-treated substrates were coated with Al₂O₃ by ALD technique at 80°C using a commercial SUNALE™ R-series ALD reactor manufactured by Picosun Oy. The targeted coating thickness was 25 nm. The ALD procedure for the Al₂O₃ depositions has been reported elsewhere.^{6–7} The precursors used for the Al₂O₃ depositions were trimethylaluminum (TMA; SAFC Hitech, electronic grade purity) and water. High purity N₂ was used as a carrier and purge gas. The precursor pulses lasted 0.1 s and the purges 5 s. The resultant film growth rates and film thicknesses on the polymer-coated boards could not be directly measured. Instead, the coating thickness was produced according to the reactor process parameters and compared with the thickness of Al₂O₃ on a silicon wafer analyzed with a Nanospec AFT4150 reflectometer. Because of the different polarities and functional groups the growth rates on the polymer-coated boards may deviate from that determined with the silicon wafer.^{17,18}

Contact angle and surface energy measurements were performed both for plain and heat-treated substrates to detect possible chemical changes caused by the heat-treatment. The measurements were made with KSV CAM 200 Optical Contact Angle Meter in a controlled atmosphere (RH 50%, temperature 23°C) and were expressed as ° for contact angle and mN/m for surface energy. The probe liquids used were H₂O and di-iodomethane (CH₂I₂). Results are given as an average of three to eight parallel measurements. The surface energy values, including dispersive and polar components, were calculated from the contact angle data using the OWRK (ext.

Fowles) theory. Contact angle values were measured at the time of 1 s from the moment the drop contacts the surface.

Atomic force microscopy (AFM tapping mode; Park Systems XE-100 with 905-ACTA cantilever) was used to study the surface topography and morphology of plain and heat-treated substrates to detect changes caused by the heat-treatment. From each sample three parallel sample areas of $5 \times 5 \mu\text{m}$ and $0.5 \times 0.5 \mu\text{m}$ were analyzed. In addition the values of average roughness (R_a) and root mean square roughness (R_q) were calculated from the larger area images. Both topography and phase images were taken. The phase lag is partially a function of the viscoelastic properties of the sample surface.¹⁹

Wide-angle x-ray scattering (WAXS) was measured from the samples in perpendicular transmission geometry to observe the morphological changes caused by the heat-treatment. The radiation was produced with a rotating anode X-ray generator using Cu K α radiation ($\lambda = 1.541 \text{ \AA}$) monochromatized with a Si(111) crystal and a totally reflecting mirror. An image plate detector (MAR345, Marresearch) was used to detect the scattered radiation in perpendicular transmission geometry. Additionally, the air scattering with an empty sample holder and the "dark current" without beam were measured. These, as well as corrections due to the measurement geometry, measurement time, and absorption were considered during the analysis. The measured q -range was 0.3–3.1 $1/\text{\AA}$ with the definition $q = (4\pi \sin \theta)/\lambda$ for the length of the scattering vector.

Water vapor and oxygen transmission rates were measured from untreated and heat treated samples with and without the ALD- Al_2O_3 layer. The water vapor transmission rate (WVTR) was measured from three to five parallel flat samples according to the modified gravimetric methods ISO 2528 : 1995 and SCAN P 22 : 68, and was expressed as $\text{g}/\text{m}^2/\text{day}$. Test conditions were 23°C and 75% relative humidity. The oxygen transmission rate (OTR) was measured from two to eight parallel samples using humid gases at room temperature (23°C, 50% relative humidity) with Systech M8001 and expressed as $\text{cm}^3/\text{m}^2/10^5 \text{ Pa}/\text{day}$.

RESULTS AND DISCUSSION

Surface topography and polymer morphology

The results from the surface topography and morphology measurements are presented in Table I. The effect of heat-treatment on B(PE) was obvious. The plain substrate was rough as indicated by the high R_a and R_q values, and the large deviation between the measured areas. The smoothest B(PE) sample was heat treated at 200°C followed by quenching with

TABLE I
Average Roughness (R_a) and Root Mean Square Roughness (R_q), Both in nm, Obtained from Three Parallel Surface AFM images (area $5 \times 5 \mu\text{m}$)

Sample	R_a	R_q
B(PE)	68 ± 42	89 ± 58
B(PE), 170°C, RT	16 ± 2.4	20 ± 3.4
B(PE), 200°C, RT	20 ± 8.3	26 ± 11
B(PE), 170°C, LN	18 ± 5.4	22 ± 7.2
B(PE), 200°C, LN	13 ± 1.4	17 ± 1.7
B(PLA)	110 ± 63	137 ± 70
B(PLA), 4 min 130°C	27 ± 11	34 ± 18
B(PLA), 9 min 130°C	28 ± 21	35 ± 18
B(PLA), 16 min 130°C	26 ± 11	34 ± 15

RT refers to quenching at room temperature, LN to quenching with liquid nitrogen.

liquid nitrogen. However, taking into account the statistical scattering, all the heat-treated B(PE) samples were similar. Plain B(PLA) was rougher than the commercial PLA-coated board in our previous studies^{5–7} and the B(PE) used. Heat-treatment decreased the surface roughness, and with the longer treatment time the roughness of the surface became more uniform. The heat-treated B(PLA) samples were rougher than the heat treated B(PE) samples. However, in the case of B(PE), surfaces revealed that the amount of small scale surface features actually increased as a result of the heat-treatment. The phase images indicated more organized structures with the samples quenched at room temperature than those quenched with liquid nitrogen. This is shown in Figure 1. With B(PLA) the effect was significant which can be seen in Figure 2. The amount of spherulites increased with increased treatment time in the oven. High crystallinity of samples heat-treated for 9 and 16 min seemed also to create discontinuation points between the spherulites (Fig. 3).

When determining the crystal sizes and crystallinities of cellulose by WAXS, the measured scattering of sulfate lignin was used to approximate the amorphous background of cellulose.²⁰ The intensity pattern was integrated on a sector of 180° in the plane of the image plate. For the crystal size determination, the amorphous background was subtracted and the size was calculated with the Scherrer equation²¹ after fitting Gaussian functions to the diffraction peaks. This was possible for the 200-reflection of cellulose (1.6 1/\AA) in the B(PLA) samples only, because the diffraction peaks of LDPE in B(PE) could not be separated from the cellulose peaks. According to the results, the crystal size of cellulose in 200-direction (crystal width) was increased from 53 Å to 60 Å due to heat-treatment of B(PLA) samples, being 48 Å for an uncoated paperboard ($\pm 1 \text{ \AA}$ for all). The crystallinity of cellulose was determined for the reference sample and the plain B(PLA) substrate by fitting 24 Gaussian functions corresponding to the theoretical

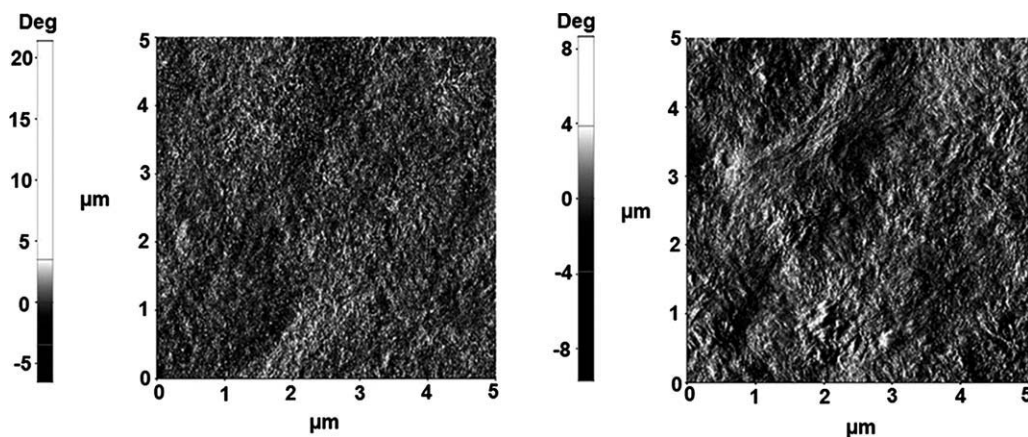


Figure 1 Phase AFM images of LDPE surfaces after 5 min heat-treatment followed by quenching with liquid nitrogen (a) and quenching at room temperature (b).

reflections of cellulose I β ²² in the data and calculating the ratio of the measured intensity and the approximation for the amorphous background. No significant difference was observed between the two samples.

The order parameter²³ describing the orientation of cellulose crystals with respect to the machine direction was calculated from the two-dimensional WAXS patterns of all samples. A narrow radial range at the peak of the 200-reflection of cellulose was chosen to minimize the contribution of the peaks of PLA and LDPE. This parameter describes

orientational order in the samples and has a value of 0 for no orientation and a value of 1 for fully oriented samples. Orientation of cellulose crystals in the machine direction (direction the web runs on board machine) was observed in all samples, with order parameters varying in the range 0.03–0.05.

Heat-treatment of the B(PLA) samples increased the level of crystallinity in PLA gradually when comparing the intensity of the sharpest peak of PLA (020-reflection at $q = 1.18 \text{ 1/\AA}^{24,25}$) obtained from the heat-treated samples to the peak of the plain B(PLA) sample (Fig. 4). This is in agreement with

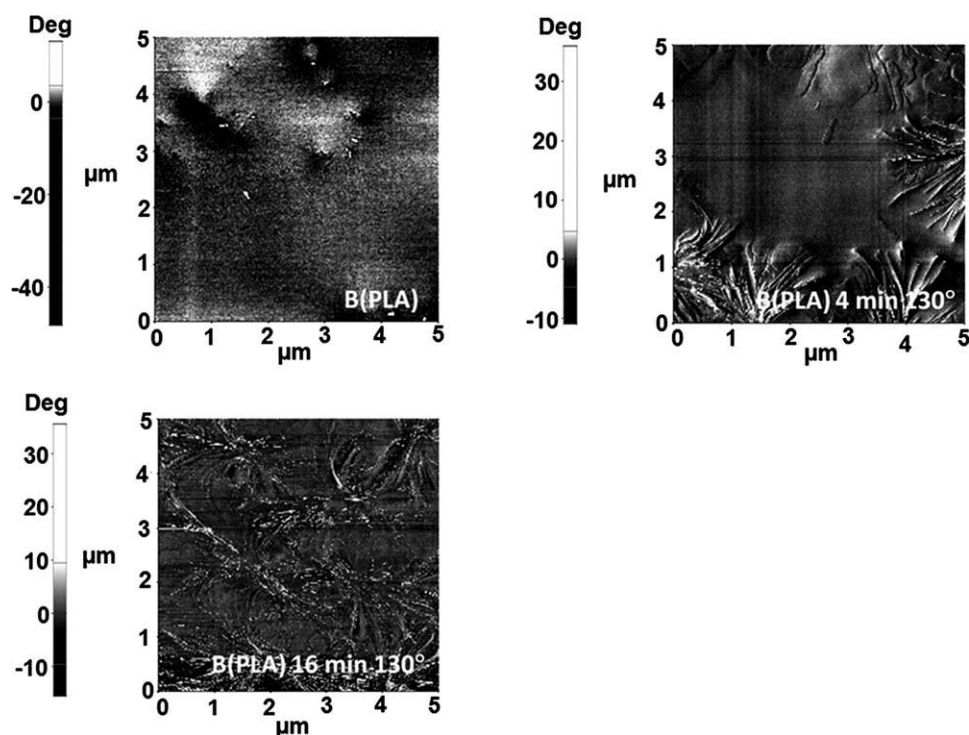


Figure 2 Phase AFM images of plain B(PLA) and B(PLA) after 4 and 16 min heat-treatment followed by quenching at room temperature.

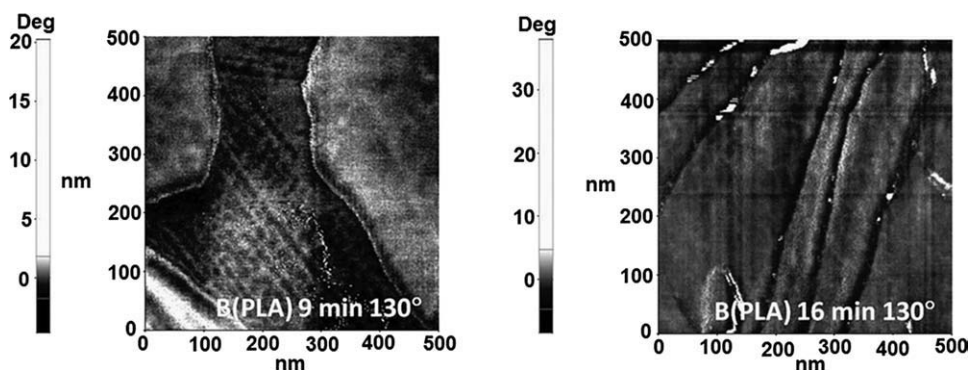


Figure 3 Phase AFM images of B(PLA) after 9 and 16 min heat-treatment followed by quenching at room temperature.

the observations from the AFM studies. The three other peaks in Figure 4 are the 101-, 023-, and 121-reflections of PLA, visible at $q = 1.05 \text{ 1/\AA}$, $q = 1.35 \text{ 1/\AA}$ and 1.58 1/\AA , respectively.^{24,25}

B(PE) samples were more challenging to analyze with WAXS due to the reason stated above. However, qualitative analysis of the data showing in Figure 5 was possible. The only diffraction peak of LDPE visible despite the cellulose background (110-reflection) is located approximately at $q = 1.52 \text{ 1/\AA}$. On the basis of visibility of this peak, it seems that plain B(PE) had the lowest crystallinity followed by B(PE) heat-treated at 200°C and the quenching with liquid nitrogen. B(PE) sample after similar heat treatment but slower quenching rate resulted in higher crystallinity. Samples heat-treated at 170°C where more crystalline regardless of the quenching process. It has to be kept in mind that more branched LDPE has lower crystallization tendency than HDPE or linear LDPE often used in such studies.

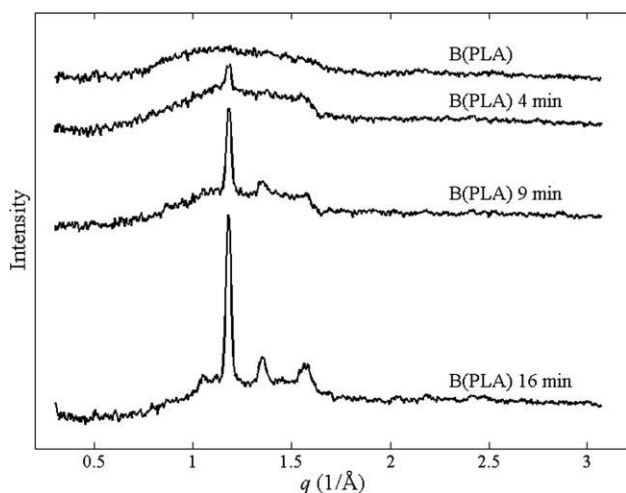


Figure 4 WAXS patterns from the plain and heat treated B(PLA) samples. The data for the uncoated reference board was subtracted from the curves.

Effect of heat-treatment on surface chemistry

Table II presents the results from the contact angle and surface energy measurements for the plain and heat-treated substrates. In the B(PLA) samples the hydrophobicity increased after 4 and 9 min of heat treatment at 130°C and then decreased after 16 min of heat treatment. This behavior can be explained by the surfaces containing both amorphous and crystalline regions, and the effect of such heterogeneity on apparent contact angles. After 16 min of heat treatment at 130°C the surface was covered with spherulites resulting in a slightly more hydrophobic surface compared with the amorphous surface. The values for the B(PE) samples were more constant. The samples which were heat-treated and quenched at room temperature had higher standard deviation in the contact angle values. These results support our findings from AFM and WAXS results. The scattering in contact angle makes also the analyses of the surface energy values based on the average contact angles difficult.

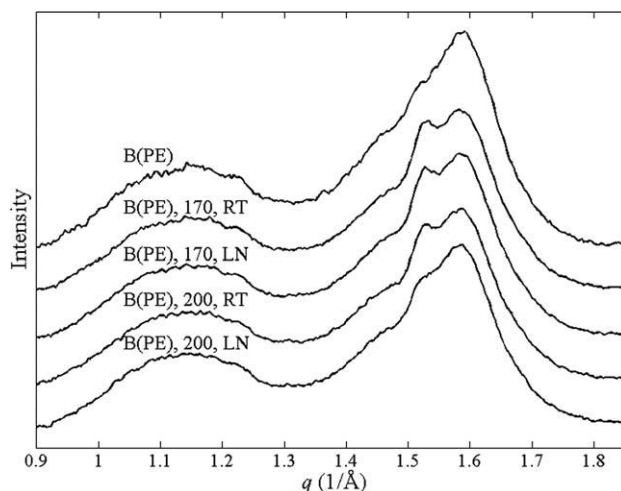


Figure 5 WAXS pattern of the plain and heat-treated B(PE) samples.

TABLE II

Average Contact Angles ($^{\circ}$) of the Samples with Water and Di-iodomethane (DIM) from Three to Eight Parallel Measurements, and Surface Energies γ (mN/m) and Relative Polarity γ_p/γ Calculated from the Contact Angle Data Using the OWRK (ext. Fowles) Theory

Sample	Contact angle, H ₂ O	Contact angle, DIM	γ	γ_p/γ
B(PE)	85 \pm 5.0	56 \pm 1.8	34	11
B(PE), 170 $^{\circ}$ C, RT	84 \pm 13	60 \pm 2.9	33	13
B(PE), 200 $^{\circ}$ C, RT	96 \pm 8.4	56 \pm 2.3	32	2.7
B(PE), 170 $^{\circ}$ C, LN	85 \pm 1.9	57 \pm 1.9	34	11
B(PE), 200 $^{\circ}$ C, LN	90 \pm 2.7	56 \pm 0.7	33	6.8
B(PLA)	76 \pm 2.2	37 \pm 7.8	46	9.8
B(PLA), 4 min 130 $^{\circ}$ C	99 \pm 3.3	34 \pm 1.0	42	0
B(PLA), 9 min 130 $^{\circ}$ C	91 \pm 9.5	65 \pm 7.6	29	10
B(PLA), 16 min 130 $^{\circ}$ C	80 \pm 6.8	36 \pm 2.0	45	7.1

The values of contact angles were measured one second after the initial contact between the sample surface and the test liquid. RT refers to quenching at room temperature, LN to quenching with liquid nitrogen.

Effect of Al₂O₃ coating on gas barrier properties of heat-treated substrates

Results from the barrier tests are presented in Tables III and IV. The water vapor barrier property of B(PE) was improved by the heat-treatment followed by quenching at room temperature. This can be explained by the increased crystallinity of LDPE. These results are similar to previous results reported.^{8,10} However, quenching of the heat-treated B(PE) with liquid nitrogen resulted in impaired water vapor barrier property. This is probably due to more amorphous structure when compared with the other samples.

The Al₂O₃ layer improved the oxygen and water vapor barrier properties of B(PE) and B(PLA) as such. In our previous studies^{5,6} increasing the thickness of the Al₂O₃ layer further from 25 nm was

TABLE III

Water Vapor Transmission Rates (g/m²/day) of Plain B(PE) and B(PLA) Substrates and Al₂O₃ Coated Substrates With and Without the Heat Treatment

Sample	Without ALD-Al ₂ O ₃	With ALD-Al ₂ O ₃
B(PE)	11 \pm 0.6	1.7 \pm 0.2
B(PE), 170 $^{\circ}$ C, RT	7.6 \pm 0.8	4.3 \pm 3.6
B(PE), 200 $^{\circ}$ C, RT	7.0 \pm 0.2	3.7 \pm 2.8
B(PE), 170 $^{\circ}$ C, LN	15 \pm 3.3	9.2 \pm 5.3
B(PE), 200 $^{\circ}$ C, LN	20 \pm 6.6	5.8 \pm 1
B(PLA)	98 \pm 2.4	5.8 \pm 2.3
B(PLA), 4 min 130 $^{\circ}$ C	88 \pm 1.7	3.0 \pm 1.9
B(PLA), 9 min 130 $^{\circ}$ C	78 \pm 5.8	3.2 \pm 0.8
B(PLA), 16 min 130 $^{\circ}$ C	76 \pm 6.8	11 \pm 2.3

Two to eight parallel measurements were performed. The results are given as average \pm standard deviation. Target thickness of Al₂O₃ layer was 25 nm. RT refers to quenching at room temperature, LN to quenching with liquid nitrogen.

TABLE IV

Oxygen Transmission Rates (cm³/m²/10⁵ Pa/day) of Plain B(PE) and B(PLA) Substrates and Al₂O₃ Coated Substrates With and Without of Heat Treatment

Sample	Without ALD-Al ₂ O ₃	With ALD-Al ₂ O ₃
B(PE)	7200 \pm 3000	450 \pm 90
B(PE), 170 $^{\circ}$ C, RT	4600 \pm 1300	8200 \pm 3700
B(PE), 200 $^{\circ}$ C, RT	85,000 \pm 35,000	9200 \pm 1200
B(PE), 170 $^{\circ}$ C, LN	71,000 \pm 41,000	9200 \pm 2800
B(PE), 200 $^{\circ}$ C, LN	>170,000	38,000 \pm 14,000
B(PLA)	530 \pm 35	120 \pm 100
B(PLA), 4 min 130 $^{\circ}$ C	650 \pm 20	40 \pm 23
B(PLA), 9 min 130 $^{\circ}$ C	3400 \pm 2300	>175,000
B(PLA), 16 min 130 $^{\circ}$ C	7500 \pm 70	>200,000

Two to eight parallel measurements were performed. The results are given as average \pm standard deviation. Target thickness of Al₂O₃ layer was 25 nm. RT refers to quenching at room temperature, LN to quenching with liquid nitrogen.

needed to significantly improve the barrier properties of B(PE). In this study the improvement was obvious already with a 25 nm layer of Al₂O₃. The improvement was clear even when we used lower deposition temperature than previously. However, after the Al₂O₃ coating the WVTR values of the plain and the heat-treated B(PE) samples quenched at room temperature were on the same level, whereas the improvement in the water vapor barrier was not necessarily as unambiguous with the amorphous B(PE) samples that can be explained by the increased thermal mobility of the amorphous polymer chains. This makes the nucleation and growth of the Al₂O₃ layer more challenging leading to poor film formation or internal/interfacial stresses. In addition, oxidation of the amorphous polymer could impair the water vapor barrier performance. Heat treatment of B(PLA) also improved the WVTR, and the longer the heat-treatment the lower the WVTR. This is in agreement with previous studies.^{9,10,13} In the previous studies with B(PLA)^{5,6} the optimal Al₂O₃ layer thickness was 25 nm. With thicker Al₂O₃ layers (e.g., 50 nm and 100 nm) the barrier properties were impaired. However, the B(PLA) samples coated with the Al₂O₃ layer were similar to each other within the limitations of the test method. This indicates that the Al₂O₃ layer made by the ALD technique dominated the water vapor barrier properties.

The oxygen barrier property of B(PE) was little affected by the over-melt-point heat treatment at 170 $^{\circ}$ C or at 200 $^{\circ}$ C. The oxygen barrier property was impaired as temperature was increased or when quenching with liquid nitrogen was used due to a more amorphous LDPE coating. The reason for increased oxygen transmission rate after treatment at 200 $^{\circ}$ C followed by quenching at room temperature could be the formation of pathways to permeants between the crystals along

the oxidized short-chain amorphous regions. Such a structure has been suggested earlier¹⁵—although for linear high-density polyethylene (HDPE). This finding of increased oxygen permeability is in disagreement with the results from others.^{8,10} In addition to different polyethylene used in these studies, one cannot rule out the effect of the base substrate which was in our case a rough paperboard. The best oxygen barrier was achieved when plain B(PE) was coated with the Al₂O₃ layer. The oxygen barrier properties with the Al₂O₃ layer were similar for the heat-treated samples quenched at room temperature and the sample heat-treated at 170°C followed by quenching with liquid nitrogen. The samples exposed to 200°C and quenched with liquid nitrogen exhibited the highest oxygen transmission rates both with and without the Al₂O₃ layer. This is in agreement with the water vapor barrier results.

In the case of B(PLA) a short heat treatment below the melting point had only a small effect on the oxygen barrier. The values were similar to the samples with the Al₂O₃ layer. However, as the heat-treatment at 130°C is prolonged to 9 or 16 min the increased crystallinity and the growing spherulites force the short-chain material with low crystallization tendency to the spherulite boundaries, as suggested for HDPE.¹⁵ If a PLA-based blend is used the different blend components might separate. Such areas had probably different response to the ALD process conditions, and the ALD layer uniformity was impaired thus creating additional pathways for oxygen molecules. In addition, oxygen barrier is more sensitive to resulting coating defects than water vapor barrier.

CONCLUSIONS

Heat-treatment of PLA-coated paperboard at 130°C and LDPE-coated paperboard at 170°C or 200°C followed by quenching at room temperature were found to be beneficial for the water vapor barrier performance. Quenching of LDPE-coated board with liquid nitrogen mainly increased the WVTR value, which was explained by changes in the polymer morphology. No systematic improvement in oxygen barrier property was observed which was explained by the spherulitic structure of PLA, and the discontinuities and low-chain material around the spherulites forming passages for oxygen molecules. An Al₂O₃ layer grown by the ALD technique improved the barrier properties of PLA and LDPE-coated substrates as such. However, heat-treatment of these substrates before applying the Al₂O₃ layer provided little or no practical means to improve the barrier performance. On the contrary, radical changes in the polymer morphology eventually impaired the barrier properties, and the thin Al₂O₃ layer could not in all

cases compensate for such changes in the substrate, probably due to an uneven nucleation and film growth and high mobility of amorphous LDPE and interspherulitic PLA chains. This indicates the importance of homogeneous surface before the Al₂O₃ coating. It was also observed that decreasing the ALD-Al₂O₃ deposition temperature from 100 to 80°C improved the barrier properties obtained with LDPE-coated board.

The authors thank Stora Enso Oyj for providing the paperboard samples.

References

- Pan, P.; Liang, Z.; Zhu, B.; Dong, T.; Inoue, Y. *Macromolecules* 2008, 41, 8011.
- Lange, J.; Wyser, Y. *Packag Technol Sci* 2003, 16, 149.
- Leterrier, Y. *Prog Mater Sci* 2003, 48, 1.
- Puurunen, R. L. *J Appl Phys* 2005; 97: 121301.
- Hirvikorpi, T.; Vähä-Nissi, M.; Mustonen, T.; Iiskola, E.; Karpinen, M. *Thin Solid Films* 2010, 518, 2654.
- Hirvikorpi, T.; Vähä-Nissi, M.; Harlin, A.; Karppinen, M. *Thin Solid Films* 2010, 518, 5463.
- Hirvikorpi, T.; Vähä-Nissi, M.; Harlin, A.; Marles, J.; Miikkulainen, V.; Karppinen, M. *Appl Surf Sci* 2010, 257, 736.
- Lahtinen, K.; Nättinen, K.; Vartiainen, J. *Polym-Plast Tech Eng* 2009, 48, 561.
- Lahtinen, K.; Kotkamo, S.; Koskinen, T.; Auvinen, S.; Kuusipalo, J. *Packag Technol Sci* 2009, 22, 451.
- Lahtinen, K. Publication 880. Tampere University of Technology, Tampere, Finland. 2010.
- Qin, Y.; Rubino, M.; Auras, R.; Lim, L. T. *J Appl Polym Sci* 2008, 110, 1509.
- Edwards, R. 1990 *Polymers, Laminations and Coatings Conference Proceedings*, Boston, MA, September 4–7, 1990; p 595.
- Tsuji, H.; Okino, R.; Daimon, H.; Fujie, K. *J Appl Polym Sci* 2006, 99, 2245.
- Al-Raheil, I. A.; Al-Share, M. *J Appl Polym Sci* 1999, 72, 1125.
- Scheirs, J.; Bigger, S. W.; Delatycki, O. *J Polym Sci Part B: Polym Phys* 1991, 29, 795.
- Kim, K. S.; Ryu, C. M.; Park, C. S.; Sur, G. S.; Park, C. E. *Polymer* 2003, 44, 6287.
- Ferguson, J. D.; Weimer, A. W.; George, S. M. *Chem Mater* 2004, 16, 5602.
- Liang, X. H.; Hakim, L. F.; Zhan, G. D.; McCormick, J. A.; George, S. M.; Weimer, A. W.; Spencer, J. A.; Buechler, K. J.; Blackson, J.; Wood, C. J.; Dorgan, J. R. *J Am Ceram Soc* 2007, 90, 57.
- Scott, W. W.; Bhushan, B. *Ultramicroscopy* 2003, 97, 151.
- Andersson, S.; Serimaa, R.; Paakkari, T.; Saranpää, P.; Pesonen, E. *J Wood Sci* 2003, 49, 531.
- Cullity, B. D.; Stock, S. R. *Elements of X-Ray Diffraction*; Prentice Hall: New Jersey, 2001.
- Nishiyama, Y.; Langan, P.; Chanzy, H. *J Am Chem Soc* 2002, 124, 9074.
- Davidson, P.; Petermann, D.; Levelut, A. M. *J de Physique II* 1995, 5, 113.
- Grijpma, D. W.; Zondervan, G. J.; Pennings, A. *J Polym Bull* 1991, 25, 327.
- Zhong, W.; Ge, J.; Gu, Z.; Li, W.; Chen, X.; Zang, Y.; Yang, Y. *J Appl Polym Sci* 1999, 74, 2546.

PUBLICATION VI

**Enhanced water vapor barrier
properties for biopolymer films by
polyelectrolyte multilayer and atomic
layer deposited Al₂O₃ double-coating**

In: Applied Surface Science 257 (2011),
pp. 9451–9454.

Reprinted with permission from the publisher.



Enhanced water vapor barrier properties for biopolymer films by polyelectrolyte multilayer and atomic layer deposited Al₂O₃ double-coating

Terhi Hirvikorpi^a, Mika Vähä-Nissi^{a,*}, Ali Harlin^a, Mikko Salomäki^b, Sami Areva^c, Juuso T. Korhonen^d, Maarit Karppinen^e

^a VTT Technical Research Centre of Finland, Biologinkuja 7, Espoo, P.O. Box 1000, FI-02044 VTT, Finland

^b University of Turku, Department of Chemistry, Laboratory of Materials Chemistry and Chemical Analysis, Vatselankatu 2, FI-20014, Finland

^c Tampere University of Technology, Department of Biomedical Engineering, Biokatu 6, P.O. Box 692, FI-33101 Tampere, Finland

^d Aalto University School of Science, Department of Applied Physics, P.O. Box 15100 FI-00076 AALTO, Espoo, Finland

^e Aalto University School of Chemical Technology, Laboratory of Inorganic Chemistry, P.O. Box 16100, FI-00076 AALTO, Espoo, Finland

ARTICLE INFO

Article history:

Received 29 April 2011

Received in revised form 3 June 2011

Accepted 6 June 2011

Available online 15 June 2011

Keywords:

Atomic layer deposition

Layer-by-layer deposition

Polyelectrolyte

Water vapor barrier

Aluminum oxide

Poly lactide

ABSTRACT

Commercial polylactide (PLA) films are coated with a thin (20 nm) non-toxic polyelectrolyte multilayer (PEM) film made from sodium alginate and chitosan and additionally with a 25-nm thick atomic layer deposited (ALD) Al₂O₃ layer. The double-coating of PEM + Al₂O₃ is found to significantly enhance the water vapor barrier properties of the PLA film. The improvement is essentially larger compared with the case the PLA film being just coated with an ALD-grown Al₂O₃ layer. The enhanced water vapor barrier characteristics of the PEM + Al₂O₃ double-coated PLA films are attributed to the increased hydrophobicity of the surface of these films.

© 2011 Elsevier B.V. All rights reserved.

1. Introduction

Growing environmental concerns related to the use of synthetic polymers in packaging industry have led to the need for new bio-based materials [1]. The bio-based packaging materials currently in the market are mainly based on starch or polylactide (PLA). These materials have many advantages, such as sustainability, recyclability and biodegradability [2]. However, the sensitivity of biopolymers towards moisture has restricted their use. To overcome the problem various surface treatment approaches have been considered to enhance the water vapor barrier properties of biopolymers.

A simple and cost-effective way to functionalize surfaces is to coat them with a polyelectrolyte multilayer (PEM) film [3]. Ultra-thin PEM films can be prepared by a layer-by-layer (LbL) technique through alternating adsorption of cationic and anionic polyelectrolyte solutions. A charged substrate of any size or shape is immersed into a polyelectrolyte solution with a net charge opposite to the surface charge. The polymer is spontaneously adsorbed onto the substrate due to the electrostatic interactions

[4,5], resulting in charge reversal at the surface [6,7]. Rinsing removes the unbound polymer from the surface. The LbL deposition technique is well suited for the construction of precise nanolevel architectures and there are several potential applications ranging from biomaterials [8] and drug delivery [9] to membranes [10].

Here we investigate the capability of PEM films together with a thin inorganic layer applied on top of it to improve water vapor barrier properties of PLA films. Our interest was to see how the PEM film as an intermediate layer would affect the surface properties of PLA and thereby the water vapor barrier properties of it after the surface is additionally coated with an Al₂O₃ layer grown by the atomic layer deposition (ALD) technique. The ALD technique is a self-limited surface controlled gas-phase deposition process perfectly suited to produce inorganic high-performance (i.e., homogeneous, pinhole-free and conformal) gas and vapor barrier coatings on polymers. Thin (5–25 nm) ALD-grown Al₂O₃ coatings have already been shown to be effective barrier layers towards gases and vapors [11–17]. The effect of surface nanostructure on the wettability properties has been demonstrated e.g., with ALD-grown ZnO coatings on cicada wings [18]. As a result of the self-limiting growth mechanism, the ALD coating follows closely the topography of the substrate, even on nanostructured surfaces [19–22].

* Corresponding author. Tel.: +35 840 530 8472; fax: +35 8946 4305.

E-mail address: mika.vaha-nissi@vtt.fi (M. Vähä-Nissi).

The nature-based polyelectrolytes sodium alginate (ALG) and chitosan (CHI) were selected for the LbL deposition of the PEM film. Chitosan is a suitable counter polyelectrolyte for moisture-sensitive ALG due to its good film-forming properties [2] and natural antibacterial and fungicidal properties make CHI an attractive polyelectrolyte for food and pharmaceutical packaging applications [23]. The fabrication of PEM films does not require any expensive equipment. The improvement in the water vapor properties of the PLA film by the intermediate PEM film could limit the amount of Al_2O_3 needed, thus improving the cost-efficiency of the fabrication process. Note that for the possible future utilization of thin Al_2O_3 coatings as a part of the fabrication line of bio-based packaging materials, the ALD is considered to be the most expensive process step.

2. Materials and methods

2.1. Fabrication of PEM films for their preliminary characterization

Polyelectrolyte multilayer films from ALG and CHI (extracted from chitin according to [24]) were first deposited on silicon wafers for preliminary tests for the film thickness and cytotoxicity. Exactly the same LbL method as used for the PLA substrates (see Section 2.2) was employed here. The LbL deposition process is also well described in literature [3,25]. The solutions of CHI and ALG were vacuum filtered in order to remove impurities. Prior to the LbL depositions the silicon (100) substrates employed were purified and silanized. The substrates were dipped into acetone (99.5 vol.%) for 15 min, rinsed with distilled water, followed by dipping into warm (60 °C) solution of 5:1:1 $\text{H}_2\text{O}:\text{NH}_4\text{OH}$ (25 vol.%) $:\text{H}_2\text{O}_2$ (30 vol.%) for 60 min. Then the substrates were rinsed again with distilled water and dipped into a warm (60 °C) solution of 3:1 H_2SO_4 (95–97 vol.%) $:\text{H}_2\text{O}_2$ (30 vol.%) for 60 min. Finally, the substrates were rinsed with distilled water and dried with pressurized air. Prior to the silanization, the silicon wafers were kept in an oven at 110 °C overnight. The silanization was performed by dipping the substrates into (3-aminopropyl)triethoxysilane in dry toluene solution (1 vol.%) at 60 °C for 4 min. After the silanization, the substrates were dipped into toluene and dried with pressurized air.

2.2. PEM and Al_2O_3 depositions on PLA biopolymer film

Commercial PLA film with a thickness of 20 μm was selected as a representative biopolymer substrate for the depositions. The substrate was first coated with a PEM film using the LbL process and subsequently with an Al_2O_3 layer. For the LbL fabrication of PEM films, four solutions were made: anionic ALG and cationic CHI solutions plus rinsing buffer and rinsing water solutions with the following concentrations: $c(\text{ALG})=c(\text{CHI})=1$ mg/ml; $c(\text{NaCl})=0.15$ M, and $c(\text{AcOH})=1$ mM. In order to improve the solubility of CHI, HCl ($c(\text{HCl})=10$ mM) was added. The pH of the solutions was adjusted to 4.5 using NaOH. The PLA substrates were sequentially dipped into ALG and CHI for 15 min. Between the dippings the substrates were dipped into rinsing solutions, three times into buffer solution for 60 s followed by dipping into distilled water for 60 s and drying with nitrogen. Eleven single layers were deposited on three parallel samples. The deposition began and ended with a layer of CHI leaving CHI as the outermost layer facing the Al_2O_3 layer.

The Al_2O_3 depositions were carried out in a commercial SUNALE™ R-series ALD reactor at 100 °C targeting at a Al_2O_3 layer thickness of 25 nm. Fig. 1 presents the targeted three-layer structure. The ALD precursors for the Al_2O_3 depositions were

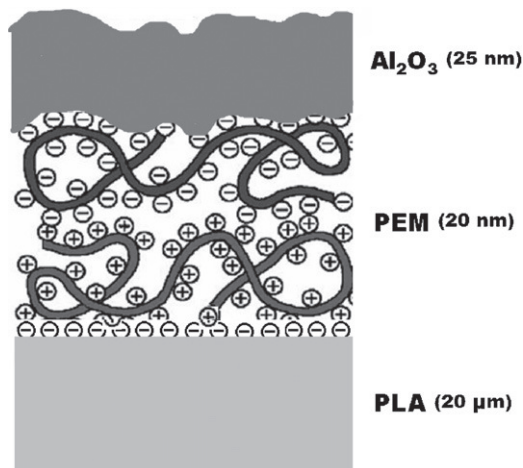


Fig. 1. Schematic illustration of the targeted multilayer structure of PEM- and Al_2O_3 -coated PLA film.

Figure modified from that of G. Decher [3].

trimethylaluminum (TMA, SAFC Hitech, electronic grade purity) and water. High purity N_2 (99.9999%) was used as a carrier and purge gas. One ALD cycle consisted of a TMA precursor pulse and a subsequent N_2 purge followed by a water precursor pulse and another N_2 purge. The precursor pulses lasted 0.1 s and the purges 5 s. The resultant film thicknesses on the polymer films could not be directly measured. Instead, the coating thicknesses were produced according to the reactor process parameters and compared to the thickness of a similarly grown Al_2O_3 layer on a silicon wafer analysed with a Nanospec AFT4150 reflectometer. The film growth rate was estimated to be ca 1.1 Å/cycle. Due to the different surface chemistries the actual growth rate on the PLA substrate may however somewhat deviate from that determined for the Al_2O_3 coating on silicon wafer [26,27].

2.3. Characterizations

Molecular weights of the polyelectrolytes affect the formation of the film and its surface properties. Therefore the molecular weights of ALG and CHI were determined. Solutions of ALG and CHI with concentrations from 0 to 6×10^{-4} g/ml were fabricated for the density and viscosity measurements. Molecular weights were determined by measuring densities with an Anton Paar DMA 45 digital density meter at 25 °C and viscosities with an Anton Paar AMVn automated microviscometer.

The Mark–Houwink equation (1) gives the relation between intrinsic viscosity $[\eta]_{\text{in}}$ and molecular weight M_v .

$$[\eta]_{\text{in}} = KM_v^a \quad (1)$$

From this equation the molecular weight of a polyelectrolyte can be determined using the intrinsic viscosity and the parameters, a and K , from literature [28,29]. The thickness and the root-mean-square (rms) roughness value of the PEM film on silicon wafer was determined by a scanning spectroscopic ellipsometer (Nanofilm EP3).

The cytotoxicity of the PEM film from ALG and CHI was investigated. Cytotoxicity measures the toxicity of a material to living cells. The disinfected PEM films deposited on silicon wafer were kept in a Medium solution (DMEM, Dulbecco's modified Eagle's medium, Sigma) for 2 h at room temperature in humid conditions. The test cells were commercial CRL-2592 cells from ATCC. In the test the value of the lactate dehydrogenase (LDH) was determined and used to evaluate the toxicity. Two control samples were used: highly toxic polyvinyl chloride stabilized with organic tin compound as a

Table 1

Molecular weights of the polyelectrolytes ALG and CHI, together with the salts and their concentrations and the Mark–Howink parameters (K and a) used in calculations.

Species	Salt	C(Salt) (M)	K (ml/g)	A	$[\eta]_{in}$ (ml/g)	M_v (g/mol)
ALG	NaCl	0.1	0.0073	0.92	760	280 000
CHI	NaOAc/AcOH	0.2/0.3	0.082	0.76	770	170 000

positive and non-toxic glass as a negative control. The cells were placed in direct contact with the samples. After 24 h the amount of LDH was measured by UV-Vis spectrophotometer and the cytotoxicity ($D\%$) was determined [30]. In the case of the $D\%$ value being 15% or higher, the sample is considered to be toxic to living cells.

The water vapor transmission rate (WVTR) was measured from three parallel samples according to the modified gravimetric methods, ISO 2528:1995 and SCAN P 22:68, and was expressed as $g/m^2/day$. The test conditions were $23^\circ C$ and 75% relative humidity. Additionally, we investigated the wettability properties of the sample surfaces through contact angle (CA) measurements. The CA measurements were performed with KSV CAM 200 Optical Contact Angle Meter in a controlled atmosphere (relative humidity 50%, temperature $23^\circ C$). The contact angle values of three parallel samples were calculated at the time of 1 s from the moment the water drop contacts the surface. The samples were also investigated by scanning electron microscopy (SEM; JEOL JSM-7500FA). For SEM, the samples were sputter-coated with a thin layer of platinum to promote conductivity.

3. Results and discussion

3.1. Properties of PEM films

The molecular weight values determined for the two polyelectrolytes, CHI and ALG, are presented in Table 1 together with the necessary parameters used to calculate these values. The values obtained for the molecular weights are consistent with those reported in literature [28,29].

Our aim was to prepare ultra-thin and PEM films from ALG and CHI. This was successfully realized and the average thickness of the films was measured (by scanning spectroscopic ellipsometry) to be 20 nm. The rms roughness in micrometer-scale of the PEM films on top of silicon wafer was determined to be 1.6 nm determined from the $300\ \mu m \times 300\ \mu m$ image. The cytotoxicity tests revealed that the $D\%$ value was 3.53% thus verifying that the films were non-toxic to living cells and accordingly suitable to be used in food and pharmaceutical packaging applications.

3.2. Properties of PEM- and Al_2O_3 -coated PLA films

The water vapor barrier and wettability properties of the PEM- and Al_2O_3 -coated PLA films were evaluated by measuring the water

Table 2

Water vapor transmission rate (WVTR) and contact angle (CA) values for the plain and variously coated PLA samples. The given numbers are average values for three parallel samples.

Sample	WVTR ($g/m^2/day$)	CA ($^\circ$)
PLA	53 ± 4	73 ± 2
PLA + PEM	106 ± 7	76 ± 4
PLA + 25 nm Al_2O_3	33 ± 6	48 ± 1
PLA + PEM + 25 nm Al_2O_3	25 ± 9	98 ± 4

vapor transmission rates and the contact angle values for a plain PLA film and for PLA films with various coatings. The results are summarized in Table 2. From Table 2 the positive effect of the PEM + Al_2O_3 double-coating on the water vapor barrier properties of PLA is clearly seen.

The PEM-film coating alone did not improve the water vapor barrier properties of the PLA film, rather the WVTR of PLA was increased from 53 to $106\ g/m^2/day$ after the PEM-film coating. This is apparently due to the dipping process in the LbL method exposing the hygroscopic PLA polymer chains to swelling. The ALD-grown Al_2O_3 layer alone enhanced the water vapor barrier properties of the PLA film considerably, as expected from our previous studies [11]. Here the WVTR value was found to decrease from 53 to $33\ g/m^2/day$. Most importantly, the PEM + Al_2O_3 double-coating improved the water vapor barrier properties even more by decreasing the WVTR value to $25\ g/m^2/day$.

The water vapor barrier level achieved here with the double-coating is close to the level required ($0.1\text{--}10\ g/m^2/day$) in commercial packaging applications for dry food and pharmaceuticals. The present results are significant due to the fact that the LbL deposition is a very cheap and easy-to-use method. It should also be emphasized that the ALD-grown Al_2O_3 layer is so thin that it should not affect the biodegradability of the material. In addition, the PLA film investigated here was relatively thin ($20\ \mu m$) when considering typical packaging materials.

From Table 2, the water vapor transmission rates seem to correlate with the wettability properties of the ALD- Al_2O_3 -coated samples such that the larger the CA is, the lower is the WVTR value. Polar H_2O molecules are apparently less readily adsorbed on the less polar surface. The contact angle value of the plain PLA film was 73° . The PEM coating alone did not change the contact angle value considerably. However, when the PEM-coated PLA film was further coated with an Al_2O_3 layer, the contact angle value increased to 98° thus making the surface more hydrophobic. On the contrary, when the PLA film was coated only with the Al_2O_3 layer, the contact angle value was found to decrease to 48° making the surface rather more hydrophilic. This is rather what was expected due to the intrinsically hydrophilic nature of Al_2O_3 surfaces [31].

From the discussions above (Table 2) the PEM intermediate layer apparently influences the hydrophobicity of the Al_2O_3 surface. The very reason for that remains to be clarified more deeply in future

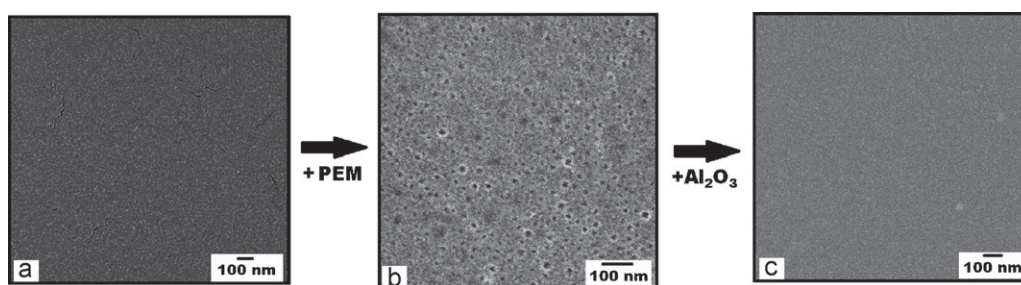


Fig. 2. SEM images for the plain and variously coated PLA films. (a) The plain PLA film appears to be smooth with small patterns due to the sputtered Pt. (b) The PEM-film-coated PLA film seems to have nanopores throughout the film. (c) After further coating with a 25-nm thick Al_2O_3 layer the surface seems to be conformally coated with the Al_2O_3 layer.

studies. However, parallel behavior (i.e., a CA value of 128°) was recently observed for a thermally grown Al₂O₃ coating with a relatively rough surface [32]. It is known that some special topologies of surface structure could produce even superhydrophobic states on intrinsically hydrophilic surfaces [33]. The LbL dipping process may alter the surface of the PLA film and increase its roughness.

In Fig. 2 we show SEM images taken from the plain and vari-ously coated PLA films. It is seen that the PLA film is a very smooth substrate, presumably due to the commercial fabrication method of the film. Small surface patterns can be observed due to the sputtered Pt. Once the PLA film is coated with a PEM film, a surface structure with small pores (10–30 nm in diameter) appears on the surface of the whole film. After the further deposition of the 25-nm thick Al₂O₃ layer the nanostructured surface seems to be conformally coated with Al₂O₃, such that the smallest pores are filled but the surface still presents some surface structure. In order to gain deeper understanding of the reasons for the increased hydrophobicity efforts should be made to investigate the surface structures and chemistries in a much more detailed way.

4. Conclusions

Ultra-thin and non-toxic polyelectrolyte multilayer (PEM) films from sodium alginate and chitosan were successfully deposited onto commercial polylactide (PLA) biopolymer film, and further coated with a 25-nm thick atomic layer deposited (ALD) Al₂O₃ layer. The water vapor barrier properties of the PLA film were considerably improved after employing the PEM + Al₂O₃ double-coating. Most importantly, the properties were improved more than by applying just the Al₂O₃ coating. This was tentatively attributed to changes in surface morphology created by the PEM layer. The use of a thin PEM film as an intermediate on the PLA film prior to the Al₂O₃ coating could extend the use of biopolymers in environmentally friendly food and pharmaceutical packaging applications.

Acknowledgements

The authors thank VTT, Metsäliitto Group, Myllykoski Corporation, Stora Enso Oyj and UPM-Kymmene Oyj for their funding. The work was also partially supported by Academy of Finland (Nos. 116254 and 126528).

References

- [1] K. Khwaldia, E. Arab-Tehrany, S. Desobry, Biopolymer coatings on paper packaging materials, *CRFSFS* 9 (2010) 82–91.
- [2] C. Andersson, New ways to enhance the functionality of paperboard by surface treatment – a review, *Pack. Technol. Sci.* 21 (2008) 339–372.
- [3] G. Decher, Fuzzy nanoassemblies: toward layered polymeric multicomposites, *Science* 277 (1997) 1232–1237.
- [4] K. Lowack, C.A. Helm, Molecular mechanisms controlling the self-assembly process of polyelectrolyte multilayers, *Macromolecules* 31 (1998) 823–833.
- [5] R. Advincula, E. Aust, W. Meyer, W. Knoll, In situ investigations of polymer self-assembly solution adsorption by surface plasmon spectroscopy, *Langmuir* 12 (1996) 3536–3540.
- [6] J.F. Joanny, Polyelectrolyte adsorption and charge inversion, *Eur. Phys. J. B* 9 (1999) 117–122.
- [7] N.G. Hoogeveen, M.A. Coheen Stuart, G.J. Fleer, M.R. Böhmer, Formation and stability of multilayers of polyelectrolytes, *Langmuir* 12 (1996) 3675–3681.
- [8] B. Thierry, F.M. Winnik, Y. Merhi, J. Silver, M. Tabrizian, Bioactive coatings of endovascular stents based on polyelectrolyte multilayers, *Biomacromolecules* 4 (2003) 1564–1571.
- [9] L. Ge, H. Möhwald, J. Li, Phospholipase A2 hydrolysis of mixed phospholipid vesicles formed on polyelectrolyte hollow capsules, *Chem. Eur. J.* 9 (2003) 2589–2594.
- [10] H.H. Rmaile, J.B. Schlenoff, Optically active polyelectrolyte multilayers as membranes for chiral separations, *J. Am. Chem. Soc.* 125 (2003) 6602–6603.
- [11] P.F. Garcia, R.S. McLean, M.H. Reilly, M.D. Groner, S.M. George, Ca-tests of Al₂O₃ gas diffusion barriers grown by atomic layer deposition on polymers, *Appl. Phys. Lett.* 89 (2006) 031915–1–031915-3.
- [12] M.D. Groner, S.M. George, R.S. McLean, P.F. Garcia, Gas diffusion barriers on polymers using Al₂O₃ atomic layer deposition, *Appl. Phys. Lett.* 88 (2006) 051907–1–051907-3.
- [13] E. Langereis, M. Creatore, S.B.S. Heil, M.C.M. van de Sanden, W.M.M. Kessels, Plasma-assisted atomic layer deposition of Al₂O₃ moisture permeation barriers on polymers, *Appl. Phys. Lett.* 89 (2006) 081905–1–081905-3.
- [14] T. Hirvikorpi, M. Vähä-Nissi, T. Mustonen, E. Iiskola, M. Karppinen, Atomic layer deposited aluminum oxide barrier coatings for packaging materials, *Thin Solid Films* 518 (2010) 2654–2658.
- [15] T. Hirvikorpi, M. Vähä-Nissi, A. Harlin, M. Karppinen, Comparison of some coating techniques to fabricate barrier layers on packaging materials, *Thin Solid Films* 518 (2010) 5463–5466.
- [16] T. Hirvikorpi, M. Vähä-Nissi, A. Harlin, J. Marles, V. Miikkulainen, M. Karppinen, Effect of corona pre-treatment on the performance of gas barrier layers applied by atomic layer deposition onto polymer coated paperboard, *Appl. Surf. Sci.* 257 (2010) 736–740.
- [17] T. Hirvikorpi, M. Vähä-Nissi, J. Vartiainen, P. Penttilä, A. Nikkola, A. Harlin, R. Serimaa, M. Karppinen, Effect of heat-treatment on the performance of gas barrier layers applied by atomic layer deposition onto polymer-coated paperboard, *J. Appl. Polym. Sci.* (2011), doi:10.1002/app.34313.
- [18] J. Malm, E. Sahramo, M. Karppinen, R.H.A. Ras, Photo-controlled wettability switching by conformal coating of nanoscale topographies with ultrathin oxide films, *Chem. Mater.* 22 (2010) 3349–3352.
- [19] M. Leskelä, M. Ritala, Atomic layer deposition chemistry: recent developments and future challenges, *Angew. Chem. Int. Ed.* 42 (2003) 5548–5554.
- [20] R.L. Puurunen, Surface chemistry of atomic layer deposition: a case study for the trimethylaluminum/water process, *J. Appl. Phys.* 97 (2005) 121301–121352.
- [21] R.H.A. Ras, M. Kemell, J. de Wit, M. Ritala, G. ten Brinke, M. Leskelä, O. Ikkala, Hollow inorganic nanospheres and nanotubes with tunable wall thicknesses by atomic layer deposition on self-assembled polymeric templates, *Adv. Mater.* 19 (2007) 102–106.
- [22] M. Knez, K. Nielsch, L. Niinistö, Synthesis and surface engineering of complex nanostructures by atomic layer deposition, *Adv. Mater.* 19 (2007) 3425–3438.
- [23] S. Quintavalla, L. Vicini, Antimicrobial food packaging in meat industry, *Meat Sci.* 62 (2002) 373–380.
- [24] R. Signini, S.P.C. Filho, On the preparation and characterization of chitosan hydrochloride, *Polym. Bull.* 42 (1999) 159–166.
- [25] M. Salomäki, P. Tervasmäki, S. Areva, J. Kankare, The Hofmeister anion effect and the growth of polyelectrolyte multilayers, *Langmuir* 20 (2004) 3679–3683.
- [26] J.D. Ferguson, A.W. Weimer, S.M. George, Atomic layer deposition of Al₂O₃ films on polyethylene particles, *Chem. Mater.* 16 (2004) 5602–5609.
- [27] X.H. Liang, L.F. Hakim, G.D. Zhan, J.A. McCormick, S.M. George, A.W. Weimer, J.A. Spencer, K.J. Buechler, J. Blackson, C.J. Wood, J.R. Dorgan, Novel processing to produce polymer/ceramic nanocomposites by atomic layer deposition, *J. Am. Ceram. Soc.* 90 (2007) 57–63.
- [28] A. Martinsen, G. Skjåk-Bræk, O. Smidsrod, F. Zanetti, S. Paoletti, Comparison of different methods for determination of molecular weight and molecular weight distribution of alginates, *Carbohydr. Polym.* 15 (1991) 171–193.
- [29] M. Rinaudo, M. Milas, P.L. Dung, Characterization of chitosan. Influence of ionic strength and degree of acetylation on chain expansion, *Int. J. Biol. Macromol.* 15 (1993) 281–285.
- [30] E.S. Säilynoja, A. Shinya, M.K. Koskinen, J.I. Salonen, T. Masuda, A. Shinya, T. Matsuda, T. Mihara, N. Koide, Heat curing of UTMA-based hybrid resin: effects on the degree of conversion and cytotoxicity, *Odontology* 92 (2004) 27–35.
- [31] D.S. Finch, T. Oreskovic, K. Ramadurai, C.F. Herrmann, S.M. George, R.L. Mahajan, Biocompatibility of atomic layer-deposited alumina thin films, *J. Biomed. Mater. Res. A* 87A (2008) 100–106.
- [32] J.E. Samad, J.A. Nychka, Wettability of biomimetic thermally grown aluminum oxide coatings, *Bioinsp. Biomim.* 6 (2011) 016004–016009.
- [33] J.-L. Liu, X.-Q. Feng, G. Wang, S.-W. Yu, Mechanisms of superhydrophobicity on hydrophilic substrates, *J. Phys.: Condens. Matter* 19 (2007) 356002-1–356002-12.

Terhi Hirvikorpi

Thin Al₂O₃ barrier coatings grown on bio-based packaging materials by atomic layer deposition

Growing environmental concerns related to the use of non-biodegradable polymers in the packaging industry have led to the need for new materials. Currently, these conventional polymers are widely used due to their relatively low cost and high performance. Bio-degradable plastics and fibre-based materials have been proposed as a solution to the waste problems related to these synthetic polymers. Fibre-based packaging materials have many advantages over their non-biodegradable competitors, such as stiffness vs. weight ratio and recyclability. However, poor barrier properties and sensitivity to moisture are the main challenges restricting their use. Application of a thin coating layer is one way to overcome these problems and to improve the barrier properties of such materials.

Atomic Layer Deposition (ALD) is a well suited technique for depositing thin inorganic coatings onto temperature-sensitive materials such as polymer-coated board and paper and polymer films. Thin and highly uniform Al₂O₃ coatings have been deposited at relatively low temperatures of 80, 100 and 130 °C onto various bio-based polymeric materials employing the ALD technique. The work demonstrates that a 25-nm-thick ALD-grown Al₂O₃ coating significantly enhances the oxygen and water vapour barrier performance of these materials. Promising barrier properties were revealed for polylactide-coated board, hemicellulose-coated board as well as various biopolymer (polylactide, pectin and nanofibrillated cellulose) films after coating with a 25-nm-thick Al₂O₃ layer.

Extremely thin Al₂O₃ coatings can improve the properties of biopolymers, enabling the use of these renewable polymers in the production of high-performance materials for demanding food and pharmaceutical packaging applications. The future roll-to-roll ALD technology for coating polymers with inorganic thin films will increase the industrial potential of these materials and could lead to further opportunities for their commercialization.

ISBN

978-951-38-7750-7 (soft back ed.)

978-951-38-7751-4 (URL: <http://www.vtt.fi/publications/index.jsp>)

Series title and ISSN

VTT Publications

1235-0621 (soft back ed.)

1455-0849 (URL: <http://www.vtt.fi/publications/index.jsp>)

Project number

Date

September 2011

Language

English, Finnish abstr.

Pages

74 p. + app. 42 p.

Name of project

Commissioned by

Keywords

Atomic layer deposition, aluminium oxide, thin film, barrier, biopolymer, packaging material

Publisher

VTT Technical Research Centre of Finland
P.O. Box 1000, FI-02044 VTT, Finland
Phone internat. +358 20 722 4520
Fax +358 20 722 4374

Terhi Hirvikorpi

Ohuet biopohjaisille pakkausmateriaaleille atomikerroskasvatetut Al₂O₃-barrierpinnoitteet

Pakkausteollisuuden tietoisuus synteettisten biohajoamattomien muovien ympäristöhaitoista on lisännyt tarvetta ekologisemmille biopohjaisille pakkausratkaisuille. Nykyisin näitä synteettisiä polymeerejä käytetään useissa pakkauksissa, koska ne ovat halpoja ja ominaisuuksiltaan hyviä. Biohajoavia muovi- ja kuitupohjaisia materiaaleja pidetään ratkaisuna öljypohjaisten synteettisten muovien aiheuttamalle jäteongelmalle. Kuitupohjaisilla pakkausmateriaaleilla on monia hyviä ominaisuuksia verrattuna niiden biohajoamattomiin kilpailijoihin, kuten painoon suhteutettu kestävyys ja kierrätettävyys. Niiden heikkoutena on kuitenkin huono kosteuden sietokyky sekä heikko vesihöyryn läpäisyn estokyky, jotka estävät tuotteiden laajamittaisemman käytön. Materiaalien läpäisyntoa voidaan parantaa sopivilla pinnoituksilla.

Työssä kasvatettiin ohuita Al₂O₃-kalvoja suhteellisen alhaisessa lämpötilassa 80, 100 ja 130 °C:ssa ALD-tekniikalla monenlaisille biopohjaisille polymeeri-substraateille. Hyvin ohuet (25 nm) ALD-tekniikalla valmistetut Al₂O₃-pinnoitteet saavat aikaan huomattavan parannuksen biopohjaisen pakkausmateriaalin hapen- ja vesihöyryn läpäisyn esto-ominaisuuksissa. Polylaktidilla ja hemiselluloosalla päällystetyt kartonkien sekä polylaktidista, pektiinistä ja nanoselluloosasta valmistettujen kalvojen huomattiin olevan lupaavia barriereja sen jälkeen, kun ne on päällystetty 25 nm:n paksuisella Al₂O₃-kerroksella.

Nämä hyvin ohuet pinnoitteet saavat aikaan niin suuren parannuksen barrier-ominaisuuksissa, että biopolymeerien käyttö vaativissakin pakkaussovelluksissa, kuten elintarvike- ja lääkepakkausissa, mahdollistuu. ALD-tekniikan kehitys kohti rullalta-rullalle-prosessia mahdollistaa epäorgaanisten pinnoitteiden valmistamisen teollisessa mittakaavassa, mikä on elintärkeää tässä työssä esiteltujen uusien pakkausmateriaalien kaupallistumiselle.

ISBN

978-951-38-7750-7 (nid.)

 978-951-38-7751-4 (URL: <http://www.vtt.fi/publications/index.jsp>)

Avainnimeke ja ISSN

VTT Publications

1235-0621 (nid.)

 1455-0849 (URL: <http://www.vtt.fi/publications/index.jsp>)

Projektnumero

Julkaisuaika

Syyskuu 2011

Kieli

Englanti, suom. tiiv.

Sivuja

74 s. + liitt. 42 s.

Projektin nimi

Toimeksiantaja(t)

Avainsanat

Atomic layer deposition, aluminium oxide, thin film, barrier, biopolymer, packaging material

Julkaisija

 VTT
PL 1000, 02044 VTT
Puh. 020 722 4520
Faksi 020 722 4374

Growing environmental concerns related to the use of synthetic, non-biodegradable polymers in packaging industry has led to the need for new, especially bio-based materials. Currently petroleum-based synthetic polymers are widely used due to their relatively low cost and high performance. Bio-based packaging materials can have many advantages over their non-biodegradable competitors, such as stiffness vs. weight ratio and biodegradability. However, poor barrier properties and sensitivity towards moisture are the main challenges for their use.

Atomic Layer Deposition (ALD) is a feasible technique to deposit thin aluminum oxide (Al₂O₃) coatings onto temperature-sensitive bio-based materials. Such coatings enhance significantly the barrier performance towards oxygen and water vapor. Even extremely thin (25 nm) Al₂O₃ coatings can provide improvement enabling the use of bio-based materials in fabrication of high-performance materials for demanding food and pharmaceutical packaging applications. The future use of roll-to-roll ALD process to coat biopolymers with ALD-grown inorganic thin-films will increase the industrial potential of these materials and is essential for the commercialization.